THEORETICAL CHEMISTRY INSTITUTE

THE UNIVERSITY OF WISCONSIN

THE POLARIZABILITY OF DIATOMIC HELIUM

by Patrick John Fortune

WIS-TCI-511

26 April 1974

MADISON, WISCONSIN

ERRATA FOR WIS-TCI-511

	Read	Instead of
p. ix, 1st line of C.1	use of DEFINE	use DEFINE
p. x, 1st line of III.2	$\beta(R)$	$\underset{\approx}{\beta}(R)$
p. 7, Eq. (1.2)	$-(\frac{\partial E}{\partial F_i})F_i=0$	$(\frac{\partial E}{\partial F_i})F_i=0$
p. 16, line 7	atom	atoms
p. 16, line before Eq. (1.30)	(spherical) system	system
p. 22, line 8	$^3\Sigma_u^+$	$^3\Sigma^+$
p. 25, line 5	29,30	29
p. 59, Eq. (2.51)	$\sum_n \lvert\langle\phi_0\rvert O\rvert\phi_n\rangle\rvert^2$	$\sum_n \lvert\langle\phi_0\rvert O\rvert\phi_0\rangle\rvert^2$
p. 65, title	A_8 are a_0^{11} .	A_8 are a_0 .
p. 68, line 9	given by:[54]	given by:[53]
p. 68, Eq. (3.3)	$\langle z_1^2\rangle$	$\langle z_1^2$
p. 98, title	diatomic	diatom
p. 101	$\beta(R)$	$\underset{\approx}{\beta}(R)$
p. 106, line 2	a(1)a(2)b(3)b(4)	a(1)a(2)b(3)c(4)
p. 122, 2nd line of table	(-.093 $cm^6/mole^2$)	(-0.93 $cm^6/mole^2$)
p. 168, reference 26	R. S. Watts, Mol. Phys. 26, 7 (1973).	R. J. Watts, to be published.
p. 169, reference 44	Doklady	Poklady

THE POLARIZABILITY OF DIATOMIC HELIUM

by

Patrick John Fortune

A Thesis Submitted in Partial Fulfillment

Of the Requirements for the Degree of

Doctor of Philosophy

(Chemistry)

University of Wisconsin

1974

THE POLARIZABILITY OF DIATOMIC HELIUM*

Patrick John Fortune

(Under the supervision of Professor Phillip R. Certain)

ABSTRACT

In this thesis, the calculation of the electric dipole polarizability tensor of the He_2 dimer is described, and the results are used in the computation of several dielectric and optical properties of helium gas, at both high (322°K) and low (4°K) temperatures. The properties considered are the second dielectric virial coefficient, the second Kerr virial coefficient, and the depolarization ratio of the integrated intensities for the Raman scattering experiments.

The thesis consists of five parts. In the first part, the polarizability and various properties are defined. In the second part, the calculation of the polarizability in the long-range region in terms of a quantum mechanical multipole expansion is described. The formulas which are obtained are applied to the H_2, He_2, and HeH diatomics, and the results are compared to those of model calculations. In the third part, the calculation of the He_2

---

* Supported by the National Aeronautics and Space Administration Grant NGL-50-002-001 and the National Science Foundation Grant GP-28213.

polarizability in the overlap region via coupled Hartree-Fock perturbation theory is described, and a basis set selection procedure is delineated which allows the Hartree-Fock limit to be approached with sets of reasonable size. It is further shown that the long-range limit of the coupled Hartree-Fock polarizability is identical to that of the point dipole model. The calculation of the quantum pair distribution function for both the ^{3}He and ^{4}He isotopes at 4°K is discussed in the fourth part. The calculated values of the properties of helium gas are given in the fifth part. The order of the computed second dielectric virial coefficients for ^{3}He and ^{4}He at 4°K is found to be opposite to that of experiment. This experimental-computational discrepancy is discussed in detail; while there is an uncertainty in the computed results due to the neglect of electron correlation, it is concluded that the discrepancy is probably due to inaccuracies in the experiments.

TABLE OF CONTENTS

Chapter		Page
	ABSTRACT.	i
	ACKNOWLEDGEMENTS.	vi
	LIST OF TABLES.	vii
	LIST OF FIGURES	x
I	INTRODUCTION.	1
	A. Motivation.	1
	B. Polarizability Definitions.	6
	C. Pressure Dependence of the Dielectric Constant.	15
	D. The Kerr Effect	24
	E. Collision Induced Raman Scattering.	29
	F. Perspective	34
II	POLARIZABILITIES OF DIATOMIC MOLECULES IN THE LIMIT OF LARGE INTERNUCLEAR SEPARATIONS	38
	A. Quantum Mechanical Multipole Expansion of the Polarizability.	38
	B. Connection between the Point Dipole Model and the Quantum Mechanical Multipole Expansion of the Polarizability	47

Chapter		Page
	C. Accurate Long-Range Polarizability Calculations for the H_2, HeH, and He_2 Systems	50
III	POLARIZABILITIES OF DIATOMIC MOLECULES IN THE OVERLAP REGION.	66
	A. Previous Calculations in the Overlap Region . . .	66
	B. Coupled Hartree-Fock Perturbation Theory.	72
	C. Basis Set Selection Procedure	79
	D. Test Calculations	83
	E. Helium Diatom Calculations.	91
	F. Extrapolation of the Hartree-Fock Polarizability to the Long-Range Region	103
IV	STATISTICAL METHODS	109
V	RESULTS AND DISCUSSION.	120
	A. Results	120
	B. Basis Set Error	124
	C. Electron Correlation Effects.	129
	D. Summary and Conclusions	132
	APPENDIX A. Symmetry Reduction Used in the Long-Range Calculation.	135

Chapter | Page

APPENDIX B. Derivation of Integrals Required in the Long-Range Helium Calculations 142

APPENDIX C. The BISON Computing System 149

APPENDIX D. Sample Input for the BISON Polarizability Load Module. 160

APPENDIX E. Conversion Factors for the Second Dielectric Virial Coefficient and the Second Kerr Virial Coefficient. 164

REFERENCES. 166

ACKNOWLEDGEMENTS

I would like to express my graditude to all who have aided me in the development of this thesis. In particular, I would like to thank the following:

Professor P. R. Certain who introduced me to the problem, and who was always available for discussion and help throughout its solution;

Professor J. O. Hirschfelder for providing an atmosphere which is both pleasant and conducive to scientific research;

Professor L. W. Bruch for his help in the quantum statistical mechanical aspects of this work;

Professor S. T. Epstein who, through several discussions and comments, helped us to view our results in the proper perspective;

Dr. A. C. Wahl for permitting the use of the BISON program, and helping in its implementation;

The University of Wisconsin Chemistry Department for much IBM 7094 computer time;

Ms. Patty Spires who typed this thesis, and Jerry Carrig who reproduced it;

My wife, Joan, whose patience and understanding were necessary ingredients for the successful completion of this work.

LIST OF TABLES

		Page
I.1	Experimental first and second dielectric virial coefficients for several rare gases	19
I.2	Experimental first and second Kerr virial coefficients for several rare gases.	28
I.3	Experimental depolarization ratios for helium liquid and gas	37
II.1	Coefficients in the expressions for $A_6^{\parallel}$ and $A_6^{\perp}$. . . .	55
II.2	Numerical parameters for the Hart-Herzberg helium atom wavefunction	57
II.3	Convergence of γ_0, $A_6^{\parallel}$, and $A_6^{\perp}$ for helium	61
II.4	Sum rule checks used in the long-range helium calculations	62
II.5	Computed properties of a ground state He atom. . . .	63
II.6	Accurate and approximate values of $A_6^{\parallel}$ and $A_6^{\perp}$ for H_2, HeH, and He_2.	65

		Page
III.1	Hirschfelder-Kirkwood approximation for the polarizability of He_2.	70
III.2	Atomic polarizabilities for He and Be.	87
III.3	Coupled Hartree-Fock first order orbital corrections for H_2 at R = 1.4 a_0	88
III.4	Coupled Hartree-Fock polarizabilities for H_2 at R = 1.4 a_0.	89
III.5	Coupled Hartree-Fock ratios, $\langle\hat{\mu}_x\rangle/F$, for several F's and two different basis sets for H_2 at R = 1.402 a_0	90
III.6	Field-free basis for He_2 at R = 4.0 a_0	93
III.7	Basis sets and values of $\alpha_\perp$ for He_2 at R = 4.0 a_0.	96
III.8	Basis sets and values of $\alpha_\parallel$ for He_2 at several internuclear separations	97
III.9	Basis sets and values of $\alpha_\perp$ for He_2 at several internuclear separations	98
IV.1	Numerical parameters in the He_2 MDD-2 pair potential	116

Page

IV.2 List of the values of the pair correlation functions for ^3He and ^4He at 4°K 117

V.1 Computed results for the second dielectric virial coefficient, the second Kerr virial coefficient, and the depolarization ratio of the integrated intensities for helium at 322°K and 4°K. 122

A.1 Symmetry reduction of spherical harmonics. 141

C.1 Illustration of the use DEFINE procedure to obtain more core for use with BISON. 153

C.2 Illustration of the use of the UNIVAC 1108 MAP processor to position data 155

D.1 Sample input for BISON for calculations of $\alpha_\perp$ for He_2. 163

LIST OF FIGURES

		Page
III.1	Mean incremental polarizability, $\Delta\alpha(R)$, for He_2, as a function of internuclear separation	100
III.2	Anisotropy, $\underset{\sim}{\beta}(R)$, in the polarizability tensor for He_2, as a function of internuclear separation	102
IV.1	Pair distribution functions for helium at 322°K and 4°K	119

CHAPTER I

INTRODUCTION

A. Motivation

> "We are perhaps not far removed from the time when we shall be able to submit the bulk of chemical phenomena to calculation." (J. L. Gay-Lussac, Memoires de la Societe' d'Archeil, 2, 207 (1808).)

> "It is also a good rule not to put overmuch confidence in the observational results that are put forward until they have been confirmed by theory." (A. Eddington in The Coming of the Golden Age by G. S. Stent.)

There is a well established paradigm for computing the macroscopic properties of the rare gases. The first step in the calculation involves treating the electronic structure of the constituent atoms or molecules of the gas via quantum mechanics. The link between the molecular properties and experiment is provided by statistical mechanics. The need for either classical or quantum statistical procedures is dictated by the parameters of the particular experiment which one is attempting to describe; low temperature experiments on light atoms, for example, necessitate the inclusion of quantum statistical effects. Then, since statistical formulas which relate experimentally observable quantities to the properties of the molecular system are available, one can, at least in principle, obtain results for the macroscopic system using a completely computational procedure.

In this light, experiments are an alternative to computation. While the approach actually taken in a given case is largely determined by convenience, the computational scheme can result in a more detailed understanding of the nature of the physical interactions which give rise to the phenomenon under investigation.

In the work which is reported in this thesis, we adopt the computational approach, and calculate a number of dielectric and optical properties of gaseous helium.

The quantities in which we are interested are: the pressure dependence of the dielectric constant;[1] the static electric-field-induced birefringence (Kerr effect);[2] and the collision induced Raman spectrum.[3] The experimental results, as well as the theory, are formulated in terms of virial expansions in powers of the density. We have considered the terms which are linear in the density and arise from interactions involving pairs of helium atoms. The calculation of each of these properties involves both the electric polarizability tensor (quantum mechanics) and the quantum radial distribution function for helium (statistical mechanics). The corresponding properties for various systems in addition to helium, including other rare gases, have been experimentally studied by other workers. We, however, restricted our work to helium because it is the only system which currently may be treated accurately using a completely non-empirical approach.

There are several reasons for undertaking this study, not the least of which is the fact that the purely computational procedure has never before been carried to completion (for helium) for a property which requires the accurate calculation of both a molecular property (other than the energy) and the quantum distribution function. Even for the relatively simple case of helium, approximations are made in both the quantum mechanical and statistical mechanical parts of the computation. While it is not our intent to question the general approach, we wish to examine the sensitivity of the experimental properties to these approximations, and to assess the interpretation of the experimental data in terms of molecular properties. One hopes that a critical comparison of experimental and computed results would either verify the utility of a given set of approximations or indicate the direction in which one should move in order to improve the approximations.

Most of our work concentrates on calculating how the polarizability of a pair of helium atoms changes as a function of internuclear separation. For collisions at thermal energies, these changes probably amount to no more than a few percent of the sum of the polarizabilities of the isolated helium atoms. Nevertheless, these changes give rise to the observable effects mentioned above. The accurate calculation of these changes is a difficult computational problem.

Quantum mechanical calculations of molecular polarizabilities have had a long history, dating from Schrödinger's second paper wherein

the polarizability of the hydrogen atom was obtained.[4] For more complicated systems than this, however, polarizability calculations are far from routine. Although semi-empirical methods have been developed which are capable of giving good upper and lower bounds to the exact polarizability,[5] most non-empirical calculations are for atoms, or molecules at fixed geometry, and are at the level of the independent particle (Hartree-Fock) model. Only recently have atomic polarizability calculations, for systems other than helium, been reported in which electron correlation is taken into account.[6] For atomic helium itself, the calculations of Buckingham and Hibbard have yielded the polarizability to six significant figures.[7] For molecules, only the fully correlated calculations of Kolos and Wolniewicz on H_2 can be considered definitive.[8]

To anticipate the pattern of our calculation of the helium pair polarizability, it is useful to briefly recall the history of calculations of the pair potential. It has been known since Lennard-Jones' successful fit of equation of state and transport data[9] that the helium pair potential is characterized by long range attraction and short range repulsion, resulting in a shallow van der Waals well at intermediate separations. Until recently, there were two separate computational approaches to explain this behavior: the multipole expansion of the potential at large internuclear separations and the Hartree-Fock approximation at shorter separations. The two approaches make different assumptions: the former assumes that the overlap

between the atomic wavefunctions is negligible and treats the interatomic correlation which gives rise to the attractive multipole interactions; the latter neglects correlation but allows the atoms to overlap, resulting in a purely repulsive interaction. It has only been within the last several years that calculations have been performed which employ a wavefunction which passes smoothly from long range to the region of the van der Waals well.[10] Calculations of the helium pair potential are now in good accord with experimental data, although there are still some questions regarding the true depth of the well.[10b,11]

In our calculations of the pair polarizability we have followed the pattern of the pair potential calculations, and have considered both the long range multipole expansion and the coupled Hartree-Fock approximation. As we shall show, in contrast to the pair potential case, the coupled Hartree-Fock model for the pair polarizability does reduce to the multipole expansion at large separations, although the multipole coefficients are incorrect due to the neglect of electron correlation. Thus, there is an uncertainty in our final results for the pair polarizability, which can only be removed by using a wavefunction which accurately describes electron correlations.

Our statistical mechanical calculation of the radial distribution function is more reliable. The essential ingredient here is an accurate pair potential function. We have used the MDD-2 potential[12] which fits well the available experimental data on macroscopic and scattering

properties of helium and also agrees with the non-empirical calculations. Further, we shall show that the dielectric and optical properties are not as sensitive to the pair potential as they are to the pair polarizability. In the calculation of the quantum distribution function, we followed methods established recently by Klemm and Storer.[13]

In the next sections, we will review the experimental and prior theoretical work on the pair polarizability of helium and on the aforementioned dielectric and optical properties, and summarize our own computations. Later chapters contain detailed explanations of the different aspects of our work.

B. Polarizability Definitions

The polarizability of an atom or molecule is a measure of how easily its electronic charge cloud is distorted by an external electric field. The electronic structure in the absence of any external forces is determined primarily by the balance of the electron-nuclear attractive forces with the electron-electron and nuclear-nuclear repulsive forces, in accord with the Schrödinger equation and the symmetry requirements of the Pauli Principle. The measure of these internal atomic fields is the ratio of the electronic charge to the square of the Bohr radius, $e/a_0^2 \sim 10^9$ volts/cm . Since most laboratory fields are considerably less than 10^5 volts/cm , the effect of such applied fields on the electronic structure of the molecule is expected to be small.

For applied electric fields which are sufficiently small, it is natural to extend the field-free treatment of molecular electronic structure to the field-dependent case via perturbation methods. Thus, one assumes that the electronic energy, E, of a molecule in an external electric field, $\underset{\sim}{F} = (F_x, F_y, F_z)$ can be expanded in powers of the components of $\underset{\sim}{F}$:

$$E = E^{(0)} - \sum_i \mu_i^{(0)} F_i - \tfrac{1}{2} \sum_{i,j} \alpha_{ij} F_i F_j - \tfrac{1}{6} \sum_{i,j,k} \beta_{ijk} F_i F_j F_k - \tfrac{1}{24} \sum_{i,j,k,\ell} \gamma_{ijk\ell} F_i F_j F_k F_\ell + \ldots . \tag{1.1}$$

In this equation, $\mu_i^{(0)}$ is the i-th component of the permanent dipole moment of the molecule, α_{ij} is the ij component of the polarizability tensor, while the hyperpolarizabilities $\underset{\approx}{\beta}$ and $\underset{\approx}{\gamma}$ refer to tensors of rank greater than 2 and reflect higher field effects. The external field also affects the total dipole moment of the molecule, and the i-th component of the dipole moment is given by

$$\mu_i = \left(\frac{\partial E}{\partial F_i}\right)_{F_i=0} . \tag{1.2}$$

Then, from Eq. (1.1) for the energy,

$$\mu_i = \mu_i^{(0)} + \sum_j \alpha_{ij} F_j + \ldots . \tag{1.3}$$

These last two equations suggest two ways by which the polarizability can be obtained. That is, it can be obtained from a second order expression which involves the energy,

$$\alpha_{ij} = -\tfrac{1}{2}\left(\frac{\partial^2 E}{\partial F_i \partial F_j}\right)_{\underset{\sim}{F}=0} ; \tag{1.4}$$

or, from a first order expression which involves the dipole moment,

$$\alpha_{ij} = \left(\frac{\partial \mu_i}{\partial F_j}\right)_{\underset{\sim}{F}=0} . \tag{1.5}$$

From Eq. (1.1) it is seen that the effect of nonzero hyperpolarizability terms is to give rise to deviations from a linear polarization law. Buckingham has written an excellent review article on induced electric moments and their modification by intermolecular interactions.[14]

To place the above definitions in a quantum mechanical framework, we consider the Schrödinger equation for a molecule in a constant electric field:

$$[H(F) - E(F)]\Psi(F) = 0 . \tag{1.6}$$

In this equation, $H(F)$ is the field-dependent Hamiltonian operator for a single molecule, and $\Psi(F)$ and $E(F)$ are the (field-dependent) wavefunction and energy respectively, for the molecule. The exact

solution of this equation is generally impossible to obtain, so that one resorts to approximate schemes. For molecules, one begins by making the Born-Oppenheimer approximation, and then applies either perturbation theory or variational methods to obtain approximate solutions to the equation which results.

For constant field, the Born-Oppenheimer Hamiltonian for a molecule having N electrons whose positions are denoted by $\underset{\sim}{r}_i$, and M nuclei of charge Z_α at $\underset{\sim}{R}_\alpha$, can be written as:

$$H = H_0 - \hat{\underset{\sim}{\mu}} \cdot \underset{\sim}{F} . \tag{1.7}$$

Here, $\hat{\underset{\sim}{\mu}}$ is the molecular dipole moment operator defined (in atomic units) by:

$$\hat{\underset{\sim}{\mu}} = -\sum_{i=1}^{N} \underset{\sim}{r}_i + \sum_{\alpha=1}^{M} Z_\alpha \underset{\sim}{R}_\alpha , \tag{1.8}$$

and H_0 is the field-free, Born-Oppenheimer Hamiltonian for the molecule. The essence of the perturbation method is that one assumes that the ground state energy, $E_0(F)$, and the corresponding wavefunction, $\Psi_0(F)$, can be expanded in a power series in $\underset{\sim}{F} = F \underset{\sim}{f}$:

$$E_0(F) = \sum_{n=0}^{\infty} F^n E_0^{(n)} , \tag{1.9}$$

and

$$\Psi_0(F) = \sum_{n=0}^{\infty} F^n \Psi_0^{(n)} . \tag{1.10}$$

Substituting these last two equations into Eq. (1.6), and setting the coefficient of each power of F equal to zero, leads to the usual set of perturbation equations. The zero and first order equations are respectively:

$$(H_0 - E_0^{(0)})\Psi_0^{(0)} = 0 , \tag{1.11}$$

and

$$(H_0 - E_0^{(0)})\Psi_0^{(1)} - (\hat{\underset{\sim}{\mu}}\cdot\underset{\sim}{f} - E_0^{(1)})\Psi_0^{(0)} = 0 , \tag{1.12}$$

where

$$E_0^{(1)} = \langle\Psi_0^{(0)}|\hat{\underset{\sim}{\mu}}\cdot\underset{\sim}{f}|\Psi_0^{(0)}\rangle .$$

The expression for the second order energy is

$$E_0^{(2)} = -\langle\Psi_0^{(0)}|\hat{\underset{\sim}{\mu}}\cdot\underset{\sim}{f}|\Psi_0^{(1)}\rangle , \tag{1.13}$$

where we have used the normalization condition

$$\langle\Psi_0^{(1)}|\Psi_0^{(0)}\rangle + \langle\Psi_0^{(0)}|\Psi_0^{(1)}\rangle = 0 . \qquad (1.14)$$

Comparing Eqs. (1.1) and (1.9) we see that the quantum mechanical analogue of Eq. (1.4) is

$$\sum_{ij} \alpha_{ij}F_iF_j = -2E_0^{(2)} F^2 , \qquad (1.15)$$

or,

$$\sum_{ij} \alpha_{ij}F_iF_j = 2\langle\Psi_0^{(0)}|\hat{\underset{\sim}{\mu}}\cdot\underset{\sim}{f}|\Psi_0^{(1)}\rangle F^2 . \qquad (1.16)$$

To obtain the analogue of Eq. (1.5), we note that quantum mechanically the dipole moment is obtained as an expectation value:

$$\underset{\sim}{\mu} = \langle\hat{\underset{\sim}{\mu}}\rangle = \langle\Psi(F)|\hat{\underset{\sim}{\mu}}|\Psi(F)\rangle . \qquad (1.17)$$

In view of Eqs. (1.9) and (1.10), this expectation value can also be represented as a power series in the field:

$$\underset{\sim}{\mu} = \sum_{n=0}^{\infty}\sum_{m=0}^{\infty} F^{n+m}\langle\Psi_0^{(n)}|\hat{\underset{\sim}{\mu}}|\Psi_0^{(m)}\rangle , \qquad (1.18)$$

$$= \langle\Psi_0^{(0)}|\hat{\underset{\sim}{\mu}}|\Psi_0^{(0)}\rangle + 2\langle\Psi_0^{(0)}|\hat{\underset{\sim}{\mu}}|\Psi_0^{(1)}\rangle F + \ldots . \qquad (1.19)$$

Comparing this last equation to Eq. (1.3) we see, of course, that the same definition of $\underset{\approx}{\alpha}$ (Eq. (1.16)) results from consideration of either the energy or the dipole moment within the context of perturbation theory.

The problem of computing the polarizability has been reduced to that of solving Eq. (1.12) for $\Psi_0^{(1)}$. Using a reduced resolvent notation, $R_0 = (E^{(0)} - H_0)^{-1}$, one writes the solution of Eq. (1.12) formally as:

$$\Psi_0^{(1)} = -R_0 \, \hat{\underset{\sim}{\mu}} \cdot \underset{\sim}{f} \, \Psi_0^{(0)} \, , \tag{1.20}$$

so that $\underset{\approx}{\alpha}$, the polarizability tensor, becomes:

$$\underset{\approx}{\alpha} = -2\langle \Psi_0^{(0)} | \hat{\underset{\sim}{\mu}} \, R_0 \, \hat{\underset{\sim}{\mu}} | \Psi_0^{(0)} \rangle \, . \tag{1.21}$$

This last equation is the immediate starting point for the multipole expansion of $\underset{\approx}{\alpha}$ which will be considered in the next chapter.

If one uses variational methods rather than perturbation theory to solve Eq. (1.6), then Eq. (1.21) is not the expression for the polarizability which is used. This is our situation in the overlap region. Here we optimize the variational functional

$$\tilde{E} = \langle \tilde{\Psi} | H(F) | \tilde{\Psi} \rangle / \langle \tilde{\Psi} | \tilde{\Psi} \rangle \, , \tag{1.22}$$

to obtain a field-dependent trial wavefunction $\tilde{\Psi}(F)$, from which the dipole moment is approximated as

$$\mu_i = \langle\tilde{\Psi}(F)|\hat{\mu}_i|\tilde{\Psi}(F)\rangle/\langle\tilde{\Psi}|\tilde{\Psi}\rangle . \tag{1.23}$$

To calculate the polarizability we return to Eq. (1.5) and use the definition of derivative explicitly:

$$\alpha_{ij} = \lim_{\underset{\sim}{F} \to 0} \frac{\mu_i - \mu_i^{(0)}}{F_j} . \tag{1.24}$$

This is the starting point of the Hartree-Fock calculations which will be discussed in Chapter III.

With respect to calculations in the short range region, one could, from a strictly formal point of view, just as easily use the definition of the polarizability in terms of the energy, Eq. (1.4). However, from a computational standpoint, the precision in the difference between the field-dependent and field-free energies is less than the corresponding dipole moment difference because one uses small applied fields (to eliminate hyperpolarizability terms) and the polarizability is a second order effect in the energy while it is a first order effect in the dipole moment.

The experimental quantities which will be given in the next section involve a knowledge of the polarizability tensor for at <u>most</u> a <u>pair</u> of interacting helium atoms. If, for a cylindrically

symmetric system such as this, we choose the z-axis to lie along the internuclear axis, the polarizability tensor is diagonal, and Eq. (1.24) becomes:

$$\alpha_{\parallel(\perp)} = \lim_{F_{\parallel(\perp)} \to 0} \frac{\mu_{\parallel(\perp)} - \mu^{(0)}_{\parallel(\perp)}}{F_{\parallel(\perp)}} , \qquad (1.25)$$

where the subscripts $\parallel$ and $\perp$ refer respectively to directions along and perpendicular to the internuclear axis. For the case of interest in this work, the term involving $\mu^{(0)}_{\parallel(\perp)}$ is absent because the field-free dipole moment of a homopolar diatom is zero.

In terms of the components given in Eq. (1.25), we define the mean polarizability of the diatom (internuclear separation R) and the anisotropy respectively as follows:

$$\alpha(R) = (\alpha_{\parallel}(R) + 2\alpha_{\perp}(R))/3 \qquad (1.26)$$

$$\beta(R) = \alpha_{\parallel}(R) - \alpha_{\perp}(R) . \qquad (1.27)$$

We further define the mean incremental polarizability by:

$$\Delta\alpha(R) = \alpha(R) - 2\alpha_0 , \qquad (1.28)$$

where α_0 is the polarizability of an isolated helium atom. Note that because of the symmetry, a knowledge of the quantities α and

β is equivalent to a knowledge of $\alpha_{\parallel}$ and $\alpha_{\perp}$. Hence, the measureable quantities discussed in the next sections provide information about the individual tensor elements.

We now turn to a consideration of the experiments which measure the polarizabilities $\Delta\alpha$ and β.

C. Pressure Dependence of the Dielectric Constant

When a rare gas sample is subjected to an external electric field, the value of the total field at a point in the sample is not equal to the applied field, because of additional fields arising from the (induced) dipole moments of the atoms. In the classical treatment of this problem, Lorentz in 1908 approximated the local field in terms of molecular polarizabilities and obtained the Clausius-Mosotti formula for the dielectric constant,[15]

$$\frac{\varepsilon-1}{\varepsilon+2} V_m = \tfrac{4}{3} \pi N \alpha_0 . \qquad (1.29)$$

Here, V_m is the molar volume, N is Avogadro's number, ε is the dielectric constant, and α_0 is the polarizability of an isolated atom. The left-hand side of this equation is known as the Clausius-Mosotti function.

Experimental determination of the Clausius-Mosotti function requires the measurement of the dielectric constant of the gas at a given temperature and pressure. This is done by measuring the ratio of the capacitance of a sample cell to that of an evacuated cell.

Early experiments by Uhlig, Kirkwood, and Keyes showed that the Clausius-Mosotti function exhibits a dependence on the gas density.[16] In an attempt to explain the discrepancy between Eq. (1.29) and experiment, Kirkwood noted that the following two assumptions which are made in the derivation of Eq. (1.29) are invalid:[17]

1. The polarizability is itself independent of density;
2. The dipole moment of an individual atoms does not change as the atom-pairs move through their various phases of thermal motion.

In reformulating the problem without these assumptions, Jansen and Mazur[18] and Buckingham and Pople[19] made use of classical statistical mechanics to relate the dielectric constant to the total induced dipole moment of the system,

$$\frac{\varepsilon-1}{\varepsilon+2} V_m = \frac{4\pi}{3} \lim_{F \to 0} \frac{\langle M(\underset{\sim}{F})\rangle}{F} , \qquad (1.30)$$

where the electric moment $\langle M(\underset{\sim}{F})\rangle$ is given by:

$$\langle M(\underset{\sim}{F})\rangle = \frac{\int [\underset{\sim}{M}(\tau,\underset{\sim}{F})\cdot\underset{\sim}{f}]\exp[-(U-\underset{\sim}{M}(\tau,\underset{\sim}{F})\cdot\underset{\sim}{F})/kT]d\tau}{\int \exp[-(U-\underset{\sim}{M}(\tau,\underset{\sim}{F})\cdot\underset{\sim}{F})/kT]d\tau} . \qquad (1.31)$$

Here, $\underset{\sim}{M}(\tau,\underset{\sim}{F})$ is the total electric moment of the system, when the molecular configuration is τ, and the applied field is $\underset{\sim}{F}$. It is assumed that $\underset{\sim}{M} = \sum_{k=1}^{N} \underset{\sim}{\mu}_k$, where $\underset{\sim}{\mu}_k$ is the dipole moment of the k-th

molecule, and N is the number of molecules in the specimen. In addition, in Eq. (1.31), $\underset{\sim}{f}$ is a unit vector in the direction of $\underset{\sim}{F}$, and U is the intermolecular potential.

By making a virial expansion of Eq. (1.30), and applying the results to S-state atoms, which have neither a permanent nor a collision-induced dipole moment, they obtained:

$$\frac{\varepsilon-1}{\varepsilon+2} V_m = A_\varepsilon + B_\varepsilon V_m^{-1} + C_\varepsilon V_m^{-2} + \ldots , \qquad (1.32)$$

where

$$A_\varepsilon = \frac{4\pi N}{3} \alpha_0 , \qquad (1.33)$$

and

$$B_\varepsilon = \frac{8\pi^2 N^2}{3} \int_0^\infty dR\, R^2\, \Delta\alpha(R) e^{-U(R)/kT} . \qquad (1.34)$$

In Eq. (1.34) the $\Delta\alpha(R)$ is the incremental mean polarizability of a pair of atoms with separation R defined in Eq. (1.28), k is Boltzmann's constant, and T is the absolute temperature. The coefficients A_ε and B_ε are called dielectric virial coefficients. McQuarrie and Levine extended these results to include the derivation of an expression for the third virial coefficient, C_ε, for the case of non-polar molecules with axial symmetry, such as H_2 or CO_2.[20]

The A_ε and B_ε were measured for several rare gases at room temperature by Orcutt and Cole.[1a] In addition, low temperature data ($T = 4°K$) for both ^3He and ^4He were taken by Kerr and Sherman.[1b] We present the results of these experiments in Table I.1.

The percent change in the Clausius-Mosotti function at room temperature is on the order of .1% for helium and 1% for argon for pressures near 2 atm. At low temperatures (near 4°K), the change is some 30% less than the room temperature change. Thus for pressures on the order of 1 atm. or less, it is very difficult to measure the pressure effects on the Clausius-Mosotti function. The helium data at 4°K of Kerr and Sherman exhibit a large amount of scatter. This is because the inherently small effect is compounded by the small amount of sample present in the cell at these pressures. The amount of scatter is reduced at higher pressures (~4 atm.), but then the validity of the virial expansion is doubtful.

Several workers have coupled the results of model polarizability calculations with classical statistical mechanics to obtain high temperature estimates of B_ε.[18,19,21] Some of the earliest of these calculations employed the point dipole approximation.[19] The simplicity of this approximation makes it particularly attractive, hence we now treat it in more detail. With this model, one assumes that the dipole moment induced in a given atom (denoted by 1) due to action of the external field $\underset{\sim}{F}$, and a second atom (denoted by 2), a distance R away, is given by:

Table I.1. Experimental first and second dielectric virial coefficients for several rare gases.[a]

System	T(°K)	A_ε(cm^3/mole)	B_ε(cm^6/$mole^2$)
He	322	0.519 ± 0.001	-0.06 ± 0.04
Ne	322	0.998 ± 0.001	-0.03 ± 0.10
Ar	322	4.142 ± 0.002	0.39 ± 0.20
Kr	322	6.267 ± 0.003	5.6 ± 0.30
^{3}He	4	0.516951 ± 0.000088	-0.030 ± 0.004
^{4}He	4	---	-0.023 ± ?

[a] The room temperature results are those of Orcutt and Cole, reference (1a); the low temperature results are those of Kerr and Sherman, reference (1b).

$$\underset{\sim}{\mu}_1 = \alpha_0(\underset{\sim}{F} + \underset{\sim}{F}_1) \ , \qquad (1.35)$$

where F_1 is the field at 1 due to the dipole at 2 . A similar expression is used for $\underset{\sim}{\mu}_2$. Using the usual expressions for the field due to a dipole, it is seen that $\underset{\sim}{\mu}_1$ can be written:

$$\underset{\sim}{\mu}_1 = \left(\frac{\alpha_0 F_x}{1+\alpha_0 R^{-3}} \ , \ \frac{\alpha_0 F_y}{1+\alpha_0 R^{-3}} \ , \ \frac{\alpha_0 F_z}{1-2\alpha_0 R^{-3}}\right) \ , \qquad (1.36)$$

where α_0 is the polarizability of an isolated atom. Differentiating Eq. (1.36) with respect to the components of $\underset{\sim}{F}$, and expanding the result for large R , yields:

$$\alpha_{\parallel}(R) = 2\alpha_0 + 4\alpha_0^2 R^{-3} + 8\alpha_0^3 R^{-6} + \ldots \ , \qquad (1.37)$$

and

$$\alpha_{\perp}(R) = 2\alpha_0 - 2\alpha_0^2 R^{-3} + 2\alpha_0^3 R^{-6} + \ldots . \qquad (1.38)$$

These results are exact through order 3 in R^{-1} . This was first shown by Jansen and Mazur, who used an exact quantum expansion of α in powers of R^{-1} .[18] This expression will be derived, and discussed in some detail in Chapter II.

The estimate of B_ε by Jansen and Mazur makes use of the Unsöld approximation.[18] In essence this represents an approximation to the

resolvent operator, R_0 , in the perturbation expansion, Eq. (1.21). This will also be discussed in more detail in Chapter II.

In the calculations of Jansen and Mazur, results were obtained for both helium and argon,[18] while Buckingham and Pople applied their method to more complicated molecules, including those in which a dipole moment in one molecule is induced by the permanent quadrupole moment of another molecule.[19,21]

Since the rare gas experiments had not been performed in 1955, the thrust of the theoretical work was to establish experimental feasibility. It must be remembered, however, that both of these early calculations used approximations to the polarizability which were meaningful in the long-range region only, thus the physical content of their theories was not complete.

Additional work on the classical statistical mechanical aspects of this problem was done by Hill in 1958,[42] and Ishihara and Hanks in 1962.[43]

Theoretical interest in the second dielectric virial coefficient was renewed by the accurate room temperature experiments of Orcutt and Cole in 1967. In particular, the reported sign change (from negative to positive) in B_ε as one goes through the series, (He, Ne, Ar) aroused considerable interest, because the early calculations predicted positive values for the entire series. This is understandable because a negative value for helium means that for some range of finite separations the polarizability of the dimer is sufficiently less

than the sum of the separated atom polarizabilities so that the integral which defines B_ε is negative. Thus since the early calculations used models which at best are valid approximations in the dispersion region only, effects in the overlap region could outweigh the positive long-range contribution to produce a negative value for B_ε.

Levine and McQuarrie in 1968 modeled the rare gas interaction using metallic spheres;[22] DuPré and McTague in 1969 used the $^3\Sigma_u^+$ state of H_2 to represent a pair of interacting rare gas atoms.[23] Both of these calculations indicated that short-range effects did produce changes relative to the long-range extrapolations in the polarizability curves, but neither result was directly applicable to the helium problem in particular.

Lim, Linder, and Kromhout in 1970 performed both coupled and uncoupled Hartree-Fock calculations on the polarizability of the He_2 dimer over the range of R from 1.0 to 6.5 a_0.[24] Their failure to produce a negative value for B_ε resulted from the failure of their short-range (negative) contribution to compensate for the positive contribution in the dispersion region. This gave rise to the possibility that previous estimates of the long-range effects had been too large.

For calculations in the low temperature regime, the expression for B_ε which includes the effects of quantum statistics has been recently derived by Bruch, and is given by:[25]

$$B_{\varepsilon} = \frac{8\pi^2 N^2}{3} \int_0^{\infty} dR\, R^2\, \Delta\alpha(R)\, g(R) \,. \qquad (1.39)$$

Here, $g(R)$ is the quantum-mechanical pair distribution function, which reflects the probability that two atoms will be found within a separation R of each other. The $g(R)$ is, of course, temperature dependent.

Formal differences between the classical and quantum treatments arise because the expression for $\langle M(\underset{\sim}{F})\rangle$ takes on a somewhat different form in quantum mechanics. For this case, $\langle M(\underset{\sim}{F})\rangle$ is expressed as:

$$\langle M(\underset{\sim}{F})\rangle = \frac{Tr[e^{-\beta H}(\underset{\sim}{M}(\tau,\underset{\sim}{F})\cdot\underset{\sim}{f})]}{Tr(e^{-\beta H})} \,, \qquad (1.40)$$

where $\beta = 1/kT$,

$$Tr(A) = \sum_{\ell} \langle \psi_{\ell}|A|\psi_{\ell}\rangle \,,$$

and ψ_{ℓ} denotes a possible state of the quantum mechanical system. Since H is now an operator, differentiation is accomplished via the formula:

$$\frac{\partial}{\partial F} e^{-\beta H} = -e^{-\beta H}\left[\int_0^{\beta} d\sigma\, e^{\sigma H} \frac{\partial H}{\partial F} e^{-\sigma H}\right] . \qquad (1.41)$$

Here H can be taken to be the Hamiltonian operator for the relative motion of a pair of atoms.

This summarizes the theoretical and experimental work on the dielectric virial coefficients up to the point at which the present work was begun.

One goal of the work reported in this thesis is to establish a definitive result for the polarizability in the long-range region. A second goal is to compute a more accurate value for the short-range effect via attainment of the Hartree-Fock limit, in that region, and to use these results to compute B_ε for both low and high temperatures.

During the time in which this work was in progress, results of additional polarizability calculations for He_2 have been reported by Buckingham and Watts,[26] and O'Brien et al.[27] Only the latter calculation resulted in a negative value for B_ε at room temperature. No attempt to match the low temperature results of Kerr and Sherman was made in either of these calculations.

D. The Kerr Effect

In the absence of external fields, the index of refraction of gaseous helium is isotropic. However, if one uses polarized light to measure the index of refraction, n, when the sample is placed in a static electric field, F, he finds that the value of n for the case in which the polarization vector of the light and the

applied field are parallel ($n_{\parallel}$) differs from that in which they are perpendicular ($n_{\perp}$) (field induced birefringence). This effect was discovered in glass by Kerr in 1875, and is known as the Kerr electro-optic effect.[28] For this phenomenon, the quantity of interest is the molecular Kerr constant, m_K which is defined as:[29]

$$m_K = \lim_{F \to 0} \frac{2(n_{\parallel} - n_{\perp})V_m}{27F^2} . \qquad (1.42)$$

In this equation, V_m again is the molar volume. More recently, Buckingham and Dunmur have measured m_K for a number of gases.[32]

In order to experimentally determine m_K, one measures the field-induced birefringence for a given pressure and temperature, as a function of electric field strength. Extrapolation of the ratio, $2(n_{\parallel} - n_{\perp})V_m/27F^2$ to zero field then yields the value for m_K.

Not surprisingly, it is found that the molecular Kerr constant, like the dielectric constant, exhibits a pressure dependence. For gases at low density, Buckingham and Pople related m_K to molecular polarizabilities.[30] Buckingham,[31] and later Buckingham and Dunmur[32] discussed the corresponding treatment for gases at higher densities, by making a virial expansion similar to that used in the dielectric constant analysis. In this last paper, it was shown that for light of low frequency (much less than the first excitation energy of the atoms), the first two terms in the density expansion of m_K for a gas of atoms are:

$$m_K = A_K + B_K \rho \ , \tag{1.43}$$

where

$$A_K = \frac{4\pi N\gamma}{81} \ , \tag{1.44}$$

and

$$B_K = \frac{8\pi^2 N^2}{405kT} \int_0^\infty dR \ R^2 (\beta(R))^2 \ e^{-U(R)/kT} \ . \tag{1.45}$$

Here the ρ is the density, $\beta(R)$ is the anisotropy in the dipole polarizability for a pair of interacting atoms at a separation R, and γ is the first nonvanishing hyperpolarizability of an isolated atom. This is a high temperature result, because the classical limit of the pair distribution function is used.

For the quantum case, Bruch has shown that replacing the factor $e^{-U(R)/kT}$ with $g(R)$ yields an upper bound to the value of B_K.[25]

Differences between the quantum mechanical and classical mechanical treatments of the Kerr effect arise because of the different form for the ensemble average in the two realms, as was observed in the corresponding treatments of the dielectric virial coefficient. The situation is even more complicated in this case than it was in the dielectric virial case, because of the need to take second derivatives, by applying Eq. (1.41) a second time.

Experimental values for A_K and B_K for several rare gases at room temperature are given in reference (32), and are listed in Table I.2. Results for B_K for helium gas are conspicuously absent from this table. This is because the pressure effect on m_K at room temperature is too small to be detected. Since low temperature experiments have not been performed as yet, it is not clear whether or not a decrease in temperature might render the effect observable. One purpose of this thesis is to estimate the magnitude of m_K at low temperatures.

There are two additional points regarding the above equations worth mentioning:

1. The field strengths used in these experiments are larger than those used in the dielectric constant experiments, hence nonlinear polarization effects (via γ) are included.
2. In the derivation of Eqs. (1.43)-(1.45) the density dependence of γ was ignored, so that the higher virial coefficients do not involve an integral over $\gamma(R)$, in this approximation.

Note that the expressions for B_ε (Eq. (1.34)) and B_K are similar, except that the respective integrands involve different functions of the polarizability components $\alpha_\parallel$ and $\alpha_\perp$. Thus, regarding the polarizability tensor, the dielectric virial and the Kerr virial measurements are complementary.

Table I.2. Experimental first and second Kerr virial coefficients for several rare gases.[a]

System	T(°K)	10^{14} A_K(esu)	10^{12} B_K(esu)
He	296	0.25 ± 0.02	---
Ne	296	0.48 ± 0.04	---
Ar	296	5.5 ± 0.4	4.1 ± 0.6
Kr	296	13.0 ± 1.0	16.0 ± 14.0
Xe	296	36.0 ± 1.0	65.0 ± 22.0

[a] Results are those of reference (2).

E. Collision Induced Raman Scattering

The change in the polarizability during a collision of a pair of rare gas atoms gives rise to a light scattering spectrum, which is called the collision induced Raman spectrum.

Experimental detection of such scattering was reported by Crawford, Welsh, and Locke[33] as early as 1949 for O_2 and N_2 gases. McTague and Birnbaum[34] in 1968, and Gersten, Slusher, and Surko[35] in 1970 reported similar observations in argon and krypton. Pike and Vaughan[36] have recently measured the light scattering spectrum of both liquid and gaseous helium, the latter at 4.2°K.

The expression which relates the intensity of the scattered light, $I(\omega)$, to the experimental parameters, has been derived and discussed by several workers, and is given by:[3,34,37,81]

$$I(\omega) = \frac{K}{2\pi} \int_{-\infty}^{\infty} F(t) e^{-i\omega t} \, dt \, . \qquad (1.46)$$

Here,

$$K = V^2 \rho^2 k_i^4 I_i / (32\pi^2 \varepsilon_p^2 R_0^2) \, , \qquad (1.47)$$

where, V is the scattering volume, ρ the number density of the sample, k_i the propagation vector of the incident beam, I_i its intensity, ε_p is the permittivity of the sample, and R_0 is the distance from the detector to an arbitrary point in the sample

(assumed to be much greater than the sample dimensions). The expression for $F(t)$ is, for light scattered at right angles,

$$F(t) = \langle \Delta\alpha(t=0)\cdot\Delta\alpha(t)\rangle (\underset{\sim}{n}_i\cdot\underset{\sim}{n}_f)^2 + \langle \beta(t=0)\beta(t)(\tfrac{1}{2}(3\cos^2\theta(t)-1))\rangle \{45^{-1}(3 + (\underset{\sim}{n}_i\cdot\underset{\sim}{n}_f)^2)\} \quad (1.48)$$

In this equation, $\underset{\sim}{n}_i$ and $\underset{\sim}{n}_f$ are unit polarization vectors of the incident and scattered beams respectively; $\theta(t)$ is the angle between the internuclear vector of a diatom at time t and an axis defined by its vector at time $t=0$; $\Delta\alpha(t)$ and $\beta(t)$ are respectively the mean incremental polarizability and anisotropy of the diatom at time t , while the brackets denote an ensemble average.

Experimentally, one often measures depolarization ratios which may be defined in a variety of ways, which depend on the geometry of the experiment. In the low temperature work of Pike and Vaughan, light from an argon ion laser was passed horizontally through a cell containing gaseous helium.[36] The incident light was introduced in either horizontal (H) or vertical (V) polarizations, and the intensity of the light scattered at 90° was analysed in both the H and V polarizations. Their data for helium gas at 0.96 atm and 4.22K is given in Table I.3 for a frequency shift of 21 cm^{-1} from the exciting line, using a spectrometer with an instrumental linewidth of 5 cm^{-1} .

Table I.3. Experimental depolarization ratios at a shift of 30K in helium liquid and gas.[a,b]

Depolarization Ratio	Liquid	Gas
V-V/V-H	1.52 ± 0.2	1.33 ± 0.2
H-V/H-H	1.1 ± 0.2	1.0 ± 0.2
V-V/H-V	1.29 ± 0.1	1.39 ± 0.2

[a] Reference (36).

[b] Gas experiments were done at 4.22°K at a pressure of 0.96 atm. Liquid experiments were done at 4.22°K and 1.15 atm.

Eqs. (1.46) and (1.48) give the following expressions for the depolarization ratios measured by Pike and Vaughan.

$$V\text{-}V/V\text{-}H = [A(\omega) + \tfrac{4}{45}B(\omega)]/[\tfrac{3}{45}B(\omega)] , \qquad (1.49)$$

$$H\text{-}V/H\text{-}H = 1 , \qquad (1.50)$$

$$V\text{-}V/H\text{-}V = V\text{-}V/V\text{-}H . \qquad (1.51)$$

Here, the Fourier transforms $A(\omega)$ and $B(\omega)$ are defined by:

$$A(\omega) = \int_{-\infty}^{\infty} <\Delta\alpha(0)\Delta\alpha(t)>e^{-i\omega t}\, dt , \qquad (1.52)$$

and

$$B(\omega) = \int_{-\infty}^{\infty} <\beta(0)\beta(t)P_2(\cos\theta(t))>e^{-i\omega t}\, dt . \qquad (1.53)$$

Here, $P_2(x) = \frac{1}{2}(3x^2-1)$ is the second Legendre polynomial. We see that the data in Table I.3 are consistent with these formulas, and, furthermore, imply that $A(\omega) << B(\omega)$ since in this limit

$$V\text{-}V/V\text{-}H \doteq \tfrac{4}{3} . \qquad (1.54)$$

Although the accuracy of the reported data is not sufficient to distinguish the contribution of $A(\omega)$ to the depolarization ratios, we shall estimate its effect computationally in order to verify that it is not observable in the present experiments and to establish its magnitude for use in planning future experiments. To avoid dealing with time-dependent correlation functions, which are difficult to compute, we shall instead deal with integrated intensities, or the zeroth frequency moments of Eqs. (1.52) and (1.53)

$$\bar{A} = \frac{1}{2\pi}\int_0^\infty A(\omega)\, d\omega = \langle \Delta\alpha(0)^2 \rangle , \tag{1.55}$$

and

$$\bar{B} = \frac{1}{2\pi}\int_0^\infty B(\omega)\, d\omega = \langle \beta(0)^2 \rangle . \tag{1.56}$$

We shall calculate the depolarization ratio corresponding to Eq. (1.49) and defined by

$$\bar{D} = [\bar{A} + \tfrac{4}{45}\bar{B}]/[\tfrac{3}{45}\bar{B}] , \tag{1.57}$$

$$= \tfrac{4}{3} + 15\bar{A}/\bar{B} . \tag{1.58}$$

Thus the interesting part of $\bar{D}$ involves averages over both the incremental mean polarizability $\Delta\alpha$ and the anisotropy β. Higher moments of (1.52) and (1.53) lead to other experimental parameters

such as linewidths, and approximations to line shapes. These extensions, however, involve more than the simple integrals of Eqs. (1.55) and (1.56).

Semi-empirical work by Levine and Birnbaum on the collision induced Raman scattering of rare gases has been directed toward obtaining a model for $\beta(R)$. Using a modification of the point dipole anisotropy,[37]

$$\beta(R) = 6\alpha_0^2 R^{-3} + BR^{-p} , \qquad (1.59)$$

they derived high temperature, two-body expressions for the first two moments of the spectral functions, $A(\omega)$ and $B(\omega)$, and obtained values for p and B by comparison to the experimental results for these moments, for argon, krypton, and xenon. Typical values so obtained for argon are on the order of 10 and -1.0×10^5 $\mathring{A}^{13}$ respectively. This is then interpreted to mean that short-range effects as represented by the Br^{-p} term are indeed significant.

Recently, Gelbart has given a quantum mechanical treatment of the depolarization and inelastic scattering of light by gases and liquids composed of atoms and/or isotropically polarizable molecules.[38] Effects due to collisions of more than two particles were also included.

F. Perspective

Apart from stricly formal treatises, prior theoretical work on estimating the properties of interest has been restricted to the

high temperature regime, and have involved the coupling of polarizabilities computed at different levels of approximation with classical averaging procedures. The various polarizability models which were used and the conclusions of their respective calculations are discussed in some detail in subsequent sections; however, for purposes of understanding the motivation for the present work, we note at this point that the most successful of these model approaches employed the Hartree-Fock approximation.

The meaningful use of any model depends on the existence of well-defined, reproducible model limits. In the case of the Hartree-Fock approximation, this requires assurances that in a given calculation the Hartree-Fock limit (the limit of zero basis set error in the Hartree-Fock-Roothaan scheme) has been reached.[39] This is a particularly important point when one considers the history of He_2 pair potential calculations.

In an early Hartree-Fock calculation on the ground state potential energy curve of He_2, Ransil reported that the dispersion minimum was observed.[40] This minimum was later shown, by further calculations, to be spurious, and was attributed to an idiosyncracy in the basis set which Ransil used.[41] Thus the validity of any conclusions drawn from the use of the Hartree-Fock-Roothaan scheme depends directly on the closeness of the calculation to the Hartree-Fock limit.

None of the Hartree-Fock calculations of the polarizability which have been thus far reported, purport to represent the Hartree-Fock limit.[24,26,27] It was our intent in carrying out the present work to remove this uncertainty and establish the need or lack thereof of more accurate calculations, which include electron correlation effects.

It goes without saying that even if a certain model duplicates experiment at one temperature, it does not necessarily follow that the same model will be equally useful at another temperature for which the physics of the problem might be different. This means that a given polarizability result must be tested at both high temperatures using classical statistical mechanics and low temperatures using quantum statistical mechanics if one wishes to make claims regarding the usefulness of the model from which the polarizability resulted. In addition, isotopic effects may be introduced in the low temperature region so that the ability of a given model to produce such effects must also be guaranteed.

Since no low temperature work had been carried out up to now, previous workers did not subject their polarizability results to these important tests. This is, of course, insignificant when considering models which make no claim for general usefulness.

The quantum statistical methods seem to be on somewhat firmer ground than the polarizability calculations, although they have never been used for anything other than equation of state applications.

It was the intent of the work reported in this thesis to couple the Hartree-Fock limit polarizabilities to quantum statistical mechanical results for the two helium isotopes (^{3}He and ^{4}He) in order to duplicate the results of both low and high temperature experiments. This was done with the intent of establishing a basis on which one can judge whether or not he is justified in using the same approximations in the calculation of the polarizabilities of other systems or in the calculation of different but similar molecular properties.

CHAPTER II

POLARIZABILITIES OF DIATOMIC MOLECULES IN THE LIMIT OF LARGE INTERNUCLEAR SEPARATIONS

Early estimates of the dielectric virial coefficient employed extrapolations of approximate polarizabilities from the dispersion region to the regions of smaller R.[18,19] One such approximation, the point dipole model, has already been discussed. It is apparent that if the leading contribution to the point dipole incremental mean polarizability (see Eqs. (1.37) and (1.38)),

$$\Delta\alpha(R) = 4\alpha_0^3 R^{-6} + \ldots , \tag{2.1}$$

is used for all values of R to compute a value for B_ε for a gas of ground state atoms, a positive result is obtained, in contrast to the observed negative result for helium. It is natural to ask whether this discrepancy is due to the inaccuracy of the point dipole approximation itself, or due to the use of a long-range result for all values of R.

In this chapter, we show that the point dipole model gives the leading asymptotic behavior of $\Delta\alpha$, although the magnitude of the leading multipole coefficient is too small by about a factor of four.

We derive the long-range multipole expansion of the diatomic polarizability in Section A, illustrate its connection to the point dipole model in Section B, and discuss the calculation of the leading terms for the H_2, HeH, and He_2 systems in Section C. The results of the first two sections were first obtained by Jansen and Mazur.[18]

A. The Long-Range Multipole Expansion of $\alpha(R)$

A rigorous treatment of the pair polarizability of two atoms in the long-range region can be carried out using Rayleigh-Schrödinger perturbation theory. In the long-range region, the electron clouds of the two atoms do not overlap, and it is not necessary to require the diatomic wavefunction to satisfy the Pauli Principle for electrons centered on different atoms. This greatly simplifies the calculation of the polarizability.

Let us consider two S-state atoms, a and b, separated by a distance R. The starting point of the development is the general expression for the polarizability, Eq. (1.21),

$$\underset{\sim}{\alpha} = -2\langle\Psi_0|\hat{\underset{\sim}{\mu}}\, R_0\, \hat{\underset{\sim}{\mu}}|\Psi_0\rangle \ . \tag{2.2}$$

In this expression, Ψ_0 is the wavefunction for the diatom in the absence of the electric field, R_0 is the reduced resolvent for the diatom, symbolically,

$$R_0 = (E_0 - H_0)^{-1} , \tag{2.3}$$

where H_0 is the diatomic Hamiltonian and E_0 is the ground state energy,

$$(H_0 - E_0)\Psi_0 = 0 . \tag{2.4}$$

The $\hat{\underset{\sim}{\mu}}$ is the total dipole moment operator, which is a sum of the dipole operators for atoms a and b ,

$$\hat{\underset{\sim}{\mu}} = \hat{\underset{\sim}{\mu}}^a + \hat{\underset{\sim}{\mu}}^b . \tag{2.5}$$

In the following derivation, we shall consider separately the cases that the external field is along the internuclear axis (designated the z-axis) or perpendicular to it. For simplicity of notation, the expansions of Eqs. (1.18) and (1.21) shall be written as scalar expansions with the understanding that the resulting polarizability expressions apply for the respective components.

We now wish to obtain an expansion for α in inverse powers of the separation R. The R-dependence in α occurs both in the wavefunction Ψ_0 and the resolvent R_0. We proceed by subdividing the diatomic Hamiltonian according to

$$H_0 = h_0 + V , \tag{2.6}$$

where h_0 is the sum of the atomic Hamiltonians for a and b, and V represents the Coulombic interaction between a and b. Similarly, for the energy, we have

$$E_0 = \varepsilon_0 + \Delta E \ . \tag{2.7}$$

To obtain the multipole expansion of Ψ_0, we first resolve the Schrodinger Equation (2.4) into perturbation equations based on Eq. (2.6),

$$\Psi_0 = \phi_0 + \Psi_0^{(1)} + \Psi_0^{(2)} + \ldots \ , \tag{2.8}$$

where

$$\Delta E = E^{(1)} + E^{(2)} + \ldots \ , \tag{2.9}$$

$$(h_0 - \varepsilon_0)\phi_0 = 0 \ , \tag{2.10}$$

$$(h_0 - \varepsilon_0)\Psi_0^{(1)} + (V - E^{(1)})\phi_0 = 0 \ , \tag{2.11}$$

$$(h_0 - \varepsilon_0)\Psi_0^{(2)} + (V - E^{(1)})\Psi_0^{(1)} - E^{(2)}\ \phi_0 = 0 \ , \tag{2.12}$$

with the full normalization conditions,

$$\langle\phi_0|\Psi_0^{(1)}\rangle = 0 , \tag{2.13}$$

$$\langle\phi_0|\Psi_0^{(2)}\rangle = \langle\Psi_0^{(2)}|\phi_0\rangle = -\tfrac{1}{2}\langle\Psi_0^{(1)}|\Psi_0^{(1)}\rangle . \tag{2.14}$$

The solution of these perturbation equations is well-known. The ϕ_0 is a simple product of atomic wavefunctions for atoms a and b ,

$$\phi_0 = a_0 b_0 . \tag{2.15}$$

Introducing the reduced resolvent for h_0 ,

$$r_0 = (\varepsilon_0 - h_0)^{-1} , \tag{2.16}$$

we have

$$\Psi_0^{(1)} = r_0(V - E^{(1)})\phi_0 , \tag{2.17}$$

and

$$\Psi_0^{(2)} = r_0(V - E^{(1)})\Psi_0^{(1)} - \tfrac{1}{2}\phi_0\langle\Psi_0^{(1)}|\Psi_0^{(1)}\rangle . \tag{2.18}$$

The R-dependence is still implicit in these equations. However, both V and ΔE have well-known multipole expansions in inverse

powers of R.[82] For our purposes we need consider only the leading terms,

$$V = \frac{V_3}{R^3} + \ldots , \tag{2.19}$$

and

$$E^{(1)} = 0 , \tag{2.20}$$

$$E^{(2)} = -\frac{C_6}{R^6} + \ldots ; \tag{2.21}$$

where V_3 is the dipole-dipole interaction operator,

$$V_3 = \hat{\mu}_x^a \hat{\mu}_x^b + \hat{\mu}_y^a \hat{\mu}_y^b - 2\hat{\mu}_z^a \hat{\mu}_z^b , \tag{2.22}$$

and

$$C_6 = -\langle\phi_0|V_3 \, r_0 \, V_3|\phi_0\rangle . \tag{2.23}$$

Then, introducing the multipole expansions into Eqs. (2.17) and (2.18) and collecting terms,

$$\Psi_0 = \phi_0 + R^{-3} \, r_0 V_3 \phi_0 + R^{-6}[r_0 V_3 r_0 V_3 - \tfrac{1}{2}\langle\phi_0|V_3 r_0^2 V_3|\phi_0\rangle]\phi_0 + \ldots . \tag{2.24}$$

Although we have not exhibited all the terms in Ψ_0 , we have shown those terms which contribute to α through order R^{-6} .

Finally, the R-dependence of the resolvent R_0 is obtained by invoking the operator identity,

$$(A-B)^{-1} = A^{-1} + A^{-1} B(A-B)^{-1} . \tag{2.25}$$

for $A = \epsilon_0 - h_0$ and $B = V - \Delta E$. Thus,

$$R_0 = r_0 + r_0(V - \Delta E)R_0 . \tag{2.26}$$

Iterating this equation we obtain

$$R_0 = r_0 + r_0(V - \Delta E)r_0 + r_0(V - \Delta E)r_0(V - \Delta E)r_0 + \ldots , \tag{2.27}$$

and then introducing the multipole expansion,

$$R_0 = r_0 + R^{-3}\, r_0V_3r_0 + R^{-6}[-C_6r_0^2 + r_0V_3r_0V_3r_0] + \ldots . \tag{2.28}$$

Again we have exhibited only those terms which contribute to α through order R^{-6} .

The multipole expansion of α may now be obtained by substituting the expansion for Ψ_0 , Eq. (2.24), and for R_0 , Eq. (2.28) into Eq. (2.2). When this is done, we obtain

$$\alpha = 2\alpha_0 + \frac{A_3}{R^3} + \frac{A_6}{R^6} + \ldots , \tag{2.29}$$

where

$$2\alpha_0 = -2\langle\phi_0|\hat{\mu}\, r_0\, \hat{\mu}|\phi_0\rangle , \tag{2.30}$$

$$A_3 = -4\langle\phi_0|V_3\, r_0\, \hat{\mu}\, r_0\, \hat{\mu}|\phi_0\rangle - 2\langle\phi_0|\hat{\mu}\, r_0\, V_3\, r_0\, \hat{\mu}|\phi_0\rangle , \tag{2.31}$$

and

$$\begin{aligned} A_6 = {} & -4\langle\phi_0|V_3\, r_0\, V_3\, r_0\, \hat{\mu}\, r_0\, \hat{\mu}|\phi_0\rangle - 4\langle\phi_0|V_3\, r_0\, \hat{\mu}\, r_0\, V_3\, r_0\, \hat{\mu}|\phi_0\rangle \\ & - 2\langle\phi_0|\hat{\mu}\, r_0\, V_3\, r_0\, V_3\, r_0\, \hat{\mu}|\phi_0\rangle - 2\langle\phi_0|V_3\, r_0\, \hat{\mu}\, r_0\, \hat{\mu}\, r_0\, V_3|\phi_0\rangle \\ & + 2\langle\phi_0|V_3\, r_0^2\, V_3|\phi_0\rangle\langle\phi_0|\hat{\mu}\, r_0\, \hat{\mu}|\phi_0\rangle \\ & + 2\langle\phi_0|V_3\, r_0\, V_3|\phi_0\rangle\langle\phi_0|\hat{\mu}\, r_0^2\, \hat{\mu}|\phi_0\rangle , \end{aligned} \tag{2.32}$$

where these expressions apply for the parallel component of α when $\hat{\mu} = \hat{\mu}_z$, and the perpendicular when $\hat{\mu} = \hat{\mu}_x$.

We note that the individual components of $\underset{\sim}{\alpha}$ involve terms which decrease as R^{-3}. In the next section, however, we show that

$$A_3^{\parallel} = -2A_3^{\perp} . \tag{2.33}$$

Thus, the incremental mean polarizability has the asymptotic behavior,

$$\Delta\alpha = \tfrac{1}{3}(\alpha_{\parallel} + 2\alpha_{\perp}) = 2\alpha_0 + \frac{\Delta A_6}{R^6} + \ldots , \tag{2.34}$$

where

$$\Delta A_6 = \tfrac{1}{3}(A_6^{\parallel} + 2A_6^{\perp}) . \tag{2.35}$$

The terms of α which decrease as R^{-3} yield the leading terms in the asymptotic expansion of the anisotropy

$$\beta = \alpha_{\parallel} - \alpha_{\perp} = -\frac{3A_3^{\perp}}{R^3} + \frac{(A_6^{\parallel} - A_6^{\perp})}{R^6} + \ldots . \tag{2.36}$$

For reference in later sections of this chapter, we note that the reduced resolvent operator, r_0, can be expanded in terms of the excited eigenstates of $h_0 = h_0^a + h_0^b$:

$$r_0 = \sum_K{}' \frac{|a_K b_0\rangle\langle a_K b_0|}{\varepsilon_K^a - \varepsilon_0^a} + \sum_L{}' \frac{|a_0 b_L\rangle\langle a_0 b_L|}{\varepsilon_L^b - \varepsilon_0^b} + \sum_K{}' \sum_L{}' \frac{|a_K b_L\rangle\langle a_K b_L|}{\varepsilon_K^a - \varepsilon_0^a + \varepsilon_L^b - \varepsilon_0^b} . \tag{2.37}$$

where a_K and b_L represent excited states on the respective centers and the prime means that the terms $K = L = 0$ are omitted from the sums.

B. Connection between the Point Dipole Model and the Quantum Mechanical Multipole Expansion of the Polarizability

It is instructive to relate the exact long-range behavior of the polarizability to the predictions of the point dipole model. This is the object of the present section.

Before treating the problem mathematically, we can make certain qualitative statements regarding what to expect. Since the point dipole model ignores the details of atomic structure, whereas the quantum mechanical treatment correlates interatomic electronic motions, we should expect differences in those terms which are present in both the field-free and field-dependent quantum multipole expansions of the interaction energy. On the other hand, since the point dipole model reflects modifications in the local field at a given atom due to the field-induced dipole moment in the other atom we might expect some degree of similarity between the terms of the two expansions which do not appear in the field-free quantum expansion, and represent therefore field-induced terms in the quantum expression.

The manifestation of the first of these points will be clearly seen when we consider the actual results of the calculation of the long-range coefficients for specific systems. The second point is immediately accessible, and will now be illustrated by showing that the A_3 term which results from the point dipole model is identical to that which results from the exact quantum mechanical multipole expansion. For simplicity, we consider the $A_3^{\parallel}$ term only. Since

the components of the dipole moment operator behave like the corresponding components of the vector $\underset{\sim}{r}$, and since $\hat{\mu}_z = \hat{\mu}_z^a + \hat{\mu}_z^b$, we can write Eq. (2.31) as:

$$A_3^{\parallel} = -2[-4\langle\phi_0|\hat{\mu}_z^a\,\hat{\mu}_z^b\,r_0\,\hat{\mu}_z\,r_0\,\hat{\mu}_z|\phi_0\rangle - 2\langle\phi_0|\hat{\mu}_z\,r_0\,\hat{\mu}_z^a\,\hat{\mu}_z^b\,r_0\,\hat{\mu}_z|\phi_0\rangle]$$

$$= [T1 + T2] \,. \tag{2.38}$$

Further, only those parts of r_0 which are of p-type symmetry (behave like Y_{10} spherical harmonics) can lead to nonzero contributions to $A_3^{\parallel}$. Thus, using superscripts to label the respective centers , subscripts to label different atomic states of a given symmetry, $\Delta\varepsilon_K^a$ to denote $\varepsilon_0^a - \varepsilon_K^a$, and writing $\phi_0 = a_0\,b_0$, we have:

$$T1 = 8 \sum_{K,L,M}{}' \frac{\langle a_0 b_0|\hat{\mu}_z^a\hat{\mu}_z^b|p_K^a p_L^b\rangle\langle p_K^a|\hat{\mu}_z^a|a_0\rangle\langle p_L^b|p_M^b\rangle\langle p_M^b|\hat{\mu}_z^b|b_0\rangle}{(\Delta\varepsilon_K^a + \Delta\varepsilon_L^b)\Delta\varepsilon_M^b} \tag{2.39}$$

$$+ 8 \sum_{K,L,M}{}' \frac{\langle a_0 b_0|\hat{\mu}_z^a\hat{\mu}_z^b|p_K^a p_L^b\rangle\langle p_L^b|\hat{\mu}_z^b|b_0\rangle\langle p_K^a|p_M^a\rangle\langle p_M^a|\hat{\mu}_z^a|a_0\rangle}{(\Delta\varepsilon_K^a + \Delta\varepsilon_L^b)\Delta\varepsilon_M^a}$$

Because of the orthonormality of the atomic states, this last equation can be factored, using the identity

$$(ab)^{-1} = [(a+b)a]^{-1} + [(a+b)b]^{-1} \,,$$

$$T1 = 8 \sum_{K,L}{}' \left[\frac{\langle a_0|\hat{\mu}_z^a|p_K^a\rangle^2 \langle b_0|\hat{\mu}_z^b|p_L^b\rangle^2}{(\Delta\varepsilon_K^a + \Delta\varepsilon_L^b)\Delta\varepsilon_L^b} + \frac{\langle a_0|\hat{\mu}_z^a|p_K^a\rangle^2 \langle b_0|\hat{\mu}_z^b|p_L^b\rangle^2}{(\Delta\varepsilon_K^a + \Delta\varepsilon_L^b)\Delta\varepsilon_K^a} \right] , \quad (2.40)$$

$$= 8 \left[\sum_K{}' \frac{\langle a_0|\hat{\mu}_z^a|p_K^a\rangle^2}{\Delta\varepsilon_K^a} \right] \left[\sum_L{}' \frac{\langle b_0|\hat{\mu}_z^b|p_L^b\rangle^2}{\Delta\varepsilon_L^b} \right] , \quad (2.41)$$

$$= 2\alpha_0^a \alpha_0^b . \quad (2.42)$$

Similarly,

$$T2 = 4 \sum_{K,L} \frac{\langle a_0|\hat{\mu}_z^a|p_K^a\rangle^2 \langle p_L^b|\hat{\mu}_z^b|b_0\rangle^2}{\Delta\varepsilon_K^a \, \Delta\varepsilon_L^b} + 4 \sum_{K,L} \frac{\langle b_0|\hat{\mu}_z^b|p_L^b\rangle^2 \langle p_K^a|\hat{\mu}_z^a|a_0\rangle^2}{\Delta\varepsilon_L^b \, \Delta\varepsilon_K^a} ,$$

(2.42)

$$= 2\alpha_0^a \alpha_0^b . \quad (2.43)$$

Thus,

$$A_3^{\parallel} = 4\alpha_0^a \alpha_0^b , \quad (2.44)$$

which is identical to the general point dipole result for a heteropolar diatom.

In a similar fashion, using the symmetry reduction procedure discussed in the next section and described in Appendix A, one can show that,

$$A_3^{\perp} = -2\alpha_0^a \alpha_0^b \ . \qquad (2.45)$$

Thus, as was first shown by Jansen and Mazur, the leading term in the point dipole expansion of the polarizability is identical to that obtained from the exact quantum mechanical multipole expansion.[18] A significant implication of this is that the leading contribution to the mean incremental polarizability for a diatom goes as R^{-6} , since $A_3^{\parallel} + 2A_3^{\perp} = 0$.

It does not appear possible to obtain a simple relation between the quantum mechanical and point dipole expressions for the higher multipole coefficients, however. The accurate numerical evaluation of the terms $A_6^{\parallel}$ and $A_6^{\perp}$ is described in the next section.

C. Accurate Long-Range Polarizability Calculations for the H_2, HeH, and He_2 Systems

The initial application of the equations of Section A to the calculation of the long-range contribution to diatomic polarizabilities were made by Jansen and Mazur in 1955.[18] In particular, they used the Unsöld approximation to simplify the use of Eq. (2.32), and computed a value of the second dielectric virial coefficient for helium gas. The Unsöld approximation involves the replacement of the energy denominators in r_0 (see Eq. (2.37)) with some average value, $\Delta\varepsilon$, so that r_0 can be written:

$$r_0 = \frac{1}{\Delta\varepsilon} \sum' |\phi_K><\phi_K| , \tag{2.46}$$

and using the completeness of the states ϕ_K ,

$$r_0 = \frac{1}{\Delta\varepsilon} (1 - |\phi_0><\phi_0|) . \tag{2.47}$$

With this approximation, one avoids having to compute the spectrum of atomic excited states.

The results of the Unsöld approximation calculations for helium yield values of $A_6^{\parallel}$ and $A_6^{\perp}$ of 7.59 α_0^3 and 3.94 α_0^3 respectively; here, α_0 is the helium atom polarizability.

Thus, as far as approximate calculations in the dispersion region are concerned both the point dipole and the Unsold approximation yield positive values for B_ε for helium gas. However the possibility of obtaining a negative value via the extrapolation of an <u>accurate</u> dispersion polarizability has not been completely eliminated. To test this, we have computed A_6 as given by Eq. (2.32).

The only accurate calculation of A_6 prior to the present one was that of Tulub <u>et al</u>. for H_2, in 1970.[44] In their work, they used a multipole expansion of the interaction energy of a pair of hydrogen atoms in an electric field, and averaged this energy over all orientations of the internuclear axis with respect to the field. They then solved the resulting perturbation equations variationally. A drawback of this procedure is that only the mean value of A_6 is

obtained; hence strictly speaking, no accurate detailed knowledge of the A_6 tensor was available at the time the present work was performed, even for a system as simple as H_2!

As in the Unsöld approximation, Eq. (2.32) serves as the basis for an accurate calculation in the long-range region. Ignoring, for the moment the question of how r_0 is to be obtained, we note that Eq. (2.32) is not in a computationally convenient form because the various terms contain all the Cartesian components of $\underset{\sim}{\mu}$ in V_3. Eq. (2.32), however, can be simplified so as to yield an expression which involves only the z-components of the various operators. This symmetry reduction consists of a straightforward but tedious application of the Wigner-Eckardt theorem[45] to the terms of the equation which results when Eqs. (2.22) and (2.37) are introduced into Eq. (2.32). A discussion of this simplification is given in Appendix A.

The expression for the components of A_6 which results can be written:

$$\begin{aligned} A_6 = -(1 + P_{ab})[&M_1\langle Vr_0\ Vr_0\ \mu\ r_0\ \mu\rangle_S + M_2\langle Vr_0\ Vr_0\ \mu\ r_0\ \mu\rangle_D \\ &+ M_3\langle Vr_0\ \mu\ r_0 V\ r_0\ \mu\rangle_S + M_4\langle Vr_0\ \mu\ r_0 V\ r_0\ \mu\rangle_D \\ &+ M_5\langle \mu\ r_0\ Vr_0\ Vr_0\ \mu\rangle_S + M_6\langle \mu\ r_0\ Vr_0\ Vr_0\ \mu\rangle_D \\ &+ M_7\langle Vr_0\ \mu\ r_0\ \mu\ r_0 V\rangle_S + M_8\langle Vr_0\ \mu\ r_0\ \mu\ r_0 V\rangle_D \\ &+ M_9\langle \mu\ r_0\ \mu\rangle\langle Vr_0^2\ V\rangle + M_{10}\langle \mu\ r_0^2\ \mu\rangle\langle Vr_0\ V\rangle] \ . \end{aligned} \tag{2.48}$$

In this equation, $V = \mu_z^a \mu_z^b$, $\mu = \mu_z^a$, P_{ab} is the permutation operator for the two centers, and the brackets denote an expectation value with respect to ϕ_0. The coefficients M_k are given in Table II.1. The subscripts S and D are explained below.

There are several points worth noting about Eq. (2.48). First, its use requires only atomic information as input. That is, r_0 refers to the reduced resolvent operator for the Hamiltonian, $h_0 = h_0^a + h_0^b$, so that the excited states which enter the spectral expansion of r_0, Eq. (2.37), are products of atomic eigenstates on the respective centers. This is a significant simplification as far as computations are concerned, because atomic calculations are much easier to carry out than the corresponding calculations on the diatomic systems. Second, because of the orthonormality of the atomic states, only certain symmetries enter a given r_0 so as to yield nonzero contributions to A_6. The particular symmetries required in a given r_0 depend on its position in the matrix element under consideration. As an example, consider the first term in the above expansion, and assume that the resolvents are numbered from left to right. Since $V = \mu_z^a \mu_z^b$, the only nonzero contributions from the first r_0 are due to terms which denote states of p-symmetry on each center. Similarly, the second resolvent can only involve those states which are represented by products of excited S or D functions on each center. Lastly, the third resolvent involves only those products which consist of p-states on center a and b_0 on

center b. This last statement is appropriately modified under the action of P_{ab} by using excited p-states on center b, and a_0 on center a.

The above points allow for a notational simplification which unambiguously defines the states entering each resolvent. This consists of explicitly specifying the symmetry (S or D) of the middle resolvent, so that the symmetry of the other two can be obtained via the orthogonality of the atomic states. Thus, the first two terms of Eq. (2.48) result from the two possibilities for the second r_0 which enter a single matrix element, where the subscript refers to the symmetry of the middle resolvent.

The computational ease with which Eq. (2.48) can be used rests on one's ability to compute the atomic resolvents. In most cases, the exact calculation of these operators is, of course, impossible. Thus, one generally resorts to approximate schemes to compute them. The method used in this work was to obtain "variational" approximations to the excited spectra by diagonalizing the matrix of the Hamiltonian operator in a basis set, for the atomic systems of interest.

In our work, the individual components $A_6^{\parallel}$ and $A_6^{\perp}$ were obtained by performing separate calculations for the S, P, and D parts of the resolvents. Moreover, since we also symmetry reduced the expression for $A_6^{\perp}$, only the $m_L = 0$ components of the atomic states were needed.

Table II.1. The coefficients, M_n, appearing in the expression for $A_6^{\parallel}$ and $A_6^{\perp}$.[a]

	M_1	M_2	M_3	M_4	M_5	M_6	M_7	M_8	M_9	M_{10}
$A_6^{\parallel}$	24	12	16	22	8	11	8	11	-12	-12
$A_6^{\perp}$	24	-6	4	19	2	19/2	2	19/2	-12	-12

[a] See Eq. (2.48).

The atomic basis functions for the helium calculations were taken to be of the form,

$$\psi_{n\ell} = F_{n\ell}\, a_0 \,, \tag{2.49}$$

where a_0 is Hart and Herzberg's twenty term, directly correlated, variational approximation to the He atom ground state wavefunction.[46] The form of this wavefunction and the parameters used in it are given in Table II.2.

The advantage of choosing this particular form for the basis set is that, for sufficiently accurate a_0, the matrix elements of the operator $(h_0^a - \varepsilon_0)$ are given, to sufficient accuracy by:[47,48]

$$\langle\psi_{n'\ell}|(h_0^a - \varepsilon_0)|\psi_{n\ell}\rangle = \tfrac{1}{2}\sum_{i=1}^{2}\langle a_0|\nabla_i F_{n'\ell}\cdot\nabla_i F_{n\ell}|a_0\rangle \,. \tag{2.50}$$

This last equation is exact only if a_0 is an exact eigenfunction of h_0^a. Thus, this method is equivalent to replacing h_0^a by $\tilde{h}_0^a$, so that for the particular a_0 used, one has $(\tilde{h}_0^a - \tilde{\varepsilon}_0)a_0 = 0$, while ignoring $(h_0^a - \tilde{h}_0^a)$. The justification for the use of this approximation in conjunction with the Hart-Herzberg wavefunction will be given later by comparing the results of expectation values of various operators for the ground state of He which were computed using it, to the corresponding results obtained by using more accurate wavefunctions.

Table II.2. Numerical parameters for the Hart-Herzberg He atom wavefunction.[a]

m	c_m	m	c_m	m	c_m
1	0.33729424	8	4.3290467×10^{-3}	14	6.2740944×10^{-6}
2	0.08088340	9	7.8697645×10^{-4}	15	$-6.3829315 \times 10^{-5}$
3	-0.21312975	10	$-1.7755868 \times 10^{-3}$	16	$-1.8442313 \times 10^{-4}$
4	0.02003854	11	$-7.4084122 \times 10^{-4}$	17	1.5585701×10^{-5}
5	-0.02871601	12	1.6305837×10^{-6}	18	6.4835063×10^{-4}
6	-0.01543812	13	$-2.7310618 \times 10^{-4}$	19	6.8860244×10^{-4}
7	$-9.2189670 \times 10^{-3}$				

[a] $a_0 = Ne^{-\frac{1}{2}ks}[1 + c_1u + c_2t^2 + c_3s + c_4s^2 + c_5u^2 + c_6su + c_7t^2u + c_8u^3 + c_9t^2u^2 + c_{10}st^2 + c_{11}s^3 + c_{12}t^2u^4 + c_{13}u^4 + c_{14}u^5 + c_{15}t^2u^3 + c_{16}s^2t^2 + c_{17}s^4 + c_{18}t^2u + c_{19}t^4]$,

where, $N = 0.07164092$, $k = 1.35$. The coordinates, s, t, and u are defined in terms of r_1, r_2, and r_{12} by:

$$s = r_1+r_2 \ , \quad t = r_1-r_2 \ , \quad \text{and} \quad u = r_{12} \ .$$

For these calculations, the form of the $F_{n\ell}$'s for the helium atom was taken from a calculation of the hyperpolarizability of helium.[47] It consists of the following functions:

S-symmetry:
$$(r_1^{n-2} + r_2^{n-2})|a_0\rangle \qquad 2 \leq n \leq 4$$

$$(r_1^{m-2} + r_2^{m-2})r_1 r_2 \cos\theta_{12}|a_0\rangle \qquad 2 \leq m \leq 5$$

P-symmetry:
$$(r_1^{n-1} z_1 + r_2^{n-1} z_2)|a_0\rangle \qquad 1 \leq n \leq 6$$

D-symmetry:
$$(r_1^{n-2}(z_1^2 - \tfrac{1}{3}r_1^2) + r_2^{n-2}(z_2^2 - \tfrac{1}{3}r_2^2))|a_0\rangle \qquad 2 \leq n \leq 4$$

$$(r_1^{m-2} + r_2^{m-2})(z_1 z_2 - \tfrac{1}{3}r_1 r_2 \cos\theta_{12})|a_0\rangle \qquad 2 \leq m \leq 5$$

In order to obtain a final basis for the helium atom calculations, the convergence of $A_6^{\parallel}$ and $A_6^{\perp}$ was monitored, along with that for the atomic hyperpolarizability, polarizability, and C_6 coefficient. The first of these atomic properties allowed an assessment of the completeness of that part of the resolvent with S- and D-symmetry. The second and third of these additional properties serve to test the completeness of the P part of r_0.

In the latter case, the utility of these specific properties as test properties is especially pronounced, because one obtains a rigorous upper bound to both the polarizability and the C_6 coefficient corresponding to the Hart-Herzberg a_0, as they each correspond to a second order energy. The final basis set was obtained by varying the number of functions of each symmetry type until convergence for all these quantities was achieved. The convergence of the atomic hyperpolarizability, γ_0, $A_6^{\parallel}$, and $A_6^{\perp}$ as a function of the number of terms in the basis set is given in Table II.3.

Besides testing the accuracy of our calculation in the above manner, sum rule checks were employed to test the internal consistency of our calculations. It has been shown by Dalgarno and Epstein[49] that if ϕ_0 is an exact eigenfunction of h_0, and if the basis set for a variational calculation of the states of h_0 contains the function ϕ_0, then the following sum rule holds:

$$\sum_n |\langle\phi_0|O|\phi_0\rangle|^2 = \langle\phi_0|O^2|\phi_0\rangle \ . \qquad (2.51)$$

In our case, the Hamiltonian matrix for the linear variational method was constructed as if the Hart-Herzberg wavefunction was exact. That is, the Hamiltonian matrix is that which refers to $\tilde{h}_0$. Hence, if our calculation is numerically precise, and internally consistent, the above sum rule should hold for operators O, which are of the form of our $F_{n\ell}$'s. Since the $F_{n\ell}$'s were different for each

symmetry, the numerical consistency of each part of the calculation could be independently tested. The results for the sum rule checks which we performed are given in Table II.4.

In Table II.5, we present the results of calculations for expectation values of various radial operators. The good agreement between the results obtained by using the Hart-Herzberg ground state wavefunction and those obtained through the use of the very accurate (1,078 term) Pekeris wavefunction[50] testifies to the good quality of the former, and justifies the method which we used to compute the matrix elements of the Hamiltonian.

All the integrals needed in this calculation were obtained using the method of Calais and Löwdin.[51] For the most part, their method can be used without modification. However, for certain of the integrals needed in the construction of the Hamiltonian matrix, modifications had to be made. The analytical evaluation of these integrals is discussed in Appendix B.

For the hydrogen calculations, the basis functions $\psi_{n\ell}$ for the excited states were taken to be of the form,

$$\psi_{n\ell} = F_{n\ell}\,\psi_0 \ ,$$

where

$$F_{n\ell} = r^n\, Y_{\ell 0}(\underset{\sim}{r}) \ ,$$

Table II.3. Convergence of γ_0, $A_6^{\parallel}$, and $A_6^{\perp}$ for He, as a function of the number of terms in the basis.

S Type		P Type	D Type				
N_1	N_2	N_3	N_4	N_5	γ_0	$A_6^{\parallel}$	$A_6^{\perp}$
5	0	5	5	0	38.9	54.98	25.61
3	3	6	3	3	38.7	57.71	26.56
4	3	6	4	3	42.5	60.09	28.42
5	3	6	5	3	42.6	60.09	28.43
6	3	6	6	3	42.6	60.09	28.43
4	4	6	4	4	42.5	60.09	28.43
5	3	7	5	3	42.6	60.09	28.43

Table II.4. Sum-rule check for the operator O (see Eq. (2.52)).

O	r_1+r_2	$r_1^2+r_2^2$	μ_z	$z_1^2+z_2^2-\frac{1}{3}(r_1^2+r_2^2)$	$z_1z_2-\frac{1}{3}r_1r_2\cos\theta_{12}$
$\sum\|\langle 0\|O\|n\rangle\|^2$	0.32155684	0.82473581	0.75239640	0.62955186	0.35870841
$\langle 0\|O^2\|0\rangle$	0.32155688	0.82473588	0.75239638	0.62955184	0.35870840

Table II.5. Calculation of properties of a ground-state helium atom; all properties in atomic units. N_e is the number of electrons, C_6 is the coefficient of the R^{-6} dispersion energy, α_0 is the static polarizability, γ_0 is the static hyperpolarizability.

Property	C_6	α_0	γ_0	$\langle r_1^2+r_2^2 \rangle$	$\langle r_1 \cdot r_2 \rangle$	N_e	$E_0^{(0)}$
Value, this calc	1.458	1.379	42.6	2.3867	-0.064736	2.0000000	-2.9037179
Accurate value	1.4605 ± 0.0025[a]	1.380,[b] 1.383[c]	42.8,[d] 42.6,[e] 43.1[c]	2.3870[f]	-0.064737[f]	2	-2.9037244[f]

[a] M. H. Alexander, J. Chem. Phys. 52, 3354 (1970).

[b] W. D. Davidson, Proc. Phys. Soc., (London) 87, 133 (1966).

[c] Reference (7).

[d] M. W. Grasso, K. T. Chung, and R. P. Hurst, Phys. Rev. 167, 1 (1968).

[e] Reference (47).

[f] Reference (50).

and

$$\psi_0 = \frac{1}{\sqrt{\pi}} e^{-r} .$$

Here ψ_0 is, of course, the exact ground state wavefunction. It was found that $n \leq 6$ for each symmetry was sufficient to obtain convergence for $A_6^{\parallel}$ and $A_6^{\perp}$.

For the helium-hydrogen problem, the final basis sets for the above respective parts were used together.

The values of $A_6^{\parallel}$ and $A_6^{\perp}$ obtained in this calculation for the H_2, HeH, and He_2 systems are given in Table II.6.

After this work was completed, Buckingham et al. reported the results of a variational calculation of both $\underset{\approx}{A}_6$ and $\underset{\approx}{A}_8$ for H_2.[52] This calculation was virtually identical to ours in method, and their $\underset{\approx}{A}_6$ results are in excellent agreement with ours. For reference, we include these results, those of reference (44), the point dipole, and the Unsöld results in Table II.6.

If the results of Table II.6 are used to compute a value of B_ε for helium, a positive value again results. Thus, one concludes that calculations which take only long-range interactions into account are not sufficient. This means that, not surprisingly, the overlap region contributes significantly to the measured value of B_ε, so that $\alpha(R)$ must be computed over the entire range of R if a meaningful value of B_ε is to result.

Table II.6. Accurate and approxmate values of $A_6^{\parallel}$ and $A_6^{\perp}$ for H_2, HeH, and He_2; units of A_6 are a_0^9, units of A_8 are a_0.

	H_2	HeH	He_2
$A_6^{\parallel}$(accurate)[a]	2558.59[e] (2558.59)[c,e]	517.472	60.0922
$A_6^{\perp}$(accurate)[a]	1268.25[e] (1268.25)[c,e]	258.871	28.4308
$A_6^{\parallel}$(point dipole)	729.000	146.451	21.1620
$A_6^{\perp}$(point dipole)	182.250	36.6129	5.29050
$A_6^{\parallel}$(Unsöld)[b]	1030.85		20.0874
$A_6^{\perp}$(Unsöld)[b]	552.445		10.4157
$A_8^{\parallel}$ [c]	90639.5		
$A_8^{\perp}$ [c]	22010.3		

[a] The number of figures reported in this table corresponding to the accurate calculation (see Eq. (2.48)) reflect the numerical precision obtained. Except for the H_2 calculations, the error introduced through the use of $\tilde{h}_0$ (see Eq. (2.50)) results in about four significant figures of accuracy.

[b] Reference (18).

[c] Reference (52).

[e] Reference (44) reports $\bar{A} = (A_6 + 2A_6)/3$ to be 1698 a_0^9.

CHAPTER III

POLARIZABILITIES OF DIATOMIC MOLECULES IN THE OVERLAP REGION

From the results of the previous chapter, it is clear that consideration of overlap effects is necessary if one is to accurately calculate the incremental polarizability of two helium atoms. We shall somewhat arbitrarily define the overlap region for helium to span separations from $4a_0$ to $8a_0$, which covers most of the van der Waals well region. In the overlap region, we shall apply the Hartree-Fock model to calculate the polarizability tensor of He_2 at four internuclear separations: 4, 4.7, 5.5, and 6.0 a_0 . We shall also show that the Hartree-Fock model reduces to the point dipole model at large internuclear separations, where orbital overlap is no longer important. Our results are presented in Sections C-F.

Before discussing our own work, we review previous calculations of the helium pair polarizability in the next section, and review coupled Hartree-Fock theory in Section B.

A. Previous Calculations in the Overlap Region

Early attempts at estimating the effects of overlap on the polarizabilities of rare-gas diatoms paralleled those in the

long-range region by employing model calculations. As an extension of the long-range point dipole model, Levine and McQuarrie represented a pair of interacting atoms by interacting metallic spheres.[22] The long-range asymptotic limit of the resulting polarizability is identical with that of the point dipole model presented earlier. Their short-range results indicate a sharp peak in the parallel polarizability at the point at which the spheres come in contact. The physical basis for this effect is obvious, since when the spheres touch, electronic charge can flow from one sphere to the other. They then translate this modeled result to mean that for real atoms overlap effects are indeed important. This agreement with intuition notwithstanding, their resulting value for B_ε is positive for all cases, and greater than the point-dipole result by about a factor of 2. Thus one concludes that, at least for this problem, such classical modeling is not sufficient.

To consider a model with internal structure, DuPré and McTague used the hydrogen molecule in its $^3\Sigma_u^+$ excited state to simulate the behavior of a rare-gas diatom.[23] The justification for this simulation is that this first excited triplet state of H_2 displays the qualitative features of rare-gas diatoms in their ground states. That is, the $^3\Sigma_u^+$ H_2 potential energy curve includes a short-range (overlap) repulsive part with a long-range (R^{-6}) attractive part; this situation is characteristic of the rare-gas diatomic potential curves. Also, in terms of molecular orbital configurations, triplet hydrogen is $\sigma_g\,\sigma_u$, whereas singlet helium is $\sigma_g^2\,\sigma_u^2$.

In the DuPré and McTague calculation, a one parameter variational approximation to the solution of Eq. (1.6) was used:

$$\Psi(F) = \Psi_0(1 + A(q_1 + q_2)) , \tag{3.1}$$

where Ψ_0 was chosen to be the Hirschfelder-Linnett wavefunction for the $^3\Sigma_\mu^+$ state of the unperturbed H_2 molecule;[52] here, q_1 and q_2 are the coordinates of electrons 1 and 2 , respectively in the direction of the applied field. As was shown by Hirschfelder, the components of the polarizability tensor of H_2, under these conditions, are given by:[53]

$$\alpha_{\parallel} = 8(\langle x_1^2 \rangle + \langle x_1 x_2 \rangle)^2 , \tag{3.2}$$

$$\alpha_{\perp} = 8(\langle z_1^2 + \langle z_1 z_2 \rangle)^2 , \tag{3.3}$$

where x_1 and z_1 are coordinates of electron 1 in the center of mass system, with the z-axis lying along the internuclear axis, and the $\langle\ \rangle$ denote an expectation value with respect to Ψ_0 . Eqs. (3.2) and (3.3) are a generalization to molecules of the Kirkwood approximation for atomic polarizabilities,[54,62] and were shown to give results of reasonable accuracy for the ground state of H_2. The results for the $^3\Sigma_u^+$ state of H_2 showed that the increments of $\alpha_{\parallel}$ were positive and $\alpha_{\perp}$ were negative in the intermediate region, and

that in this region, the mean incremental polarizability, $\Delta\alpha$, is negative. Thus, the second dielectric virial coefficient B_ε is less than that obtained from the dispersion models, and for some temperature range could, in fact, be negative.

The qualitative explanation of the behavior of the incremental polarizabilities is based on the notion that polarizability is related to the size of the charge cloud. When the two atoms overlap, the electrons on one atom can tunnel to the other nucleus, thereby increasing the polarizability in the parallel direction. The same effect contracts the charge cloud in the perpendicular direction, however, and decreases this component of the polarizability tensor.

For the case of the helium diatom, the Hirschfelder-Kirkwood approximation takes the form

$$\alpha_{\parallel} = 4[\langle\sigma_g|z^2|\sigma_g\rangle + \langle\sigma_u|z^2|\sigma_u\rangle - 2\langle\sigma_g|z|\sigma_u\rangle^2]^2 , \tag{3.4}$$

$$\alpha_{\perp} = 4[\langle\sigma_g|x^2|\sigma_g\rangle + \langle\sigma_u|x^2|\sigma_u\rangle]^2 , \tag{3.5}$$

for a field-free wavefunction of the Hartree-Fock form,

$$\Psi_0 = |\sigma_g\, \bar{\sigma}_g\, \sigma_u\, \bar{\sigma}_u| . \tag{3.6}$$

As a preliminary to our main calculation, we chose for Ψ_0 the Kestner wavefunction and evaluated Eqs. (3.4) and (3.5). The

Table III.1. Hirschfelder-Kirkwood approximation for the polarizabilities of He_2 (see Eqs. (3.4) and (3.5)).[a,b]

R	$2\langle\sigma_g\|z^2\|\sigma_g\rangle$	$2\langle\sigma_u\|z^2\|\sigma_u\rangle$	$2\langle\sigma_g\|z\|\sigma_u\rangle$	$2\langle\sigma_g\|x^2\|\sigma_g\rangle$	$2\langle\sigma_u\|x^2\|\sigma_u\rangle$	$\alpha_\parallel$	$\alpha_\perp$	$\Delta\alpha$
1.0	0.7443	4.7418	1.1520	0.4507	1.4220	17.100	3.5446	5.567
2.0	2.3397	3.6952	2.1042	0.7797	0.7430	2.5832	2.3186	-0.089
3.0	4.9164	5.7783	3.0246	0.8241	0.7322	2.3916	2.4221	-0.084
4.0	8.5505	9.0511	4.0042	0.8184	0.7546	2.4586	2.4743	-0.027
4.7	11.6793	11.9986	4.7013	0.8079	0.7699	2.4828	2.4895	-0.008
5.2	14.2004	14.4096	5.1982	0.8021	0.7756	2.5240	2.4891	-0.005
5.5	15.8274	16.0043	5.5002	0.7998	0.7796	2.4948	2.4945	-0.001
6.0	18.7322	18.8489	6.0003	0.7949	0.7841	2.4885	2.4932	-0.004
∞	$\langle a\|z_u^2\|a\rangle$ = 0.39494					2.4956	2.4956	

[a] All entries in this table are in atomic units.

[b] The ψ_0 (Eq. (3.6)) is that of reference (41).

results are shown in Table 3.1. It is seen that this approximation gives negative values for $\Delta\alpha$ in the region of the van der Waals well.

To proceed beyond these model calculations, several workers have applied Hartree-Fock theory.[24,26,27] The first Hartree-Fock computation of the polarizability of the helium diatom was carried out by Lim, Linder, and Kromhout.[24] Their calculation used a Gaussian basis set and was unable to produce a negative value for the dielectric virial coefficient, B_ε. However, their calculated asymptotic results also differed from the Hartree-Fock limit for the separated atoms by about 25%. Thus, their calculation is of questionable accuracy.

Buckingham and Watts have also used coupled Hartree-Fock theory to compute an $\alpha(R)$ curve for He_2 using a Gaussian basis set.[26] They obtain negative values for the incremental mean polarizability in the region of strong overlap. These negative contributions, however, occur at too short a separation to produce a negative value for B_ε. Their results are plagued by instabilities in the values of $\alpha(R)$ with respect to basis set variation. To this extent, the authors themselves point out that their results should be regarded as tentative, and no claim for attainment of the Hartree-Fock limit is made.

Recently, O'Brien et al. have also published results of a coupled Hartree-Fock calculation of the polarizability of He_2.[27] Their calculation was similar in motivation and method to ours, so

that a discussion of their results will be deferred to the final section, at which time a comparison of results will be presented.

B. Coupled Hartree-Fock Perturbation Theory

Langhoff, Karplus, and Hurst have reviewed several of the forms of perturbed Hartree-Fock theory currently in use.[56] The method which was used in our work is known as the coupled Hartree-Fock perturbation method (method a of reference (56)).

The Born-Oppenheimer Hamiltonian, in atomic units, for a pair of helium atoms relative to an origin at the center of mass, in a constant, static electric field $\underset{\sim}{F}$ is given by:

$$H = -\tfrac{1}{2}\sum_{i=1}^{4}\nabla_i^2 - \sum_{i=1}^{4}\left(\frac{2}{r_{iA}} + \frac{2}{r_{iB}}\right) + \sum_{i>j}^{4}\frac{1}{r_{ij}} + \sum_{i}\underset{\sim}{r}_i\cdot\underset{\sim}{F}\ , \qquad (3.6)$$

where $\underset{\sim}{R}_A$ and $\underset{\sim}{R}_B$ represent the position vectors of the nuclei. Invoking the Hartree-Fock approximation for this case involves the assumption that the eigenstates of H can be represented by a single determinant of orthonormal spin orbitals:

$$\tilde{\Psi} = \det[\chi_1(1)\ \chi_2(2)\ \chi_3(3)\ \chi_4(4)]\ , \qquad (3.7)$$

where the spin orbitals χ are to be chosen by minimizing the energy functional, Eq. (1.22). The derivation and use of the resulting one-electron (Fock) equations is well known for the unperturbed

problem.[39] To extend the formalism to the problem at hand, we need only note that since the perturbation is a symmetric sum of one-electron operators, it will carry through the usual Hartree-Fock derivation in the same way that the nuclear attraction terms do in the unperturbed case. One then obtains the perturbed canonical Hartree-Fock equations:

$$(h(1) + \underset{\sim}{r}_1 \cdot \underset{\sim}{F} - \varepsilon_i)\chi_i(1) = 0 , \qquad i = 1,2 , \tag{3.8}$$

where $h(1)$ is the one-electron Fock operator:

$$h(1) = -\tfrac{1}{2}\nabla_1^2 - \frac{2}{r_{1A}} - \frac{2}{r_{1B}} + \sum_{j=1}^{4} \langle \chi_j | r_{12}^{-1} (1 - P_{12}) | \chi_j \rangle_2 , \tag{3.9}$$

and ε_i is the perturbed orbital energy. The subscript "2" on the fourth term means that one integrates the indicated expression over the coordinates of electron 2 only. For helium, Eq. (3.8) represents a pair of coupled integrodifferential equations for the orbitals χ_1 and χ_2. The solution of these equations can be approached either directly or by using perturbation methods.

With the direct method, one leaves the electric field explicitly in the Fock equations. This means that the perturbed Fock equations differ from the usual unperturbed Fock equations only in the electric field term. Thus, a standard Hartree-Fock program can be used for

the field-dependent problem with a relatively small number of modifications. This method was first used by Cohen and Roothaan[57,58] in atomic polarizability calculations, and is known as the finite-field method; it is the one used in our work.

In using the perturbation method to solve Eq. (3.8), one proceeds as in Chapter I, and introduces the expansions:

$$\chi_i = \chi_i^{(0)} + F\,\chi_i^{(1)} + \cdots , \tag{3.10}$$

and

$$\varepsilon_i = \varepsilon_i^{(0)} + F\,\varepsilon_i^{(1)} + \cdots , \tag{3.11}$$

into Eq. (3.8), and, using the usual linear independence arguments, one gets, to zero and first order respectively:

$$[h^0(1) - \varepsilon_i^{(0)}]\chi_i^{(0)} = 0 , \tag{3.12}$$

and

$$\begin{aligned}[h^0(1) - \varepsilon_i^{(0)}]\chi_i^{(1)}(1) - [r_{1q} + \varepsilon_i^{(1)}]\chi_i^{(0)}(1) \\ + \sum_{j=1}^{4} [\langle\chi_j^{(1)}|r_{12}^{-1}(1 - P_{12})|\chi_j^{(0)}\rangle_2 \\ + \langle\chi_j^{(0)}|r_{12}^{-1}(1 - P_{12})|\chi_j^{(1)}\rangle_2]\chi_j^{(0)} = 0 ,\end{aligned} \tag{3.13}$$

where

$$h^0(1) = -\tfrac{1}{2}\nabla_1^2 - \frac{2}{r_{1A}} - \frac{2}{r_{1B}} + \sum_{j=1}^{4} \langle \chi_j^{(0)} | r_{12}^{-1} (1 - P_{12}) | \chi_j^{(0)} \rangle_2 , \tag{3.14}$$

and r_{1q} refers to the component of $\underset{\sim}{r}_1$ in the direction of $\underset{\sim}{F}$. Eq. (3.13) represents a set of coupled integrodifferential equations for the first order contributions to the perturbed orbitals and energies.

To obtain the polarizability using these two methods, we refer back to Eqs. (1.5) and (1.24). The field-dependent dipole moment for He_2 in the Hartree-Fock approximation is given by:

$$\langle \underset{\sim}{\mu} \rangle = \langle \tilde{\Psi}(F) | \hat{\underset{\sim}{\mu}} | \tilde{\Psi}(F) \rangle , \tag{3.15}$$

where $\tilde{\Psi}(F)$ is defined in Eq. (3.7). Denoting the orthonormal closed shell α-spin orbitals for the field-dependent problem by χ_1 and χ_2, we see that Eq. (3.15) can be written as:

$$\langle \underset{\sim}{\mu} \rangle = 2\langle \chi_1 | \hat{\underset{\sim}{\mu}}_1 | \chi_1 \rangle + 2\langle \chi_2 | \hat{\underset{\sim}{\mu}}_1 | \chi_2 \rangle . \tag{3.16}$$

This expression is used directly in the finite-field method by extrapolating the ratio μ/F to zero field. For use with the perturbation method, Eq. (3.16) can be written:

$$\begin{aligned}\langle \underset{\sim}{\mu} \rangle &= 2\langle \chi_1^{(0)} + F\,\chi_1^{(1)} + \ldots | \hat{\underset{\sim}{\mu}}_1 | \chi_1^{(0)} + F\,\chi_1^{(1)} + \ldots \rangle \\ &\quad + 2\langle \chi_2^{(0)} + F\,\chi_2^{(1)} + \ldots | \hat{\underset{\sim}{\mu}}_1 | \chi_2^{(0)} + F\,\chi_2^{(1)} + \ldots \rangle \qquad (3.17) \\ &= 4F[\langle \chi_1^{(0)} | \hat{\underset{\sim}{\mu}}_1 | \chi_1^{(1)} \rangle + \langle \chi_2^{(0)} | \hat{\underset{\sim}{\mu}}_1 | \chi_2^{(1)} \rangle] + O(F^2) \ .\end{aligned}$$

Here, we have used fact that the dipole moment of the free He_2 diatom is zero. Differentiating Eq. (3.17) with respect to F, and evaluating the result at zero field yields the following expression for the polarizability:

$$\alpha_{qq} = 4 \sum_{i=1}^{2} \langle \chi_i^{(1)} | \hat{\mu}_{1q} | \chi_i^{(0)} \rangle \ . \qquad (3.18)$$

In both the finite-field and perturbation methods, exact solution of the Hartree-Fock equations is not in general possible, so that one makes use of basis set expansions to obtain analytical solutions. That is, in the finite-field method, one uses the Hartree-Fock-Roothaan procedure by introducing a basis set expansion for the field-dependent orbitals χ_i. This converts Eq. (3.8) to a set of coupled matrix equations for the expansion coefficients. In the perturbation method, one converts to a matrix scheme by introducing a basis set expansion for the first order orbitals, $\chi_i^{(1)}$. The resulting coupled matrix equations are solved iteratively in either case. It is readily seen that for small field strengths, the two methods are equivalent.

In both the finite-field and perturbation methods, one begins with a zero-order Hartree-Fock wavefunction which, except for certain atomic cases, is itself obtained by the Hartree-Fock-Roothaan procedure. The basis sets used in such calculations usually consist of either Slater type functions (STF) or Gaussian type functions (GTF). The STF sets are generally more efficient than the GTF, with the size of the latter often being three or more times larger than the former for the same accuracy.

The symmetry of the zero order basis functions is dictated by the molecular orbital correlation diagram for the particular molecule of interest.[59] The set of functions which one introduces to reflect the distortion of the zero order wavefunctions by the electric field is known as the polarization set. For polarizability calculations, the symmetry of these functions is chosen to be such that they couple to the zero order molecular orbitals via the dipole moment operator. Sitter and Hurst have this discussed this problem for calculations of atomic hyperpolarizabilities.[60]

In view of the expansion nature of the solutions of Eq. (3.8), it is important to ask how the result obtained compares to that which would be obtained if the Hartree-Fock equations could be solved exactly. This latter limit is referred to as the Hartree-Fock limit, and it corresponds to the use of an infinitely large basis set. The difference between it and the analytical result is known as the basis set error, and is exactly known only for atomic calculations. The

"art" of carrying out such computations, therefore, involves the minimization of the size of the basis set used, while, at the same time, getting as close as possible to the Hartree-Fock limit result. For field-free diatomi molecules, this problem is considered to be solved, and Gilbert and Wahl have illustrated it in detail for the He_2, Ne_2, and Ar_2 rare-gas diatoms.[61] Additional references to this problem and its solution for field-free calculations can be found in Chapters I and III of reference (63).

The method which we used for the selection of the perturbed basis set will be discussed in the next section.

From a formal point of view, the finite-field procedure is the same whether one is discussing atoms or molecules. From a computational standpoint, however, this is no longer true because of the additional amount of work that one must do in computing and processing the requisite two-center, two-electron integrals. For this reason it is desireable to recast the above procedure to take advantage of optimized computer codes which currently exist.

The program which we used in our calculations is a modification of the BISON computer program of A. C. Wahl, P. J. Bertoncini, R. Land, and K. Kaiser of Argonne National Laboratory.[64] The modifications are those required for field-dependent calculations, and are discussed in more detail in Appendix C.

The basic change needed involved the introduction of the appropriate products of the dipole moment matrix elements and the

electric field strength in the one-electron contributions to the Fock matrix. Since the field variation was done in the SCF part of the program, unit field strengths were used in the one-electron integral calculations; this means that the integrals need to be computed only once per each R value considered. This was especially important in that convergence problems which appeared in the calculations of $\alpha_{\parallel}(R)$, made it necessary to turn the field on slowly.

For basis set variation purposes, auxiliary programs were written to remove those one- and two-electron integrals which involved a given basis function from a "master" integral tape. This allowed step-by-step basis set reduction to be performed using the integrals corresponding to a single, large set. One, of course, must be careful to guarantee that the cost of computing the integrals for the large set is less than the sum of the costs of the individual, smaller sets.

Once the appropriately modified Hartree-Fock program was working, the problem remained of delineating a basis set selection procedure which would allow us to approach the Hartree-Fock limit economically. The procedure which we used is discussed in the next section.

C. Basis Set Selection Procedure

In order to compute the Hartree-Fock limit for the polarizability, one introduces basis functions which reflect the electric field polarization of a zero-field Hartree-Fock limit wavefunction and

carries out the Hartree-Fock-Roothaan prescription with this augmented basis set. This procedure for the polarizability calculation can be capsulized as follows:

1. Obtain a field-free Hartree-Fock limit wavefunction using the Hartree-Fock-Roothaan method.
2. Choose polarization functions for the above.
3. Redo the Hartree-Fock-Roothaan calculation with the zero-order plus polarization basis set in the presence of an electric field F. Compute the dipole moment μ of the resulting field-dependent wavefunction and extrapolate the ratio μ/F to zero field to get α.

We now assume that step 1 has been carried out. The choice of a polarization set for a given field-free basis is a playoff between two competing requirements:

1. The set must be flexible enough to adequately represent the distortion of the field-free orbitals by the electric field.
2. The size should be minimized, within the above constraint, so as to minimize the number of integrals which must be computed.

The prescription which we used for the selection of polarization functions will now be described.

As a first step, the polarization functions are chosen to polarize individual field-free basis functions. For a given normalized Slater orbital, $\phi^{(0)}$ we define the <u>orbital polarizability</u> by the maximum value of the second-order variational functional:

$$\alpha(\Phi^{(1)}) = -2\langle\Phi^{(1)}|(H_0 - E_0)|\Phi^{(1)}\rangle + 4\langle\Phi^{(1)}|z|\Phi^{(0)}\rangle , \tag{3.19}$$

where $\Phi^{(1)}$ is a trial polarization function, z is the polar axis of coordinates, and H_0 is an unperturbed Hamiltonian which defines $\Phi^{(0)}$:

$$H_0 = -\tfrac{1}{2}\nabla^2 - \zeta n r^{-1} - [\ell(\ell+1) - n(n-1)]/2r^2 , \tag{3.20}$$

$$E_0 = -\zeta^2/2 , \tag{3.21}$$

$$\Phi_0^{(0)} = N r^{n-1} e^{-\zeta r} Y_{\ell m}(\theta,\phi) . \tag{3.22}$$

We expand $\Phi^{(1)}$ as a linear combination of STO's and maximize $\alpha(\Phi^{(1)})$ with respect to the linear coefficients and the orbital exponents. A general nodeless STO is the ground state of the corresponding H_0 , so that for a sufficiently flexible choice of $\Phi^{(1)}$, the maximization procedure yields the exact polarizability of the ground state of H_0 . Following the optimization of $\Phi^{(1)}$, we generate a more flexible basis of polarization functions by adding the STO's which represent $\Phi^{(1)}$, to the finite-field basis individually; that is, we use the variational procedure to choose optimum orbital exponents and principle quantum numbers for the finite-field basis.

If the procedure described in the preceding paragraph is followed to polarize an extended field-free basis, a linearly dependent basis set is usually obtained. Even if the linear dependencies are removed, we have found that the basis is much larger than is necessary to give converged results for the molecular polarizability. We then consider the following modifications to reduce the size of the polarization basis:

a. Primary attention is paid to polarizing the STO's which fall into the following categories: those which are dominant in the field-free orbitals; those which are the most polarizable; and those which constitute a leading contribution to the tail of the orbitals.

b. The less dominant basis functions are polarized collectively. Let $\phi_p^{(0)}$ and $\phi_q^{(0)}$ denote two STO's which have expansion coefficients c_p and c_q in a field-free occupied orbital, and let $\phi_p^{(1)}$ and $\phi_q^{(1)}$ denote their polarization functions. Then we construct a new polarization function θ, which also is represented by an expansion in STO's, in a weighted least-squares sense. We minimize

$$\Delta = \int |\theta(\vec{r}) - \phi^{(1)}(\vec{r})|^2 \, d\tau , \qquad (3.23)$$

where

$$\phi^{(1)} = a_p c_p \phi_p^{(1)} + a_q c_q \phi_q^{(1)} , \qquad (3.24)$$

$$a_p = \alpha(\phi_p^{(1)})/[\alpha(\phi_p^{(1)}) + \alpha(\phi_q^{(1)})] . \qquad (3.25)$$

The optimum expansion functions of θ give a smaller set of STO's to add to the polarization basis than the two functions $\phi_p^{(1)}$ and $\phi_q^{(1)}$ taken individually.

Other factors affecting the choice of basis functions depend on the case under consideration and are discussed below.

D. Test Calculations

Before computing the polarizability of He_2, we obtained the polarizabilities for the united and separated atoms, Be and He, respectively, in order to test our procedure for basis set selection; the idea being to obtain the coupled Hartree-Fock limit for the polarizability of these atomic limits. The results for the atomic tests are given in Table III.2. These results agree quite well with the accepted coupled Hartree-Fock values ($\alpha(He) = 1.322\ a_0^3$; $\alpha(Be) = 45.5\ a_0^3$).[57,58,65]

The atomic basis set selection followed closely the procedure outlined in the previous section. The field-free basis for Be is taken from Clementi[66] while that for He is taken from Kestner.[41] The 3p orbital exponent in the He atom calculation was selected by variationally solving Eq. (3.19), for each 2s basis orbital, using a

two-term basis set (2p,3p) for $\Phi^{(1)}$; the combined result was then fitted to a single 3p via the least-squares procedure (see Eq. (3.23)). For the Be atom, the selection of candidates for collective polarization is not clear-cut, because the second occupied orbital has a dominant contribution from the 2s orbitals, while the first has a dominant contribution from the 1s orbitals. Thus, these orbitals were polarized separately.

In addition to these atomic limits, a series of test calculations were performed on the hydrogen molecule, at an internuclear separation of 1.402 a_0 . These tests were made both to check the modified BISON program and to examine features of the finite-field method and our basis set selection procedure peculiar to a diatomic example.

The program checks were of two types: the first involved a comparison with a coupled Hartree-Fock calculation which was carried out by hand; and the second involved the duplication of results obtained by other workers who used the iterative method.

The former check is possible without iteration because H_2 has an electronic configuration which can be represented by $1\sigma_g^2$, so that there is only one perturbed orbital, $1\sigma^{(1)}$, hence only one equation of the form of Eq. (3.13) to solve. This means that expansion of $1\sigma^{(1)}$ in a Slater basis set leads to a single matrix equation of the form:

$$\underset{\sim}{A}\underset{\sim}{c} = \underset{\sim}{b} , \qquad (3.26)$$

which is solved by inverting the matrix A. The second method involved the duplication of the coupled Hartree-Fock H_2 polarizability calculations by Caves and Karplus[67] and Gutschick and McKoy.[68]

For the first test, Eq. (3.13) for the field perpendicular to the internuclear axis can be written:

$$\begin{aligned}[-\tfrac{1}{2}\nabla_1^2 - \frac{1}{r_{1A}} - \frac{1}{r_{1B}} + \langle\sigma_0|r_{12}^{-1}|\sigma_0\rangle_2 - \varepsilon_0]\sigma_1 \\ + [\chi_1 + 2\langle\sigma_0|r_{12}^{-1}|\sigma_1\rangle_2 - \varepsilon_0]\sigma_0 = 0 .\end{aligned} \tag{3.27}$$

Here, ε_1 is given by $(\sigma_0\sigma_1|\sigma_0\sigma_0)$. If we now introduce the expansion,

$$\sigma_1 = \sum_K c_K \phi_K , \tag{3.28}$$

into Eq. (3.13) we obtain Eq. (3.25), with,

$$\begin{aligned}A_{LK} = [\langle\phi_L|-\tfrac{1}{2}\nabla_1^2 - \frac{1}{r_{1A}} - \frac{1}{r_{1B}}|\phi_K\rangle + (\sigma_0\sigma_0|\phi_L\phi_K) - \varepsilon_0\langle\phi_L|\phi_K\rangle \\ + 2(\sigma_0\phi_L|\sigma_0\phi_K) ,\end{aligned} \tag{3.29}$$

and

$$b_L = -\langle\sigma_0|\chi|\phi_L\rangle . \tag{3.30}$$

The required integrals were computed using the two-center integral program of H. F. Schaefer III. The results of this check for $\alpha_\perp$ are given in Table III.3. The minor differences reflect the (arbitrary) convergence tolerance of 10^{-5} for the coefficient vectors in the SCF part of BISON. This check lends confidence to the correctness of our working version of BISON.

To further check the program, we used the basis set of Caves and Karplus, and computed $\alpha_\parallel$ and $\alpha_\perp$ for H_2 at $R = 1.40\ a_0$. The results are given in Table III.4. Again, the slight discrepancies result from differences in numerical parameters used in the respective calculations. These results serve to re-enforce the above conclusions regarding the accuracy of our working version of BISON.

A further concern which one has in using the finite-field method is that hyperpolarizability terms can contribute to the computed value of the dipole moment. If these additional effects are not correctly interpreted and accounted for, erroneous results for the polarizability will be obtained.

For a calculation in which the polarizability is the only quantity of interest, the hyperpolarizability terms can be removed by using a sufficiently small field strength. However, the field strength must be kept large enough so that the computed dipole moment has numerical significance. The particular value of the field strength used in these calculations was .001 au. This value was chosen by test calculations on both H_2 and He_2.

Table III.2. Basis sets and polarizabilities for atomic helium and beryllium.

Atom	Field-Free Basis[a]	Polarization Basis[a]	Polarizability[b]
He	1s(1.450) 2s(1.641) 2s(1.723)	2p(1.450) 3p(1.450) 3p(1.655)	1.322 a_0^3
Be	1s(3.3370) 1s(5.5063) 2s(0.6040) 2s(1.0118)	2p,3p(3.3370) 2p,3p(5.5063) 2p,3p(0.6040) 2p,3p(1.0118)	45.574 a_0^3

[a] Slater-type basis. Orbital exponents given in parentheses.

[b] Here a_0 is the Bohr radius.

Table III.3. Comparison between the first order perturbed orbital for H_2 at $R = 1.40\ a_0$ computed using Eq. (3.27) and that obtained from BISON.[a]

	A_{11}[a]	A_{12}	A_{22}	b_1	b_2	F	c_1	c_2
Eq. (3.27)	2.4111	2.4658	3.5624	-1.1667	-1.0919	0.025	-0.01458	0.00243
BISON	---	---	---	---	---	0.025	-0.01457	0.00243

[a] In the basis set definitions, the subscripts A and B refer to the respective centers:

$\sigma_0 = -3.6218\phi_1 - .17759\phi_2 - .02817\phi_3$

$\phi_1 = \chi_{100}(1.06)_A + \chi_{100}(1.06)_B$

$\phi_2 = \chi_{100}(1.43)_A + \chi_{100}(1.43)_B$

$\phi_3 = \chi_{210}(1.82)_A + \chi_{210}(1.82)_B$

$\sigma_1 = c_1\ \phi_4 + c_1\ \phi_5$

$\phi_4 = [\chi_{211}(.935)_A + \chi_{21-1}(.935)_A + \chi_{211}(.935)_B + \chi_{21-1}(.935)_B]$

$\phi_5 = [\chi_{211}(1.509)_A + \chi_{21-1}(1.509)_A + \chi_{211}(1.009)_B + \chi_{21-1}(1.509)_B]$.

The χ's are defined by Eq. (3.22).

Table III.4. Coupled Hartree-Fock polarizabilities and basis sets for H_2 at R = 1.40 .

	Field-Free Basis[a]	Polarization Basis[a]	Polarizability
$\alpha_{\parallel}$	1s(1.06) 1s(1.43) $2p_{\sigma}$(1.82)	$2p_{\sigma}$(0.945)	6.478 a_0^3 (6.478 a_0^3)[b]
$\alpha_{\perp}$	1s(1.06) 1s(1.43) $2p_{\sigma}$(1.82)	$2p_{\pi}$(0.935) $2p_{\pi}$(1.509)	4.601 a_0^3 (4.602 a_0^3)[b]

[a] Numbers in parentheses are the orbital exponents used, with a Slater-type basis centered on the respective nuclei.

[b] Reference (67).

Table III.5. Coupled Hartree-Fock ratios at $\langle\mu_x\rangle/F$, for H_2 at $R = 1.402\ a_0$.[a]

F	$\mu_x(F)_I$[b]	$\mu_x(F)_{II}$[c]
0.005	4.290	4.290
0.008	4.289	4.290
0.010	4.289	4.290
0.025	4.281	4.292
0.050	4.253	4.294

[a] Units of field strength are atomic units, units of μ_x/F are a_0^3.

[b] I refers to the basis set: 1s(1.197), $2p_\pi$(1.050), $3p_\pi$(1.197) on each center.

[c] II refers to the above basis set (b) augmented by the function $3d_\Delta$(1.197) on each center.

The hyperpolarizability of a diatomic molecule will depend on basis functions of Σ, π, and Δ symmetry. Thus if one hopes to extract hyperpolarizability information from a finite-field calculation (this capability makes the finite-field method attractive), basis functions of all the appropriate symmetries for a given direction of the applied field must be included. Failure to do so can result in the wrong sign for the hyperpolarizability, as evidenced by the H_2 data of Table III.5.

In addition to the tests described above, we repeated the test calculations of Gutschick and McKoy on H_2, and verified their results.

E. Helium Diatom Calculations

For our calculation of the polarizability of the helium diatom, the field-free wavefunction of Kestner was chosen.[41] This wavefunction is defined in terms of a Slater orbital basis set, with orbital exponents optimized at each internuclear separation. The basis set error in Kestner's calculation, as inferred from the extremely accurate calculation of Gilbert and Wahl, is about 1 part in 10^7 for the energy. A reduction in the size of this zero-order set can be justified only by numerical experimentation.

For the purpose of calculating statistical averages, one is interested in the polarizability for those internuclear separations for which the statistical pair distribution function is non-zero. As will be seen later, this implies that the smallest internuclear

separation for which we need to compute α is about $4a_0$. Thus, for this range of separations, it is reasonable to attempt to achieve a reduction of the size of the basis set by experimentation at $R = 4a_0$, and assume that the results are valid for larger separations.

In the H_2 test calculations, it was observed that it was unnecessary to include basis functions which polarize the $2p_\sigma$ zero-order basis function. This is presumably due to two effects: the $2p_\sigma$ does not easily distort in a direction perpendicular to the orbital axis, and the coefficient of the $2p_\sigma$ in the zero-order occupied orbitals is small relative to those of the s-type basis functions. For the case of He_2, the coefficient of the p-type basis functions is less than .5% of the coefficients of the s-type functions, for internuclear separations greater than or equal to $4a_0$. Thus, it was assumed at the outset that for the calculations of $\alpha_\perp$, the $2p$ need not be polarized.

The zero-order basis set for $R = 4a_0$, is given in Table III.6. From this table, it is seen that for a calculation of $\alpha_\perp$ a reasonable initial polarization set would consist of the following functions on each center:

$$2p_\pm(1.458)\ ,\quad 3p_\pm(1.458)\ ,\quad 2p_\pm(1.175)\ ,\quad 3p_\pm(1.644)\ .$$

The last two polarization functions represent collective polarization of the two $2s$ zero-order basis functions. Since the zero-order set

Table III.6. Field-free basis set for He_2 at $R = 4.0\ a_0$.

Basis[a]	Field-Free Basis
1	1s(1.458)
	2s(2.631)
	2s(1.723)
	$2p_\sigma$(1.748)

[a] Slater-type functions centered on nuclei A and B . Orbital exponents given in parentheses.

consists of eight functions, this yields a total of 24 basis functions, or 45,150 two-center, two-electron integrals which need to be computed. The systematic reduction in the basis set size for $R = 4a_0$ is given in Table III.7. The most noticeable conclusion warranted by these results is that in the calculations of $\alpha_\perp$, the $2p_\sigma$ basis function does not have to be included. This result coupled with the collective polarization of the two 2s functions by a single 3p yields a basis set of 18 functions, or 14,706 two-center, two-electron integrals. This corresponds to a 65% decrease in the cost of computing <u>each point</u> on the $\alpha_\perp(R)$ curve (with calculations done in double precision on the UNIVAC 1108).

For the parallel direction, a set of 18 basis functions was used for size-consistency with the calculations for the perpendicular direction. The size here represents a linear independent combination of an essentially complete polarization set; for the purposes of this calculation, the linear independence criterion which was adopted was that the smallest eigenvalue of the overlap matrix could not be less than 10^{-6}. The specific polarization sets and the results for the polarizabilities are given in Table III.8 ($\alpha_\parallel$) and Table III.9 ($\alpha_\perp$). The mean incremental polarizability, $\Delta\alpha$, which is computed from the data in these tables is plotted in Figure III.1. The cross-hatched area in this graph reflects our estimates of the basis set error in the polarizability calculations, and will be discussed in Chapter V.

From the data of Tables III.8 and III.9, it is apparent that, in the overlap region, $\alpha_\parallel$ first increases and then decreases as

the internuclear separation decreases. This is opposed to the trend for the corresponding $\alpha_\perp$ values which decrease monotonically with decreasing R. Hence, our results indicate that the incremental parallel and perpendicular polarizabilities have opposite signs for the range of internuclear separations which we have considered. This, as noted in references (23) and (37), is in accord with the general features of the polarizability curves which are necessary to obtain agreement with the dielectric constant experiments. The Kerr effect experiments, on the other hand, are affected by the variation in the anisotropy as a function of R. Our computed $\beta(R)$ curve is given in Figure III.2, and will be discussed later.

In order to cast this data in a form which is useful for the property calculations, we fit the incremental mean polarizability, $\Delta\alpha(R)$ and the anisotropy $\beta(R)$ to the following forms:

$$\left.\begin{aligned} \Delta\alpha(R) &= -12.9\exp(-1.45)R + .00116a_0^3 \\ \text{and} \\ \beta(R) &= \alpha_\parallel - \alpha_\perp = 6\alpha_0^2 R^{-3} - 42.5\exp(-1.645R) \end{aligned}\right\} R \leq 6.5a_0 \,. \qquad (3.31)$$

For internuclear separations greater than $6.5a_0$, we used the asymptotic results:

Table III.7. Basis sets and perpendicular polarizabilities for diatomic helium, $R = 4.0\ a_0$.

Basis[a]	Field-Free Basis	Polarization Basis	Polarizability[b]
1	1s(1.458) 2s(2.631) 2s(1.723) $2p_\sigma$(1.748)	$2p_\pm$(1.458) $3p_\pm$(1.458) $2p_\pm$(1.175) $3p_\pm$(1.644)	2.570 a_0^3
2	1s(1.458) 2s(2.631) 2s(1.723)	$2p_\pm$(1.458) $3p_\pm$(1.458) $2p_\pm$(1.175) $3p_\pm$(1.644)	2.570 a_0^3
3	1s(1.458) 2s(2.631) 2s(1.723)	$2p_\pm$(1.458) $3p_\pm$(1.458) $3p_\pm$(1.644)	2.570 a_0^3

[a] Slater-type basis centered on nuclei A and B . Orbital exponents given in parentheses.

[b] Here a_0 is the Bohr radius.

Table III.8. Basis sets and parallel polarizabilities of diatomic helium.

$R(a_0) \rightarrow$ Basis ↓	4.0	4.7	5.5	6.0	∞
		Orbital Exponents			
1s	1.458	1.454	1.450	1.451	1.450
2s	2.631	2.635	2.630	2.638	2.641
2s'	1.723	1.723	1.721	1.720	1.720
$2p_\sigma$	1.250	1.250	1.250	1.250	1.250
$2p_\sigma$	1.458	1.454	1.450	1.451	1.450
$3p_\sigma$	1.458	1.454	1.450	1.451	1.450
$3p_\sigma$	1.655	1.655	1.655	1.655	1.655
$3d_\sigma$	1.458	1.454	1.450	1.451	1.450
$4d_\sigma$	1.458	1.454	1.450	1.451	1.450
		Parallel Polarizabilities (a_0^3)			
(a)	2.675	2.685	2.681	2.672	2.644
(b)	2.678	---	2.681	2.675	2.650

(a) This work. Here a_0 is the Bohr radius.

(b) Gaussian basis set results of reference (27).

Table III.9. Basis sets and perpendicular polarizabilities of diatom helium.

Basis ↓ $R(a_0)$ →	4.0	4.7	5.5	6.0	∞
			Orbital Exponents		
1s	1.458	1.454	1.450	1.450	1.450
2s	2.631	2.635	2.630	2.641	2.641
2s'	1.723	1.723	1.721	1.723	1.723
$2p_{\pm}$	1.458	1.454	1.450	1.450	1.450
$3p_{\pm}$	1.458	1.454	1.450	1.450	1.450
$3p_{\pm}$	1.6550	1.6550	1.6550	1.6550	1.6550
			Perpendicular Polarizabilities (a_0^3)		
(a)	2.570	2.602	2.623	2.628	2.644
(b)	2.582	---	2.630	2.635	2.650

(a) This work. Here a_0 is the Bohr radius.

(b) Gaussian basis set results of reference (27).

Figure III.1. Mean Incremental Polarizability, $\Delta\alpha(R)$, for He_2, as a Function of R .

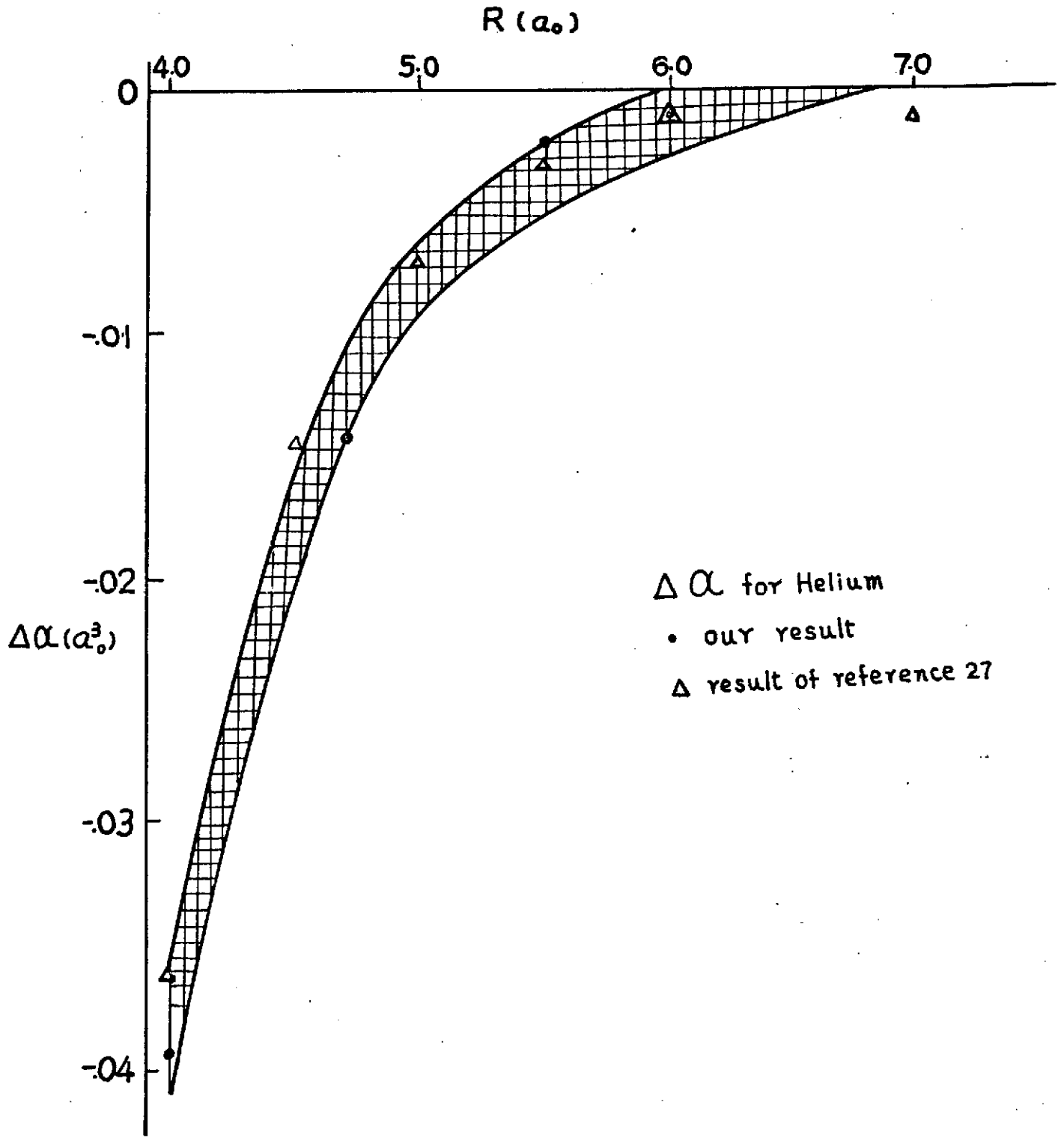
R (a₀)
4.0
5.0
6.0
7.0
0
-.01
-.02
-.03
-.04
Δα (a₀³)
Δ α for Helium
• our result
Δ result of reference 27

Figure III.2. Anisotropy in the Polarizability Tensor, $\underset{\sim}{\beta}(R)$, as a Function of R .

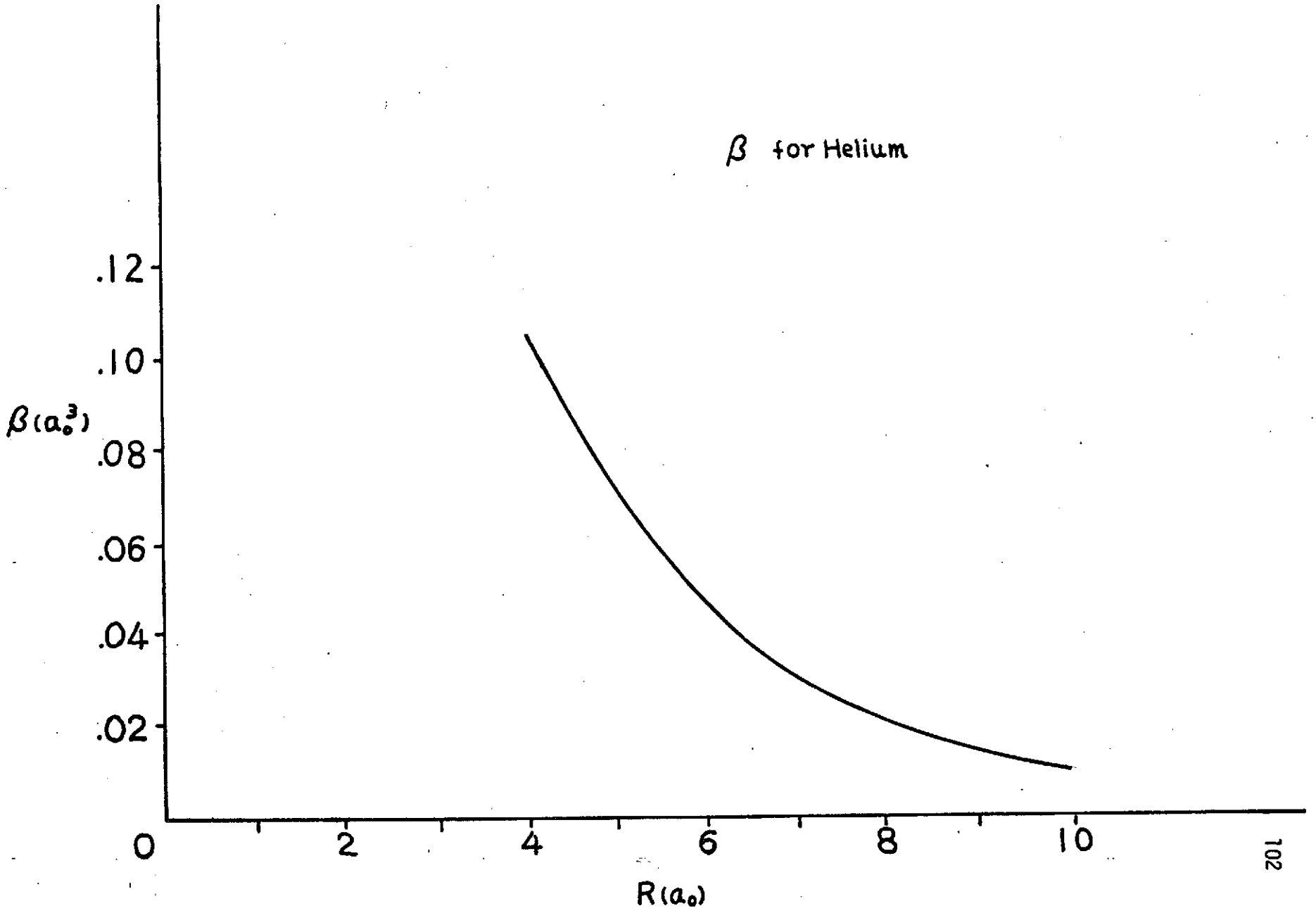
β for Helium
.12
.10
.08
.06
.04
.02
β(a₀³)
0
2
4
6
8
10
R(a₀)

$$\left.\begin{aligned} \Delta\alpha(R) &= 4\alpha_0^3 R^{-6} \\ \text{and} \\ \beta(R) &= 6\alpha_0^2 R^{-3} + 12.07R^{-6} \end{aligned}\right\} R > 6.5a_0 \ . \qquad (3.33)\ (3.34)$$

The successful use of an exponential function to fit our computed mean incremental polarizabilities in the overlap region bears no special physical or mathematical significance. In fact, attempts at fitting the computed parallel and perpendicular curves individually, using a similar functional form, were unsuccessful, so that one cannot justify the use of an exponential fit to our data on any grounds other than convenience. Here, α_0 is the computed atomic polarizability of helium ($1.322a_0^3$) . The use of the long-range extrapolation is justified in the next section.

F. Extrapolation of the Hartree-Fock Polarization to the Long-Range Region

Our calculations do not extend beyond an internuclear separation of $6a_0$ because the increment in the polarizability compared to the atomic limit becomes zero to the accuracy of our calculation. However, the asymptotic atomic limit of the coupled Hartree-Fock polarizability can be derived without explicit calculation.

It is well established computationally that the Hartree-Fock potential energy curves for interacting closed shell atoms are strictly repulsive and do not account for van der Waals (R^{-6}) binding. Qualitatively this occurs because the effective potential for the localized orbitals on one atom is obtained by spatial averaging of the instantaneous multipole moments of the other atom. Since the atoms have no permanent multipole moments, the interactions average to zero, leaving only the repulsive overlap forces as nonvanishing.

In considering the incremental polarizability, a similar situation occurs with the uncoupled Hartree-Fock method.[56,69] Here one calculates the polarizability of the field-free orbitals separately, without allowing the remaining occupied orbitals to simultaneously polarize. Hence, at long range where overlap effects can be neglected, the polarizability of each localized atomic orbital in the diatom is equal to its atomic value, and there are no multipole contributions from the other spherical atom. The asymptotic limit of the uncoupled theory is then, for either component $\alpha_{\parallel}$ or $\alpha_{\perp}$,

$$\alpha(\text{uncoupled}) \sim 2\tilde{\alpha}_0 + \text{overlap terms} ,$$

where $\tilde{\alpha}_0$ is the uncoupled Hartree-Fock polarizability of the atom.

A more interesting situation occurs in a coupled theory,[58,69] such as we have used. Here the polarizability of each orbital is computed with the orbital in the presence of the remaining polarized orbitals. Thus, at large internuclear separations, a localized orbital on one atom feels not only the external field, but also the field due to the induced dipoles on the other atom. This picture is reminiscent of the classical point-dipole model of the incremental polarizability. In fact, we can show that the long-range limit of the coupled Hartree-Fock theory gives precisely the point-dipole model results; namely,

$$\alpha_{\parallel} \sim 2\alpha_0 + 4\alpha_0^2 R^{-3} + 8\alpha_0^3 R^{-6} + \ldots , \tag{3.35}$$

$$\alpha_{\perp} \sim 2\alpha_0 - 2\alpha_0^2 R^{-3} + 2\alpha_0^3 R^{-6} + \ldots , \tag{3.36}$$

where α_0 is the coupled Hartree-Fock polarizability of an isolated helium atom. (We restrict attention to helium, although the results of this section are general for interacting closed shell atoms.)

To prove Eqs. (3.35) and (3.36) we consider two helium atoms at large separations R. The Hartree-Fock energy of the diatom in the presence of an external field $\underset{\sim}{F}$ may be written

$$E \sim 2h_a + J_{aa} - 2\underset{\sim}{\mu}_a \cdot \underset{\sim}{F} + 2h_b + J_{bb} - 2\underset{\sim}{\mu}_b \cdot \underset{\sim}{F} + 4R^{-3}(\underset{\sim}{\mu}_a \cdot \underset{\sim}{\mu}_b - 3\mu_{az}\mu_{bz}) , \tag{3.37}$$

where we have used a localized representation of the wavefunction, $\psi = a(1)a(2)b(3)c(4)$, and the orbital a is centered on nucleus A . We have retained only the leading (R^{-3}) multipole interaction. The various terms in Eq. (3.37) are expectation values of the corresponding operators; e.g.

$$\underset{\sim}{\mu}_a = \langle a|\underset{\sim}{\mu}_a|a\rangle / \langle a|a\rangle \ , \tag{3.38}$$

and

$$J_{aa} = \langle a|\hat{J}_a|a\rangle / \langle a|a\rangle \ , \tag{3.39}$$

where $\hat{J}_a$ is the Coulomb operator,

$$\hat{J}_a = \int a^2(2) r_{12}^{-1} \, d\tau_1 \int a^2(2) \, d\tau_2 \ . \tag{3.40}$$

The Fock equation for the orbital a is obtained by varying the energy E with respect to a , while holding the orbital b fixed. Requiring the energy to be stationary results in the equation

$$[\hat{h}_a + \hat{J}_a - \underset{\sim}{\mu}_a \cdot \underset{\sim}{F} + 2R^{-3}(\underset{\sim}{\mu}_b \cdot \hat{\underset{\sim}{\mu}}_a - 3\mu_{bz}\hat{\mu}_{az}) - \varepsilon]a = 0 \ . \tag{3.41}$$

The proof of the point-dipole model now rests on showing that a self-consistent solution of Eq. (3.41) has the form of a scaled atomic orbital,

$$a = a_0(\zeta F) , \tag{3.42}$$

where ζ is a constant to be determined. Here the orbital a_0 satisfies Eq. (3.41) for $R = \infty$. By symmetry a similar solution holds for the orbital b.

Let us consider two geometries. First suppose F is perpendicular to the internuclear (z) axis; then Eq. (3.42) for b gives

$$\underset{\sim}{\mu}_b = \langle b|\underset{\sim}{\mu}_b|b\rangle/\langle b|b\rangle \equiv p(\zeta F)\zeta\vec{F} . \tag{3.43}$$

The leading term in p is one-half the atomic polarizability α_0, while higher-order terms in F give hyperpolarizabilities. Substituting Eq. (3.43) into Eq. (3.41) we see that the effect of the multipole term is simply to scale the external field. Thus the condition that Eq. (3.42) be a solution to Eq. (3.41) is

$$\zeta = [1 + 2p(\zeta F)R^{-3}]^{-1} . \tag{3.44}$$

With this result for ζ, the dipole moment of the diatom is

$$2\underset{\sim}{\mu}_a + 2\underset{\sim}{\mu}_b = 4p(1 + 2p\ R^{-3})^{-1}\ \underset{\sim}{F} .$$

The diatomic polarizability is the leading term of the expansion of the dipole moment in powers of F ; thus,

$$\alpha_{\perp} = 2\alpha_0(1 + \alpha_0 R^{-3})^{-1} . \qquad (3.45)$$

This is the point-dipole result.

Similarly, an external field parallel to the internuclear axis gives

$$\alpha_{\parallel} = 2\alpha_0(1 - 2\alpha_0 R^{-3})^{-1} , \qquad (3.46)$$

which is also the point-dipole result.

If higher multipoles are retained in Eq. (3.37), more complicated expressions involving quadrupole polarizabilities, etc. are obtained. This also occurs in the classical point-dipole model if field-gradient effects are considered. Such terms do not affect the polarizability through order R^{-6} , however.

In our computations using the finite field method, we did not achieve sufficient numerical accuracy in the long-range region ($R > 6a_0$) to observe the asymptotic limits. Nevertheless, in using the computed polarizability functions, it is legitimate to extrapolate to large internuclear separations via the point-dipole model.

CHAPTER IV

STATISTICAL METHODS

In Chapter I it was noted that, in addition to the polarizability curves, $\alpha_{\parallel}(R)$ and $\alpha_{\perp}(R)$, the computation of the properties in which we are interested require a knowledge of the function $g(R)$ for gaseous helium. This function is the density independent part of the first term in a cluster development of the pair distribution function; that is, it is the pair distribution function for a dilute gas. For high temperatures, this simply involves a knowledge of the interaction potential $U(R)$ for a pair of atoms. In the low temperature regime, however, things are not quite so easy, and one needs to compute the so-called Slater sum, $W_2(q)$, where q represents a complete set of generalized coordinates.

The differences between the classical and quantum mechanical cases arise because the state of a quantal system is specified by a wavefunction, rather than the exact values of the coordinates and momenta, as it is in classical mechanics. In addition, it follows that spin effects give rise to terms in the quantum mechanical $g(R)$ which have no counterpart in the classical expression. In fact, the quantum mechanical $g(R)$ can be written as a sum of two terms:

$$g(R) = g(R)_{direct} \pm g(R)_{exchange} , \qquad (4.1)$$

where the first term is the quantal $g(R)$ for a Boltzmann gas, and reduces to the classical Boltzmann factor in the limit of high temperature. The second term represents spin effects, and is associated with the Bose-Einstein (+) or Fermi-Dirac (-) character of the gas. A discussion of this latter point has been given by Yang and Lee,[70] and several workers have illustrated it with model calculations. Larsen has computed the two terms of Eq. (4.1) for a gas of hard spheres;[71] Larsen, Witte, and Kilpatrick have obtained results for ^4He at low temperatures using a Lennard-Jones 12-6 pair-potential;[72] while Poll and Miller also used a 12-6 potential to compute g_{dir} and $g_{exchange}$ for H_2 gas for temperatures in the range of $2°K$ to $80°K$.[73]

The method used in this work to compute $g(R)$ is that of Klemm and Storer.[74,75] For high temperatures, one can approximate the statistical density matrix $\rho(R,R';\beta)$ $(\beta = 1/kT)$, by expanding it in powers of β, and neglecting terms which are greater than second order in β. The density matrix, ρ, is then given by:

$$\rho = \rho_1 \rho^{(0)} \rho_1 , \qquad (4.2)$$

where the operators ρ_1 and $\rho^{(0)}$ satisfy the differential equations

$$\tfrac{1}{2}H_1\rho_1 = -\frac{\partial\rho_1}{\partial\beta}\,, \tag{4.3}$$

and

$$H_0\rho^{(0)} = -\frac{\partial\rho^{(0)}}{\partial\beta}\,, \tag{4.4}$$

respectively, with boundary conditions

$$\lim_{\beta\to 0}\rho^{(0)}(\underset{\sim}{R},\underset{\sim}{R}';\beta) = \delta(\underset{\sim}{R}-\underset{\sim}{R}') = \lim_{\beta\to 0}\rho_1(\underset{\sim}{R},\underset{\sim}{R}';\beta)\,. \tag{4.5}$$

Here, H_1 and H_0 refer to a partitioning of the Hamiltonian of relative motion, H_r, for a pair of particles. It is generally taken to be the case that H_1 contains the interatomic potential term $U(R)$ of H_r.

Once this high temperature limit has been obtained, one can proceed to lower temperatures in a recursive manner, using the following formula due to Storer:[76,77]

$$\rho(\underset{\sim}{R},\underset{\sim}{R}';2\beta) = \int d\underset{\sim}{R}_2\ \rho(\underset{\sim}{R},\underset{\sim}{R}_2;\beta)\rho(\underset{\sim}{R}_2,\underset{\sim}{R}';\beta)\ d\underset{\sim}{R}_2\,, \tag{4.6}$$

which is a matrix form of the operator relation

$$e^{-2\beta H} = e^{-\beta H}\,e^{-\beta H}\,.$$

If the assumption that the interatomic potential $U(R)$ is spherically symmetric is made, the eigenfunctions of H_r can be expanded in terms of spherical harmonics, so that the density matrix is expanded in the following manner:

$$\rho(\underset{\sim}{R},\underset{\sim}{R}';\beta) = \sum_{\ell=0}^{\infty} \frac{2\ell+1}{4\pi RR'} \rho_\ell(R,R';\beta)\, P_\ell(\cos\omega) \ , \qquad (4.7)$$

where P_ℓ is the Legendre polynomial of order ℓ, ω is the angle between $\underset{\sim}{R}$ and $\underset{\sim}{R}'$, and $\rho_\ell(R,R';\beta)$ is defined by the differential equation,

$$\frac{2\mu}{\hbar^2}\frac{\partial\rho_\ell}{\partial\beta} = \frac{\partial^2\rho_\ell}{\partial R^2} - \left[\frac{\ell(\ell+1)}{R^2} + \frac{2\mu}{\hbar^2}V(R)\right]\rho_\ell = -H_\ell\,\rho_\ell \ , \qquad (4.8)$$

where μ is the reduced mass. The boundary conditions are:

$$\lim_{\beta \to 0} \rho_\ell(R,R';\beta) = \delta(R - R') \qquad \text{for } R,R' > 0 \ , \qquad (4.9)$$

and

$$\rho_\ell(R,R';\beta) = 0 \quad \text{for } R,R' = 0 \ . \qquad (4.10)$$

These equations can be transformed to be compatible with the form of Eqs. (4.3) and (4.4), by defining,

$$H_\ell^0 = -\frac{\partial^2}{\partial R^2} + \frac{\ell(\ell+1)}{R^2} , \tag{4.11}$$

and

$$H_\ell^1 = U(R) , \tag{4.12}$$

so that the analogues of Eqs. (4.3) and (4.4) are respectively:

$$\tfrac{1}{2}U(R)\rho_1 = -\frac{\partial \rho_1}{\partial \beta} , \tag{4.13}$$

and

$$\frac{\partial^2 \rho_\ell^{(0)}}{\partial R^2} - \frac{\ell(\ell+1)}{R^2}\rho_\ell^{(0)} = \frac{\partial \rho_\ell^{(0)}}{\partial \beta} . \tag{4.14}$$

The solutions of this latter equation are the ℓ-th partial wave contributions to the free particle density matrix,

$$\rho_\ell^{(0)}(R,R';\beta) = \left(\frac{2\pi\hbar^2\beta}{\mu}\right)^{-3/2} 4\pi RR' \exp\left[-(R^2 + R'^2)/\left(\frac{2\hbar^2\beta}{\mu}\right)\right] i_\ell\left(\frac{RR'}{2\beta}\right) , \tag{4.15}$$

where i_ℓ is the Modified Spherical Bessel function of the first kind, defined by:[78]

$$i_\ell(z) = \sqrt{\frac{\pi}{2z}}\, I_{\ell+\frac{1}{2}}(z) . \tag{4.16}$$

Thus, we can make the initial high temperature approximation:

$$\rho_\ell(R,R';\beta) \cong e^{-(\beta/2)U(R')}\, \rho_\ell^{(0)}(R,R';\beta) e^{-(\beta/2)U(R)} , \qquad (4.17)$$

and extend this lower temperatures using Eq. (4.6), which for the partial wave expansion becomes:

$$\rho_\ell(R,R';2\beta) = \int_0^\infty \rho_\ell(R,R_2;\beta)\rho_\ell(R_2,R';\beta)\, dR_2 . \qquad (4.18)$$

In practice, one evaluates the various functions over a finite grid, so that Eq. (4.18) becomes an $n \times n$ matrix. Thus one can use a Simpson's rule quadrature to evaluate the right of Eq. (4.18) to reduce it to a square of the $n \times n$ density matrix. One then proceeds to lower temperatures by performing standard matrix multiplication.

The expression for g_{dir} and $g_{exchange}$ for a given value of β, in terms of the partial wave expansion are:

$$g_{dir}(R) = \left(\frac{2\pi\hbar^2\beta}{\mu}\right)^{3/2} \sum_{\ell=0}^{\infty} \frac{2\ell+1}{4\pi R^2} \rho_\ell(R,R;\beta) , \qquad (4.19)$$

and

$$g_{exchange}(R) = \left(\frac{2\pi\hbar^2\beta}{\mu}\right)^{3/2} (2S+1)^{-2} \sum_{\ell=0}^{\infty} \frac{2\ell+1}{4\pi R^2}(-1)^\ell \rho_\ell(R,R;\beta) . \qquad (4.20)$$

A detailed account of this method and a listing of the computer program which is used to carry it out, can be found in reference (75).

For the helium isotopes ^3He and ^4He (the masses used in this work are respectively 3.0160 and 4.0026 amu) low temperature calculations of $g(R)$ were made at $T = 4°K$. To get down to this temperature, a starting temperature of $1024°K$ was used, so that eight iterations were required. The adequacy of this starting temperature was established by comparison of our ^4He results at $2°K$ (9 iterations) with those of reference (72); agreement to at least three places was obtained. In this work, we used a mesh size of .025 (in units of $\sigma = 2.556$ Å) at higher temperatures, and .10 at lower temperatures for the Simpson's rule integration of Eq. (4.18). By numerical experimentation, we found that twenty partial waves were sufficient for three decimal place accuracy. In this work, the MDD-2 pair potential of Bruch and McGee was used.[12] This potential combines a Morse potential for separations less that $6.96a_0$, with a dispersion dipole plus quadrupole result for separations greater than or equal this core. The potential parameters for helium along with the resulting asymptotic forms of $g(R)$ are given in Table IV.1.

For future reference, a plot of the values of $g(R)$ for ^3He and ^4He at $T = 4°K$ is given in Figure IV.1, and the $g(R)$ values are listed in Table IV.2.

Table IV.1. MDD-2 pair-potential and long-range g(R) for helium.[a,b,c]

MDD-2 Pair-Potential:

$$\frac{1}{k} V(R) = -\frac{36.4778}{R^6} - \frac{15.0935}{R^8} \qquad R > 1.44085 \ \sigma\text{-units}$$

$$\frac{1}{k} V(R) = 10.75[e^{[2c(1-x)]} - 2e^{[c(1-x)]}]^{d} \qquad R \leq 1.44085 \ \sigma\text{-units}$$

Long-Range g(R) Expressions:

$$g(R) = 1 - \frac{V(R)}{kT} - \frac{\hbar^2}{6mk^2T^2} V^{e} \qquad R > 3.1 \ \sigma\text{-units}$$

^{3}He, T = 4°K $\qquad g(R) = 1 + \frac{9.11945}{R^6} + \frac{31.8405}{R^8} + \frac{21.6784}{R^{10}}$

^{4}He, T = 4°K $\qquad g(R) = 1 + \frac{9.11945}{R^6} \quad \frac{24.9223}{R^8} \quad \frac{16.3349}{R^{10}}$

[a] See reference (12).

[b] R is assumed to be in σ-units (σ = 2.556 Å), $\frac{1}{k} V(R)$ is obtained in °K.

[c] k = Boltzmann's constant = 1.38062 ergs/°K.

[d] x = R/1.8302, c = 6.1277.

[e] This expression is valid for large R values, the use of R = 3.1 σ-units was chosen in our calculation by convenience.

Table IV.2. Radial distribution functions for ^3He and ^4He at T = 4°K .[a]

R(σ-units)	g(^{3}He)	g(^{4}He)	R(σ-units)	g(^{3}He)	g(^{4}He)
0.700	0.000	0.000	2.000	1.251	1.282
0.800	0.008	0.006	2.100	1.205	1.217
0.900	0.076	0.076	2.200	1.164	1.164
1.000	0.284	0.330	2.300	1.129	1.123
1.100	0.606	0.755	2.400	1.101	1.092
1.200	0.931	1.181	2.500	1.078	1.069
1.300	1.177	1.480	2.600	1.060	1.052
1.400	1.326	1.626	2.700	1.046	1.040
1.500	1.395	1.655	2.800	1.036	1.031
1.600	1.408	1.613	2.900	1.028	1.024
1.700	1.388	1.536	3.000	1.022	1.019
1.800	1.348	1.447	3.100	1.017	1.015
1.900	1.300	1.360			

[a] 1σ-unit = 2.556 Å .

Figure IV.1. Pair Distribution Functions for Helium at 4°K and 322°K as a Function of R .

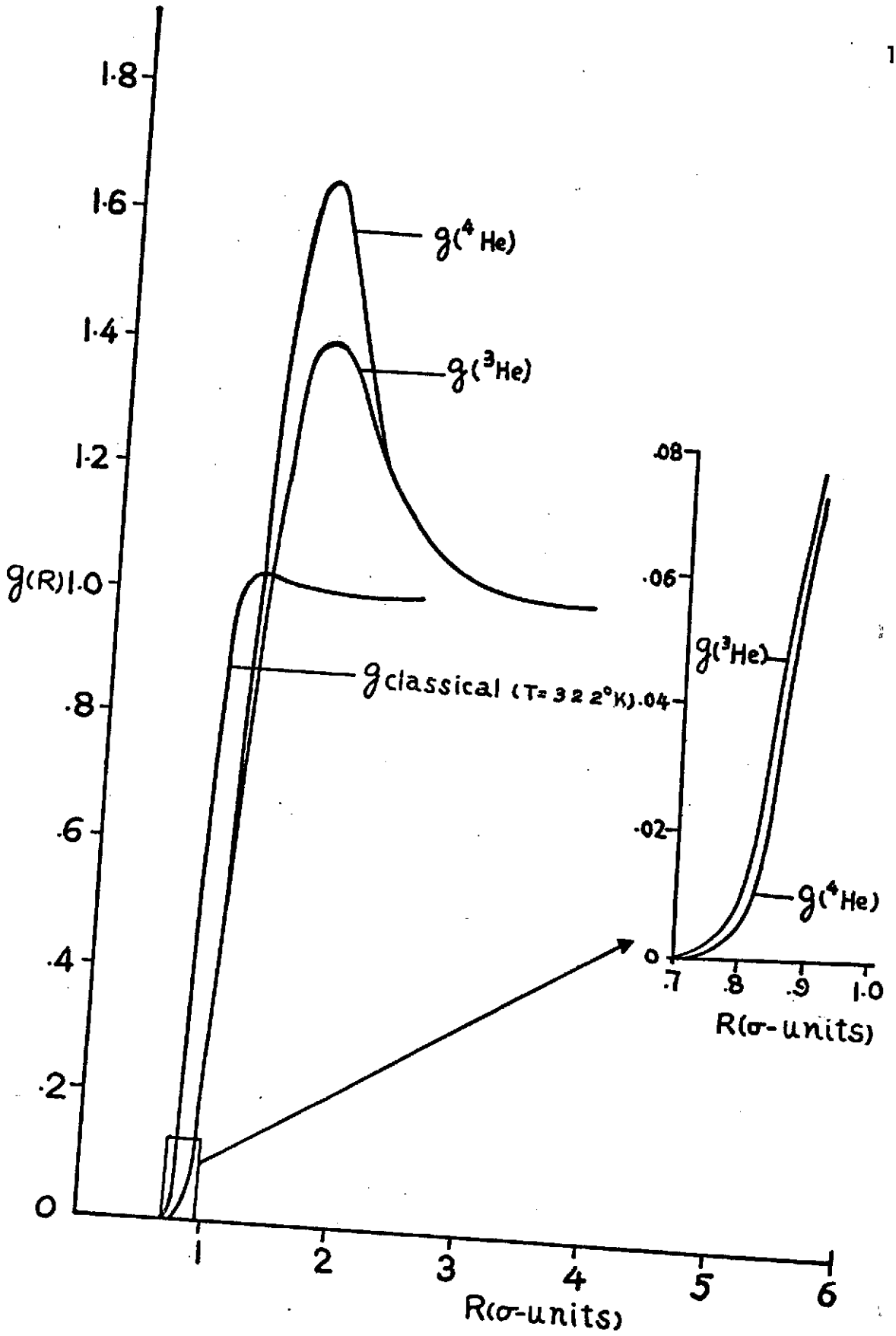
1·8
1·6
1·4
1·2
g(R) 1·0
·8
·6
·4
·2
0
g(⁴He)
g(³He)
g classical (T= 3 2 2°K)
1
2
3
4
5
6
R(σ-units)
·08
·06
·04
·02
0
g(³He)
g(⁴He)
·7
·8
·9
1·0
R(σ-units)

CHAPTER V

RESULTS AND DISCUSSION

A. Results

A problem worthy of attack
Proves its worth by striking back.

--A Grook by Piet Hein

In Chapters II and III we have discussed the calculation of the polarizability functions $\Delta\alpha$ and β for the helium diatom. The results of the calculation are summarized in Eqs. (3.31)-(3.34) and in Tables III.8 and III.9 and Figures III.1 and III.2. In Chapter IV we have discussed the helium radial distribution function $g(R)$, which is given in Table IV.2 and Figure IV.1. We are now ready to put these results together to calculate the experimental quantities introduced in Chapter I.

The macroscopic quantities are related to the corresponding molecular properties through integrals weighted with $g(R)$. The second dielectric virial coefficient B_ε (see Eqs. (1.34) and (1.39)) is an average of the mean incremental polarizability $\Delta\alpha$. The second Kerr virial coefficient B_K (see Eq. (1.45)) is an average of the anisotropy β^2. The Raman depolarization ratio $\bar{D}$ (see Eq. (1.58)) reflects both $\Delta\alpha^2$ and β^2, but is dominated by β. Thus

the experimental quantities are complementary with respect to the components of the polarizability tensor.

The integrals involved in B_ε , B_K and $\bar{D}$ were evaluated numerically by Simpson's Rule quadrature. The final integration grids were chosen by varying the number of points in the grid until further reduction of mesh size left the value of the integrals unchanged, to the number of places to which the results are reported. The upper limit at which the integration was truncated was determined in the same manner. It was found sufficient to use integration steps of .04 σ-units over the range .65 to 4.55 σ-units. The B_ε results were checked by transforming the corresponding range of integration to the interval $[-1,1]$, and numerical integrating the result using a 64-point Gausian quadrature. The conversion factors from atomic units to the experimental units is given in Appendix E.

The results of our calculations of B_ε , B_K , and $\bar{D}$ are presented in Table V.1. They are summarized as follows. Our calculated value of B_ε is within the rather large experimental error bars at 322K. We are also in order of magnitude agreement with the results at 4K, but we predict the isotopic dependence to be opposite to that observed experimentally; we shall discuss this discrepancy in further detail below, where the quantities B_ε^U and B_ε^L will be explained.

Our calculated B_K at 300K verifies the null experimental result. We predict that the contribution of the second virial term

Table V.1. Dielectric and light scattering properties of fluid helium.

Property	T = 322°K	T = 4°K	
		^{3}He	^{4}He
Second dielectric virial coefficient, B_ε	-.094 cm^6/mole^2 (-0.93 cm^6/mole^2)[a] (-.06 ± .04 cm^6/mole^2)[b]	-.025 cm^6/mole^2 (-.030 cm^6/mole^2)[c]	-.030 cm^6/mole^2 (-.023 cm^6/mole^2)[c]
B_ε^U	-.086 cm^6/mole^2	-.012 cm^6/mole^2	-.015 cm^6/mole^2
B_ε^L	-.135 cm^6/mole^2	-.034 cm^6/mole^2	-.041 cm^6/mole^2
Second Kerr virial coefficient, B_K	2.4 × 10^{-15} esu (3.1 × 10^{-15} esu)[a]	1.2 × 10^{-13} esu	1.4 × 10^{-13} esu
Depolarization ratio for Raman scattering, $\overline{D}$	4/3 + .37 4/3 + .44[a]	4/3 + .08	4/3 + .07 (1.33 ± .20)[d] (1.39 ± .20)[d]

[a] Calculation of reference (27); temperature used was 300°K.

[b] Experimental results of reference (1a).

[c] Experimental results of reference (1b).

[d] Experimental results of reference (36).

to the observed Kerr constant of helium to be .1% at room temperature and pressures of 50 atm., which is not observable. However at 4K, the B_K is larger than the room temperature result by a factor of 50, and the second virial term contributes 14%, at a pressure of 1 atm. Thus it may well be possible to detect the B_K at 4K.

Our calculated value of $\overline{D}$ differs from the purely geometrical value of $\frac{1}{3}$ by only 7%. Thus, it is not likely that Raman scattering from $\Delta\alpha$ can be observed by measuring depolarization ratios.

We turn now to a consideration of errors in our calculation. In particular we wish to assess the significance of the discrepancy with experiment in the isotopic dependence of B_ε at low temperatures. The values of B_ε reported in Table V.1 were obtained using the Hartree-Fock polarizability curve given in Eqs. (3.31) and (3.32). Thus, the use of our computed $\Delta\alpha$ curve can be questioned on two main points: there is a basis set error associated with the fact the Hartree-Fock-Roothaan prescription is carried out with a (necessarily) finite basis set; and, there is an inherent (correlation) error associated with even the exact Hartree-Fock result. In Section B, the former point is discussed, and our calculation is compared to that of O'Brien et al. In Section C, the correlation error is discussed, while Section D contains our conclusions.

With respect to errors in $g(R)$, we have pointed out that at 2°K, our $g(R)$ values are in agreement with the calculation of

reference (72) to at least three decimal places. Variation of computational parameters in the direction which would produce a more accurate g(R) produced changes in, at worst, the fifth decimal place. Further, the method used here was shown to give good values of the second pressure virial coefficient in the calculations of reference (74).

B. Basis Set Error

As has been pointed out in earlier chapters, one of the main objectives of our work was to compute the Hartree-Fock limit for the polarizability of the helium dimer for those internuclear separations which contribute to certain experimental observables.

By definition, the Hartree-Fock limit for a given property is that which is obtained through the exact solution of the Hartree-Fock equations. Except for field-free atoms, however, the Hartree-Fock equations are generally solved as we have done, via basis set expansion of the molecular orbitals, using the Hartree-Fock-Roothaan scheme. This means that the Hartree-Fock limit corresponds to zero basis set error in this analytical method of solution.

In terms of basis set selection procedures, the problem of obtaining the Hartree-Fock limit for field-free diatomic molecules is solved, and, in fact, actual calculations have been performed for many diatomic molecules, including the one of interest here, He_2.[63] From the viewpoint of perturbation theory, one should require that

the Hartree-Fock limit of the perturbed problem should relax to the field-free Hartree-Fock limit as the field is turned off. Thus, if the effect of the field is to couple the zero-order basis functions to functions of a different symmetry (this is the case for fields applied perpendicular to the internuclear axis of a diatomic molecule), it is clear that this can be accomplished by augmenting the optimized field-free basis set with functions which describe their distortion by the applied field. For cases in which the polarization functions are of the same symmetry (as is the case for fields applied parallel to the internuclear axis of a diatomic molecule) one follows the same prescription. The reason for this is that if the field-free wavefunction truly represents the Hartree-Fock limit, the effect of the polarization functions on the energy and properties for the zero-field case will be minimal.

The manner in which we selected the basis set in this work, was described earlier (Section C of Chapter III). With respect to assessing the success of our approach in light of the foregoing discussion, the following three points are significant:

1. Our zero-order set was essentially a Hartree-Fock limit set, with orbital exponents optimized (by Kestner) at each internuclear separation.
2. Any reduction in either the zero-order or polarization set was made only after it was justified by numerical experimentation.

3. The Hartree-Fock limit of the polarizability was obtained for both the separated and united atom limits, using atomic extensions of the diatomic prescription.

Based on his own basis set variations, and on the results of the more elaborate calculations of Gilbert and Wahl, Kestner asserts that the total energies computed with his wavefunction differ from the Hartree-Fock limit values by less than one part in 10^7. To this extent, one can be confident that the choice of Kestner's wavefunction is a reasonable one. Although we used the same basis functions for both the σ_g and σ_u occupied orbitals, whereas Kestner used different ones for each, the effect of this difference is expected to be small, since the corresponding change in the field-free energy is on the order of a few parts in 10^6. This means that as the field is turned off, we still relax to a function which obtains essentially the Hartree-Fock limit for the energy.

It, of course, does not follow that any function which yields the Hartree-Fock limit for the zero-order energy is as good for second-order property calculations as any other which also yields this limit. However, additional credence is lent to our results because our basis goes smoothly into that for the separated atom limit, for which we obtain the correct coupled Hartree-Fock limit polarizability.

In comparing our results to those of O'Brien et al., three points are especially noteworthy: first, in their calculation, they used

the same (Gaussian) basis set for all values of the internuclear separation; second, the difference between the Hartree-Fock limit for the total energy and their total energy is on the order of a part in 10^4; third, they failed to obtain the coupled Hartree-Fock limit for the polarizability of the helium atom.

The use of a single basis set for all internuclear separations has the advantage that smoothness is automatically built into the polarizability curve. For the case in which the single basis is an atomic set, one thereby introduces the so-called distortion error.[61] Using our basis set, this amounts to an error of about .003 a_0^3 in $\alpha_\perp$ at $R = 6.0\ a_0$. This and the use of a Gaussian basis set are probably the major source of error in the computed, zero-order potential curve of O'Brien et al.

The most significant difference between our results and theirs is that they do not obtain the Hartree-Fock limit for the polarizability at the separated atom limits. In fact, while our values of $\alpha(R)$ are slightly below theirs, our values of $\Delta\alpha(R)$ are about the same; this is because their value of $2\alpha_0$ is greater than the Hartree-Fock limit by about the same amount that their values of $\alpha(R)$ are greater than ours.

We estimate that our results are within about .002 a_0^3 of the Hartree-Fock limit of the polarizability for R values between $4.0\ a_0$ and $5.5\ a_0$, and are within about .001 a_0^3 for R values between $5.5\ a_0$ and $6.0\ a_0$. Curves for $\Delta\alpha$ which correspond to our error estimates are given as follows:

$$\alpha^U(R) = -14.5\exp(-1.48R) + .0085/R \ , \quad R \leq 6.0 \ a \ , \quad (5.1)$$

$$\alpha^L(R) = -12.9\exp(-1.45R) - .0127\exp(-.462R) \ , \quad R \leq 7.0 \ a \ . (5.2)$$

For large values of R we use the point dipole result, Eq. (1.37) and (1.38). These curves are shown as the bounding curves in Figure III.1. The corresponding values of the second dielectric virial coefficient are denoted by B_ε^U and B_ε^L in Table V.1. In this table the "U" superscript refers to the result obtained using Eq. (5.1) while the "L" superscript refers to the result obtained using Eq. (5.2). We should emphasize that these bounds are based on "best guesses" of errors, and are not quantitative. The anisotropy curve which is of interest for the B_K calculations is given in Figure III.2.

It is apparent from Table V.1 that the magnitude of B_ε depends markedly on which $\Delta\alpha(R)$ curve one uses; in fact, the value of B^L at room temperature is seen to be out of the experimental range. It is equally apparent, however, that the isotopic ordering of the low temperature results is the same regardless of which $\Delta\alpha(R)$ curve is used. Thus, we conclude that basis set error does not account for the low temperature isotopic discrepancy.

C. Electron Correlation Effects

This section is not intended to be a general comment on the effects of electron correlation on molecular polarizabilities, but rather, it concerns itself with whether or not this effect can account for the isotopic reversal of our values of the second dielectric virial coefficient for ^3He and ^4He relative to experiment.

To get a better feeling for the problem, one can examine Figure IV.1, which shows a plot of the $g(R)$ values we obtain for ^3He and ^4He at 4°K, along with that for room temperature helium gas. Our $\Delta\alpha(R)$ points are plotted in Figure III.1. The isotopic differences between the $g(R)$ curves at this temperature is due to mass effects: that is, the larger mass of ^4He results in an increase of ^4He density over the well, while the smaller mass of ^3He allows it to tunnel further into the barrier than ^4He. The order of the B_ε values which results is then a resolution of the question whether or not the slightly greater penetration into the barrier by ^3He to regions of more negative $\Delta\alpha(R)$ can overcome the significant increase in ^4He density over the well.

In order to effect the reversal of our results by invoking correlation effects, one must argue that the effect of correlation is to "pull up" the $\Delta\alpha(R)$ curve for internuclear separations over the well and "pull it down" in the tunneling region. This latter effect is limited for two reasons: first, $\Delta\alpha(R)$ is bounded from below because $\alpha(R)$ must be positive for a molecule in its ground state;

second, even within the constraint introduced by the above point, a decrease in the Hartree-Fock $\Delta\alpha(R)$ curve in the tunneling region for a broad range of R values will destroy the agreement between the room temperature experiments and the Hartree-Fock calculation. Thus, in order to agree with experiment, one would have to require that the effect of correlation on the incremental polarizability curve is to make $\Delta\alpha(R)$ positive over the well, negative and sharply decreasing in the region where $g(^3He) > g(^4He)$, and negative but increasing in the region where the classical $g(R)$ is large, and the quantal $g(R)$ curves are small.

The results of earlier chapters indicate that the correlation contribution to the mean incremental polarizability in the dispersion region is positive, and is given by:

$$\alpha_{Corr}(\text{long-range}) = (38.98 - 9.24)R^{-6}\, a_0^3 .$$

Here, $38.98\, a_0^9$ is the accurate A_6 result of Chapter II, and $9.24\, a_0^9$ is the corresponding point dipole value. If one assumes that the multipole expansion is valid into $R = 6.5\, a_0$, this results in slight increase in B_ε for ^4He relative to ^3He.

For separations in the overlap region, the correlation correction is not known, and any conclusions are therefore speculative. To obtain an idea of what one is up against in this region, we denote the exact (correlated) result by α, and the

Hartree-Fock result by $\tilde{\alpha}$, $\Delta\alpha$(correlated) by $\Delta\alpha$, $\Delta\alpha$(Hartree-Fock) by $\widetilde{\Delta\alpha}$, and consider the following:

$$\Delta\alpha = \alpha(R) - 2\alpha_0 ,$$

$$\widetilde{\Delta\alpha} = \tilde{\alpha}(R) - 2\tilde{\alpha}_0 ,$$

or,

$$\Delta\alpha = \Delta\tilde{\alpha} - .122a_0^3 + (\alpha(R) - \tilde{\alpha}(R)) ,$$

where we have used the known result, $\alpha_0 - \tilde{\alpha}_0 = 0.061a_0^3$.[65] The sign of $\Delta\alpha$ in a given range of R is determined by the sign of the last term on the right-hand side of this equation, since the first two terms are both negative. Intuitively, one might expect this term to be negative in the region of the van der Waals well, corresponding to the greater diffuseness of the Hartree-Fock wavefunction compared to the correlated function. This is the case for most atoms and for H_2 at its equilibrium separation. However, definitive statements regarding He_2 can be made only by actually performing the correlated polarizability calculation.

In an attempt to match the isotopic dependence and magnitude of the experimental data at 4°K and 322°K, we adopted several ad hoc models. These models served to distort the Hartree-Fock $\Delta\alpha(R)$

curve in a manner which is consistent with the ideas discussed earlier in this section. The resulting $\Delta\alpha(R)$ curve required a maximum of .10 a_0^3 in the region of the well, and a minimum of about -.30 a_0^3 in the tunneling region. While this general shape is not implausible, the actual numbers involved, require that the correlation correction to the mean incremental polarizability be an order of magnitude larger than $\Delta\alpha$(Hartree-Fock).

The effect of correlation of the mean incremental polarizability on the properties other than B_ϵ listed in Table V.1, is minimal, so that no insight as to its magnitude can be inferred from those experiments.

D. Summary and Conclusions

The largest part of the discussion has dealt with the dielectric constant experiments, as this is the only place where a conflict between the present work and experiment has appeared. To summarize our dielectric constant results, we see that we get good agreement between our computed results and those of the room temperature measurements, and order of magnitude agreement with the low temperature experiments, but with reversed isotopic dependence. Ad hoc modification of the incremental mean polarizability curve within what we take to be reasonable limits does not reverse this result. Our estimates of the other properties which we considered all agree with experiment where such experiments have been performed; agreement with

other calculations of the high temperature properties is also good, although the corresponding polarizability curves are somewhat different. In this respect, we believe our calculations represent the Hartree-Fock limit more closely than the others do.

Further, it is our opinion that the disagreement with experiment is a consequence of using too small error assignments in the difficult experiments. This reflects on the analysis of the experiment in two ways: first, in the region of low densities where the virial expansion is certainly valid, the data exhibits a large amount of scatter, so as to render these points relatively useless as data in a linear least-squares fit. On the other hand, in the region in which the scatter is smallest the number densities are quite high. At these densities, a two-term virial expansion of the equation-of-state is known to be a poor approximation. Thus the density coefficient quoted by Kerr and Sherman may be an <u>average</u> slope, as distinct from the <u>initial</u> slope which defines B_ε. Neither of these problems appear in the room temperature data of Orcutt and Cole.

Our results indicate that <u>à priori</u> calculations of the molecular properties of helium can now make meaningful contributions to the interpretation of experimental data, and we believe that renewed experimental and computational efforts on the dielectric properties of helium is very desireable. In this connection, additional calculations on X-ray structure factors for liquid helium; third

pressure virial coefficients for the gas, and Raman scattering line shapes are presently being carried out in this laboratory.

APPENDIX A

SYMMETRY REDUCTION PROCEDURE USED IN THE LONG-RANGE CALCULATION

The reduction of Eq. (2.32) to (2.48) is long but straightforward. We shall illustrate the technique for a simple example, and then present a table of results. Consider the single-center matrix element,

$$I = \langle \phi_0 | \mu_m \mu_{-m} | \phi_0 \rangle , \qquad (A.1)$$

where $\mu_{\pm m} \sim Y_{1,\pm m}$, and $Y_{\ell m}$ represents the usual spherical harmonic. In this work, we used the phase convention, $Y^*_{\ell,m} = (-1)^m Y_{\ell m}$.

The intent of the symmetry reduction is to relate the matrix elements of the form (A.1) which have $m \neq 0$ to those which have $m = 0$, so that Eq. (2.32) can be simplified. To effect this, it is natural to make use of the Wigner-Eckart theorem.[45] This theorem states that, in a standard representation $\{\hat{J}^2, \hat{J}_z\}$, whose basis functions are denoted by $|\tau, J, M\rangle$, the matrix element $\langle \tau JM | T^{(K)}_q | \tau' J' M' \rangle$ of the q-th standard component of the k-th

order irreducible tensor operator, $T^{(K)}$, is equal to the product of a Clebsch-Gordon coefficient, $\langle J'KM'q|JM\rangle$ and a quantity which is independent of M, M', and q . That is,

$$\langle \tau JM|T_q^{(K)}|\tau'J'M'\rangle = \langle \tau J||T^{(K)}||\tau'J'\rangle\langle J'KM'q|JM\rangle , \qquad (A.2)$$

where the quantity $\langle \tau J||T^{(K)}||\tau'J'\rangle$ is known as the reduced matrix element, and can be evaluated by using a particular value of M for which the left-hand side of Eq. (A.2) can be easily evaluated directly.

In the following, we ignore the radial part of the functions μ_m , as they are independent of m , so that we take,

$$\langle \phi_0|\mu_m \mu_{-m}|\phi_0\rangle \sim \langle \phi_0|Y_{1,m} Y_{1,-m}|\phi_0\rangle \qquad (A.3)$$

Then,

$$\langle \phi_0|Y_{1,m} Y_{1,-m}|\phi_0\rangle = (-1)^m \langle Y_{1,m} \phi_0|Y_{1,m} \phi_0\rangle \qquad (A.4)$$

$$= (-1)^m \sqrt{4\pi} \langle Y_{1,m} \phi_0|Y_{0,0}|Y_{1,m} \phi_0\rangle , \qquad (A.5)$$

and

$$\langle \phi_0|Y_{1,0} Y_{1,0}|\phi_0\rangle = \sqrt{4\pi} \langle Y_{1,0} \phi_0|Y_{0,0}|Y_{1,0} \phi_0\rangle . \qquad (A.6)$$

Now, since the $2k+1$ spherical harmonics $Y_{k,q}$ ($q = -k, -k+1, \ldots, k-1, k$) considered as operators, are the standard components of an irreducible tensor operator of order k, $T^{(k)}$, we can write Eq. (A.5) as:

$$(-1)^m \sqrt{4\pi} \langle Y_{1,m}\phi_0 | Y_{0,0} | Y_{1,m}\phi_0 \rangle = (-1)^m \sqrt{4\pi} \langle Y_{1,m}\phi_0 | T_{0,0} | Y_{1,m}\phi_0 \rangle . \quad (A.7)$$

Further, since ϕ_0 has S-type symmetry, the right-hand side of this last equation is of the form of Eq. (A.2), so that we can apply the Wigner-Eckart formula to Eq. (A.7) for the two cases $m = 0,1$:

$$\langle Y_{1,1}\phi_0 | T_{0,0} | Y_{1,1}\phi_0 \rangle = \begin{pmatrix} 1 & 0 & 1 \\ -1 & 0 & 1 \end{pmatrix} \langle \tau,1 || T_0 || \tau',1 \rangle , \quad (A.8)$$

and

$$\langle Y_{1,0}\phi_0 | T_{0,0} | Y_{1,0}\phi_0 \rangle = (-1) \begin{pmatrix} 1 & 0 & 1 \\ 0 & 0 & 0 \end{pmatrix} \langle \tau,1 || T_0 || \tau',1 \rangle , \quad (A.9)$$

where we have replaced the Clebsch-Gordon coefficient of Eq. (A.2) with the corresponding Wigner 3-j symbol. Thus,

$$\langle \phi_0 | Y_{1,m} Y_{1,-m} | \phi_0 \rangle = (-1)\sqrt{4\pi} \begin{pmatrix} 1 & 0 & 1 \\ -1 & 0 & 1 \end{pmatrix} \langle \tau,1 || T_0 || \tau',1 \rangle , \quad (A.10)$$

and

$$\langle\phi_0|Y_{1,0}Y_{1,0}|\phi_0\rangle = (-1)\sqrt{4\pi}\begin{pmatrix}1 & 0 & 1\\ -1 & 0 & 1\end{pmatrix}\langle\tau,1||T_0||\tau',1\rangle \quad . \quad (A.11)$$

but since

$$\begin{pmatrix}1 & 0 & 1\\ 0 & 0 & 0\end{pmatrix} = -\frac{1}{\sqrt{3}} ,$$

and

$$\begin{pmatrix}1 & 0 & 1\\ -1 & 0 & 1\end{pmatrix} \quad \frac{1}{\sqrt{3}} ,$$

we get:

$$\langle\phi_0|\mu_0\mu_0|\phi_0\rangle = -\langle\phi_0|\mu_1\mu_{-1}|\phi_0\rangle \quad . \quad (A.12)$$

We needed a number of relations such as Eq. (A.12). They are collected together in Table A. These results can also be obtained by using explicit relations for the $Y_{\ell m}$'s or by raising-lowering operator techniques.

Let us now outline the symmetry reduction of Eq. (2.32) for A_6 . First we note two simplifications:

1. The dipole moment operator can be replaced by $\hat{\mu}^a$, the dipole operator for atom a , since the cross terms involving $\hat{\mu}^a$

and μ^b vanish. The final expression is symmetrized by multiplying by $(1 + P_{ab})$, where P_{ab} exchanges the labels of a, b.

2. The resolvent r_0 is spherically symmetric about each center, and hence the excited atomic states behave like the spherical harmonics $Y_{\ell m}$.

The dipole-dipole interaction operator can be written

$$V_3 = -\tfrac{1}{2}\mu_+^a \mu_-^b - \tfrac{1}{2}\mu_-^a \mu_+^b - 2\mu_0^a \mu_0^b ,$$

where $\mu_0 = \mu_z$, $\mu_+ = -\mu_x - i\mu_y$ and $\mu_- = \mu_x - i\mu_y$. Then one of the nonzero terms in A_6 is

$$\langle\phi_0|V_3\, r_0\, V_3\, r_0\, \hat{\mu}_+ r_0\, \hat{\mu}_-|\phi_0\rangle = (1+P_{ab})\langle\phi_0|V_3\, r_0^{ab}\, V_3\, r_0^a\, \mu_+^a\, r_0^a\, \mu_-^a|\phi_0\rangle$$

$$= \tfrac{1}{4}(1+P_{ab})\langle\phi_0|\mu_+^a\, \mu_-^b\, r_0^{ab}\, \mu_-^a\, \mu_+^b\, r_0^a\, \mu_+^a\, r_0^a\, \mu_-^a|\phi_0\rangle + \ldots .$$

For the excitations involving atom b, we have

$$\langle Y_{1-1}Y_{11}\rangle\langle(Y_{11})^* Y_{11}\rangle = -\langle Y_{1-1}Y_{11}\rangle^2 = -\langle Y_{10}\rangle^2 .$$

For atom a, the middle resolvent can involve either excited $S(Y_{00})$ or $D(Y_{2m})$ states. Thus, there are two possibilities:

$$\langle Y_{11}Y_{1-1}\rangle\langle Y^{*}_{1-1}Y_{1-1}Y_{00}\rangle\langle Y_{00}Y_{11}Y_{1-1}\rangle\langle Y^{*}_{1-1}Y_{1-1}\rangle$$

$$= (-1)(+1)(-1)(+1)\langle Y_{10}Y_{10}\rangle\langle Y_{10}Y_{10}Y_{00}\rangle\langle Y_{00}Y_{10}Y_{10}\rangle\langle Y_{10}Y_{10}\rangle$$

and

$$\langle Y_{11}Y_{1-1}\rangle\langle Y_{1-1}Y_{1-1}Y_{20}\rangle\langle Y_{20}Y_{11}Y_{1-1}\rangle\langle Y_{1-1}Y_{1-1}\rangle$$

$$= (-1)(-\tfrac{1}{2})(\tfrac{1}{2})(+1)\langle Y_{10}Y_{10}\rangle\langle Y_{10}Y_{10}Y_{20}\rangle\langle Y_{20}Y_{10}Y_{10}\rangle\langle Y_{10}Y_{10}\rangle \ .$$

This gives

$$\langle\phi_0|\mu_+^a\,\mu_-^b\,r_0^{ab}\,\mu_-^a\,\mu_+^b\,r_0^a\,\mu_+^a\,r_0^a\,\mu_-^a|\phi_0\rangle$$

$$= \langle\phi_0|\mu_0^a\,\mu_0^a\,r_0^{ab}\,\mu_0^a\,\mu_0^b\,r_0^a\,\mu_0^a\,r_0^a\,\mu_0^a|\phi_0\rangle_S$$

$$+ \tfrac{1}{4}\langle\phi_0|\mu_0^a\,\mu_0^a\,r_0^{ab}\,\mu_0^a\,\mu_0^b\,r_0^a\,\mu_0^a\,r_0^a\,\mu_0^a|\phi_0\rangle_D \ ,$$

where the subscript S and D refer to the symmetry of the excited states in the middle resolvent.

In the way we have just illustrated, we reduced Eq. (2.32) to Eq. (2.48), with the coefficients given in Table II.1.

Table A.1. Symmetry reduction of sperical harmonics. The angular brackets < > denote spherical averages.

$\langle Y_{11}Y_{1-1}\rangle = -\langle Y_{10}^2\rangle$
$\langle Y_{10}Y_{11}Y_{2-1}\rangle = -\frac{r_3}{2}\langle Y_{10}^2 Y_{20}\rangle$
$\langle Y_{11}Y_{1-1}Y_{20}\rangle = {}^1{}_2\langle Y_{10}^2 Y_{20}\rangle$
$\langle Y_{21}Y_{2-1}\rangle = -\langle Y_{20}^2\rangle$

APPENDIX B

DERIVATION OF INTEGRALS REQUIRED IN THE LONG-RANGE HELIUM CALCULATIONS

The basic reference for integral evaluation for the long-range calculations is the atomic integral work of Calais and Löwdin. The general integral for which they derive closed-form expressions is:

$$(ac|bd) = \iint f_a(r_1)Y^*_{\ell_1 m_1}(\theta_1,\phi_1)f_b(r_2)Y^*_{\ell_2 m_2}(\theta_2,\phi_2)h(r_{12}) \times f_c(r_1)Y_{\ell_3 m_3}(\theta_1,\phi_1)f_d(r_2)Y_{\ell_4 m_4}(\theta_2,\phi_2)d\underset{\sim}{r}_1\, d\underset{\sim}{r}_2 \ . \tag{B.1}$$

In reference (51) this integral is reduced to a sum of simpler integrals of the form:

$$I^{m\mu}_{\ell\lambda} = \iint f(r_1)Y_{\ell m}(\theta_1,\phi_1)h(r_{12})g(r_2)Y_{\lambda\mu}(\theta_2,\phi_2)d\underset{\sim}{r}_1\, d\underset{\sim}{r}_2 \ . \tag{B.2}$$

For our purposes, the functions f,g, and h are of the form $r^\nu e^{-\mu r}$. We use the following notation,

$$[k\ell m] = \int_0^\infty r_1^k e^{-ar_1}\, dr_1 \int_0^\infty r_2^\ell e^{-br_2}\, dr_2 \int_{|r_1-r_2|}^{r_1+r_2} r_{12}^m e^{-cr_{12}}\, dr_{12} \ , \tag{B.3}$$

where

$$[0,0,0] = \frac{2}{(a+b)(a+c)(b+c)} , \qquad (B.4)$$

and

$$\frac{\partial^k}{\partial a^k}\frac{\partial^\ell}{\partial b^\ell}\frac{\partial^m}{\partial c^m}[0,0,0] = [k,\ell,m] . \qquad (B.5)$$

Thus, knowing the fundamental integral $[0,0,0]$, one can generate formulas for the set $[k,\ell,m]$ by carrying out the differentiations indicated in Eq. (B.5), and $(ac|bd)$ can be computed. The general expression for the $[k,\ell,m]$ is given in reference (51).

In the present calculation, construction of the Hamiltonian matrix requires, in addition to the $\Gamma_{\ell\lambda}^{m\mu}$, expressions for the basic integral:

$$\gamma_{\ell\lambda}^{m\mu n} = \iint f(r_1)Y_{\ell m}(\theta_1,\phi_1)e^{in\phi_1}\, g(r_2)Y_{\lambda\mu}(\theta_2,\phi_2)h(r_{12})d\underset{\sim}{r}_1\, d\underset{\sim}{r}_2 . \qquad (B.6)$$

One purpose of this appendix is to derive a computationally useful expression for this integral.

Following Calais and Löwdin, we first integrate over ϕ_1, ϕ_2, and θ_1 and express the remainder as an integral over r_1, r_2, and the relative angle, $\theta_{12} = \theta_2 - \theta_1$. To accomplish this, we first

rotate the coordinate system so that the polar axis for $\underset{\sim}{r}_2$ coincides with $\underset{\sim}{r}_1$. Denoting the new polar angles as θ_{12} and ϕ_{12} , we have that $Y_{\lambda\mu}(\theta_2,\phi_2)$ becomes:

$$Y_{\lambda\mu}(\theta_2,\phi_2) = \sum_{m'} (-1)^{\mu-m'} e^{i\mu\phi_1} d^{\lambda}_{-\mu,-m'}(\theta_1) Y_{\lambda m'}(\theta_{12},\phi_{12}) . \tag{B.7}$$

Here, the factor $e^{i\mu\phi_1} d^{\lambda}_{-\mu,-m'}(\theta_1)$ is an element of the rotation matrix representing rotation through the Euler angles $\alpha = \phi_1$, $\beta = \theta_1$, $\gamma = 0$. Using Eq. (B.7) in (B.6), we can integrate over ϕ_{12} and see that only the $m' = 0$ term contributes to the above sum. Thus, since,

$$Y_{\ell m}(\theta,\phi) = [\frac{(2\ell+1)}{4\pi}]^{1/2} P_{\ell m}(\cos\theta) e^{im\phi} , \tag{B.8}$$

and

$$d^{\lambda}_{-\mu,0}(\theta) = [\frac{(\lambda-\mu)!}{(\lambda+\mu)!}]^{1/2} P_{\lambda\mu}(\cos\theta) , \tag{B.9}$$

we get

$$\gamma^{m\mu n}_{\ell\lambda} = (-1)^{m+\mu} [\frac{(\lambda-\mu)!}{(\lambda+\mu)!} \cdot \frac{2\lambda+1}{4\pi} \cdot \frac{(2\ell+1)(\ell-m)!}{4\pi(\ell+m)!}]^{1/2}$$
$$\times \int f(r_1) g(r_2) h(r_{12}) P_{\ell m}(\cos\theta_1) P_{\lambda m}(\cos\theta_1) P_{\lambda}(\cos\theta_{12}) e^{i(m+n+\mu)\phi_1} d\tau , \tag{B.10}$$

where

$$d\tau = r_1^2\, r_2^2 \sin\theta_1 \sin\theta_{12}\, dr_1\, dr_2\, dr_{12}\, d\theta_1\, d\theta_{12}\, d\phi_1 \,.$$

Integrating over ϕ_1 yields a factor $\delta_{m+\mu,-n}$, so that $\gamma_{\ell\lambda}^{m\mu n}$ can be written,

$$\begin{aligned}\gamma_{\ell\lambda}^{m\mu n} = {} & (-1)^m\, 2\pi\, \delta_{m+\mu,-n} \int_0^\infty f(r_1) r_1^2\, dr_1 \int_0^\infty g(r_2) r_2^2\, dr_2 \\ & \times \int_0^\pi h(r_{12}) P_\lambda(\cos\theta_{12}) \sin\theta_{12}\, d\theta_{12} \\ & \times (-1)^\mu \left[\frac{(\lambda-\mu)!}{(\lambda+\mu)!} \frac{2\lambda+1}{4\pi} \frac{(2\ell+1)(\ell-m)!}{4\pi(\ell+m)!}\right] 2\pi \int_{-1}^{1} P_{\ell m}(u) P_{\lambda\mu}(u)\, du \,.\end{aligned} \tag{B.11}$$

Comparing this result to Eq. (17) of reference (51), we get

$$\begin{aligned}\gamma_{\ell\lambda}^{m\mu n} = {} & \left[(-1)^\mu \left[\frac{(\lambda-\mu)!}{(\lambda+\mu)!} \frac{2\lambda+1}{4\pi} \frac{(2\ell+1)(\ell-m)!}{4\pi(\ell+m)!}\right]^{1/2} 2\pi \int_{-1}^{1} P_{\ell m}(u) P_{\lambda\mu}(u)\, du\right] \\ & \times \Gamma_{\ell\lambda}^{m+n,\mu} \,.\end{aligned} \tag{B.12}$$

Hence, $\gamma_{\ell\lambda}^{m\mu n}$ can be done by computing $\Gamma_{\ell\lambda}^{m+n\ \mu}$ via the method of Calais and Löwdin, and modifying it by the above multiplicative factor. The integrations involving the associated Legendre functions were done explicitly for the particular $P_{\ell m}$'s which we required.

This result, Eq. (B.12), can be duplicated by expanding the factor $e^{in\phi_1}$ in terms of spherical harmonics, and using the addition theorem for spherical harmonics to reduce the result to the form of $\Gamma_{\ell\lambda}^{m+n,\mu}$.

As mentioned earlier in this appendix, the integrals of Eq. (B.6) can be reduced to sums of integrals of the form of Eq. (B.3), with Eqs. (B.4) and (B.5) forming the basic computational units. For our purposes, however, we also need the additional integral:

$$I = \int_0^\infty r_1^{-1} e^{-kr_1} dr_1 \int_0^\infty r_2^b e^{-kr_2} dr_2 \int_{|r_1-r_2|}^{r_1+r_2} r_{12}^c dr_{12} , \tag{B.13}$$

for $-1 \leq b \leq s$ and $1 \leq c \leq t$.

We proceed by integrating over r_{12} first, then over r_2 , and finally over r_1 , using standard expressions for the intermediate integrals which occur. The final result which is obtained for the integral I is:

$$I = I_1 + I_2 ,$$

where

$$I_1 = \left\{\frac{1}{(c+1)k^{b+c+2}}\right\}\left\{[1+(-1)^{c+2}](b+c+1)!\ \ell n2 + \sum_{p=1}^{c}[1+(-1)^{p+1}]\right.$$

$$\times \frac{(c+1)!\ (b+p)!\ (c-p)!}{p!(c+1-p)!}\left[1 - \frac{1}{2^{c-p+1}}\right] - \sum_{p=1}^{c+1}{\sum_{q=0}^{b-p-1}}'[1+(-1)^{p+1}]$$

$$\left.\times \frac{(c+1)!\ (b+p)!\ (b+c-q)!}{p!(c+1-p)!\ (b+p-q)!\ 2^{b+c-q+1}}\right\}. \qquad (B.14)$$

For I_2, we have different results depending on whether $b = -1$, or $b > -1$:

<u>$b = -1$</u> :

$$I_2 = \frac{1}{c+1}\frac{c!}{k^{c+1}}[1+(-1)^{c+2}]\ell n2 + \frac{1}{c+1}\frac{1}{k^{b+c+2}}\left\{\sum_{p=1}^{c}[1+(-1)^{p+1}]\right.$$

$$\times \frac{(c+1)!}{p!(c+1-p)!}(p-1)!\ (b+c+1-p)!\left[1 - \frac{1}{2^{b+c+2-p}}\right] - \sum_{p=1}^{c+1}{\sum_{q=0}^{p-2}}' \qquad (B.15)$$

$$\left.\times [1+(-1)^{p+1}]\frac{(c+1)!}{p!(c+1-p)!}\frac{(p-1)!}{(p-q-1)!}\frac{(b+c-q)!}{2^{b+c+1-q}}\right\}.$$

$\underline{b > -1}$:

$$I_2 = \frac{1}{c+1}\frac{1}{k^{b+c+2}}\left\{\left[1-\frac{1}{2^{b+1}}\right]b!c!\left[1+(-1)^{c+2}\right]+\sum_{p=1}^{c}\left[1+(-1)^{p+1}\right]\right.$$

$$\times\frac{(c+1)!}{p!(c+1-p)!}(p-1)!\,(b+c+1-p)!\left[1-\frac{1}{2^{b+c+2-p}}\right]-\sum_{p=1}^{c+1}\sum_{q=0}^{p-2}{}' \qquad \text{(B.16)}$$

$$\left.\times\left[1+(-1)^{p+1}\right]\frac{(c+1)!}{p!(c+1-p)!}\,\frac{(p-1)!}{(p-q-1)!}\,\frac{(b+c-q)!}{2^{b+c+1-q}}\right\}.$$

Eqs. (B.12), (B.13), (B.14), (B.15), and (B.16) taken together with the results of Calais and Löwdin comprise all the necessary expressions for computing the integrals needed in the long-range helium calculation.

APPENDIX C

THE BISON COMPUTING SYSTEM

BISON is a self-contained FORTRAN computer system for the calculation of analytic self-consistent-field wavefunctions, properties, and charge densities for diatomic molecules, using a basis of Slater type orbitals. BISON was written by A. C. Wahl, P. J. Bertoncini, K. Kaiser, and R. H. Land of Argonne National Laboratory and is described in reference (64). In the initial construction of this package, care was taken to guarantee that the code would be computationally optimized, modular, machine transferable, and capable of continuous growth and revision. For these reasons it is particularly attractive for our purposes.

Before the program could be modified to allow for computation of diatomic polarizabilities, the standard working version had to be made operative on the University of Wisconsin UNIVAC 1108. The version of BISON with which we began, consisted of ten overlays (independent program segments) which are defined as follows:

main - basic executor, remains core-resident throughout the computations;

overlay 1 - input driver and data-screening segment;

overlay 2 - compute J-type exchange integrals;

overlay 3 - compute J-type coulomb-hybrid integrals;

overlay 4 - compute K-type exchange integrals;

overlay 5 - compute K-type coulomb-hybrid integrals;

overlay 6 - compute one-electron integrals;

overlay 7 - construct P and Q matrices;

overlay 8 - carry out SCF iterations;

overlay 9 - compute properties;

overlay 10 - contour hunting and drawing.

A description of the notation and definitions of terms can be found in the BISON manual.

The initial problem was simply enough storage space to store intermediate results. The data bank (d-bank) size of the above overlays was on the order 130 thousand machine words $(130k)_{10}$ (double precision version) except for overlays 1, 7, 9, and 10 which were considerably smaller. The data divided up among several arrays, with one array of dominant size in the two-electron integral overlays and several arrays of similar size in the one-electron integral overlay. In each case, however, the sizes were such that no matter how the arrays were arranged in core, at least one array would begin beyond the nominal memory size $(65k)_{10}$. This comprised a main problem in adapting the program to the 1108; because the UNIVAC 1110 series of computers uses a 16-bit address field in its instruction words, thus the base address of any array must be less than $(65k)_{10}$ relative to the beginning of the program. However, special data

arrangement procedures can be used to extend this limit to $(256k)_{10}$. This is done by collecting a sufficient number of arrays into a master array using the FORTRAN V DEFINE procedure, such that the base address of this master array is less that $(65k)_{10}$.[79] The words beyond the $(65k)_{10}$ boundary are addressed by the operating system via the base address plus an index offset. This clearly implies that this master array must be stored as the (physically) last part of the d-bank for the given overlay. This is accomplished by declaring the master array to be in labelled COMMON, and manipulating the position of this COMMON block in core using the EXEC-8 MAP processor (MAP is the local name for the EXEC-8 COLLECTOR).[80]

These points are best illustrated by an example from the 1108 version of BISON. Figure (C.1) is a partial listing of the source code for subroutine SUT, which is the main subroutine in the one-electron integral overlay. Figure (C.2) is a listing of the output of the MAP processor for the same overlay.

In Figure (C.1), the COMMON block of interest is EXCORE (a); since this is a double precision program, the array STRAGE requires $(130,000)_{10}$ words. Part (b) of Figure (C.1) shows the actual arrays which are contained in STRAGE, and the manner in which they are imbedded. The statement which defines the function MM(I,J) is of additional interest, because it illustrates the procedure used to imbed a two-dimensional array in a one-dimensional array. The offsets given in Part (c), are not to be confused with the operating

Table C.1. Illustration of the Use of the DEFINE Procedure in BISON.

SEGMENT SUT• 014070 017740 054761 502377
FOLLOWS SEGMENT MAIN

OFFSET (COMMON BLOCK)				054761	054763
SUTMAT (COMMON BLOCK)				054764	100403
SUTPUT (COMMON BLOCK)				100404	100547
SUTDUM (COMMON BLOCK)				100550	100713
SUTDAT (COMMON BLOCK)				100714	102077
SUTCOM (COMMON BLOCK)				102100	103537
SUT	1	014070 015662	0	103540	103770
	3	INPUT	2	FLOAT	
	5	FLAGS	4	PARM	
	7	SUTDUM	6	SUTDAT	
	9	EXCORE	8	SUTPUT	
	11	SUTCOM	10	DIPLM	
	13	OFFSET	12	SUTMAT	
			14	IBLCKS	
GAUSS	1	015663 016175	0	103771	104113
	3	SUTDAT	2	FLOAT	
	5	SUTCOM	4	EXCORE	
STOSUT	1	016176 016535	0	104114	104175
	3	SUTPUT	2	FLOAT	
	5	SUTCOM	4	EXCORE	
			6	OFFSET	
LEGSUT	1	016536 017354	0	104176	104323
	3	EXCORE	2	FLOAT	
			4	OFFSET	
ADDSTO	1	017355 017411	0	104324	104335
			2	SUTDUM	
BLKCTC			0	104336	104336
			2	SUTDAT	
DPARAM	1	017412 017660	0	104337	104435
	3	DIPLM	2	EXCORE	
	5	OFFSET	4	SUTCOM	
PUTLEG	1	017661 017740	0	104436	104457
	3	SUTPUT	2	PARM	
EXCORE (COMMON BLOCK)				104460	502377

Table C.2. Illustration of the Use of the MAP Processor to Position Data.

```
      SUBROUTINE SUT
      IMPLICIT REAL*8 (A-H,O-Z)
      REAL*8 MM
      REAL*8 MATEL
      REAL GRID
      COMMON/FLOAT/FLINT(176),FACTL(57)
      COMMON/INPUT/ Z(100),NN(100),NL(100),NM(100),NNEU,NSIMP,NXI,NETA,
     1   NSYM,NBIAS,ICH,NLAMDA(10)
      COMMON/PARM/ ZA,ZB,RR,RMAX,BETA,MMMIN,MMMAX,LLMIN,LLMAX,IPMAX,NMAT
      COMMON/FLAGS/ IPRINT,IDEBUG,ISTO,IPUNCH
      COMMON/SUTDAT/GRID(628)
      COMMON/SUTDUM/ IDUM(100)
      COMMON/SUTPUT/ JPLACE(100)
      COMMON/EXCORE/STRAGE(65000)                                    } a
      COMMON/DIPLM/IDIPL,FIELDS
      COMMON/SUTCOM/GDPT(2,100),GDWT(2,100)
      COMMON/SUTMAT/ MATEL(1000,5)
      COMMON/OFFSET/IOFST1,IOFST2,IOFST3
      COMMON/IBLCKS/NBLCKS
      DEFINE PLMNX(I)=STRAGE(I)                                      }
      DEFINE CHI(I)=STRAGE(I+IOFST1)                                 }
      DEFINE R(I)=STRAGE(I+IOFST2)                                   }
      DEFINE COS(I)=STRAGE(I+IOFST3)                                 }  b
      DEFINE MM(I,J)=STRAGE(J*NROWS-NROWS+I+IOFST4)                  }
      DEFINE ZVALU(I,J)=STRAGE(J*NRSP-NRSP+I+IOFST5)                 }
      DEFINE XVALU(I)=STRAGE(I+IOFST6)                               }
      IOFST1=10000                                                   }
      IOFST2=20000                                                   }
      IOFST3=25000                                                   }
      IOFST4=30000                                                   }
      IOFST5=58000                                                   }  c
      IOFST6=60000                                                   }
      NROWS=7                                                        }
      NRSP=1000                                                      }
```

system offset indices mentioned above, which are transparent to the user. The program offsets (c) are user defined and are equal to the total number of words in the individual "sub-arrays".

In Figure (C.2), we see that the COMMON BLOCK EXCORE has been forced to the end of the d-bank of the overlay, SUT; this, in fact, forces it to the absolute end of the overlay, as the I-bank is stored first. This positioning is accomplished by placing the card, IN EXCORE (left-justified in column 1) as the last card in the set which defines SEGMENT SUT. Note that since EXCORE begins at $(64772)_8$ and ends at $(502377)_8$ (relative addresses), it could not have fit into the addressable memory in any other way.

Besides the core requirements, BISON uses eleven periferal files. These may be tape files, disk files, drum files, or any combination thereof. For production runs, the program was copied from tape on which the relocatable elements were stored to a temporary drum file, and collected. The rest of the periferals used, consisted of an integral save tape, and eight (scratch) drum files. The logical unit numbers assigned to the scratch files were:

40, 41, 42, 49, 51, 52, 53, 54 .

Of these, all but unit 52 were allotted a maximum of 128 tracks (1 track = $(1,792)_{10}$ words); unit 52 required somewhat more, the actual number depended on the basis set used. LUN 43 was assigned

to the integral save tape; the 7-channel tape was taken to be of medium density (556 bpi). We used 7-channel tapes in order to be compatible with the 1108's 36-bit word structure.

Once the original version of BISON was working, the primary modifications which were necessary to enable us to compute polarizabilities took place mainly in the integral overlays. The original BISON was designed to take advantage of the $D_{\infty h}$ or $C_{\infty v}$ symmetry of diatomic molecules. The symmetry is lowered when an external field is present in the perpendicular direction, and this required modifying some of the algorithms of integral evaluation. These changes consisted of four basic steps:

1. Compute the dipole moment matrix elements in the one-electron segment. This is equivalent to constructing $\underset{\sim}{\mu}\cdot\underset{\sim}{F}$ for unit field strength. The basic code was extracted from the properties segment.
2. Modify the two-electron integral overlays to allow for Slater orbitals of different m-values (including those with m-values of opposite sign) to be handled in a single symmetry block. This included insertion of new selection rules and phase factors. It was also necessary to restrict the MCYCLE DO-loop parameters of subroutines KEX and KCH to a single value, as it was no longer necessary to compute both the K^+- and K^--type integrals separately;

3. Modify the PQ overlay to take the loss of permutational symmetry in the two-electron integrals into account;
4. Modify the SCF part of the program to include the dipole moment terms in the one-electron contributions to the Fock operator, and to allow for field variation in those terms.

Various and sundry additional changes in other parts of the code were also necessary, but these will be discussed elsewhere. A description of the (free-format) input to the polarizability load module is given in Appendix D.

The final verison of the program which we used, typically required about 41 minutes of CPU time to compute a value of $\alpha_{\parallel}$ or $\alpha_{\perp}$ for a given value of R, with an 18-term basis set, using three different field strengths. Of the 41 minutes, 39 minutes were spent in evaluating integrals, with the remainder spent in the SCF calculation. A significant cost factor was the core usage and I/O changes, as illustrated in the typical breakdown shown below:

CPU time	$99.00
IO requests	16.00
IO word transferred	2.50
CORE usage	54.00

Shortly after the computations reported in this thesis were completed, the University of Wisconsin Academic Computing Center upgraded their 1108 to an 1110. Although they made the claim that programs which operated on the 1108 would operate on the 1110 without

modifications, our initial attempts to run BISON were unsuccessful due to decreased available core size on the 1110. However, since the final form of the 1110 operating system was not available, no attempt was made to re-organize the BISON code to fit into the 1110 core.

APPENDIX D

SAMPLE INPUT FOR BISON POLARIZABILITY LOAD MODULE

A sample of the (format-free) input to the BISON load module which is used in the polarizability calculations is given on the Figure D.1. The input, except for the second and third cards, is identical to that described in the BISON manual, reference (64). The data which is entered on the second and third cards is now described.

The ninth (MASSA) and tenth (MASSB) entries on the second card represent the masses of centers A and B respectively, in atomic mass units. The eleventh (IDIPL) and fourteenth (NBLCKS) can be considered together as follows:

IDIPL = 2 , NBLCKS = 1 ; computes the matrix elements of z in the one-electron part of the program, for unblocked input.

IDIPL = 2 , NBLCKS $\neq$ 1 ; computes the matrix elements of x in the one-electron part, for unblocked input.

IDIPL = 1 , NBLCKS $\neq$ 1 ; computes matrix elements of z for blocked input.

The twelfth entry (FIELDS) is the field strength used in the one-electron part of the program, to compute the $\underset{\sim}{\mu}\cdot\underset{\sim}{F}$ terms. The thirteenth entry (DEPTOL) is the linear independence tolerance, and execution is terminated if the smallest eigenvalue of the overlap matrix is less than this threshold.

The first entry on the third card (NFIELD) indicates the number of field strengths to be employed in the current run, and the next NFIELD entries on this card are the specific values of the field strengths which will be used. The field variation is done in the SCF part of the program, so that the use of the field strengths given on the third card presupposes that a value of FIELDS = 1.0 is used on the second card.

Table D.1. Sample Input for BISON for Calculation of $\alpha_{\perp}$ for He_2.

```
HE2 CALCN. OF ALPHA-PERP. AT R=6.0. BASIS OF 18 FNS.
6.0 30 50 50 0 0 2.0 2.0 4.0 4.0 2 1.0 .1D-6 0
1 .001
14 60 20
0 1 0 7 7 5 6 7 0 0 0 0 0
18 2 2 0
2.0 2.0
1     0     0     1.450
2     0     0     2.641
2     0     0     1.723
2     1     1     1.450
2     1    -1     1.450
3     1     1     1.450
3     1    -1     1.450
3     1     1     1.655
3     1    -1     1.655
1     0     0    -1.450
2     0     0    -2.641
2     0     0    -1.723
2     1     1    -1.450
2     1    -1    -1.450
3     1     1    -1.450
3     1    -1    -1.450
3     1     1    -1.655
3     1    -1    -1.655
-.9400
 .0800
 .1900
-.0001
 .0001
-.0002
 .0002
 .0001
-.0001
-.9400
 .0800
 .1900
-.0001
 .0001
-.0002
 .0002
 .0001
-.0001
 .9700
-.0800
-.1900
 .0001
-.0001
 .0003
-.0003
-.0001
 .0001
-.9700
 .0800
 .1900
-.0001
 .0001
-.0003
 .0003
 .0001
-.0001

END OF /RUN
```

APPENDIX E

CONVERSION FACTORS FOR B_ε AND B_K

In our work, we have computed the polarizabilities in units of a_0^3 (atomic units). The results for the second dielectric virial coefficient, B_ε, and the second Kerr virial coefficient, B_K, however, are reported in units of $cm^6/mole^2$, and electrostatic units (esu) respectively (see Table V.1). The conversion factors which are therefore required are obtained in this appendix.

To convert the units of B_ε, Eq. (1.39) is quite straightforward. We have,

$$B_\varepsilon = \frac{8\pi^2 N^2}{3} \int_0^\infty dR\, R^2\, \Delta\alpha(R)\, g(R) ,$$

where we assume that the integral is computed in atomic units (au), which, in this case, means that it has units of a_0^6. Using $N = 6.022169 \times 10^{23}/mole$ and $1a_0 = .529177\ \mathring{A} = .529177 \times 10^{-8}$ cm, we have immediately that,

$$B_\varepsilon(cm^6/mole^2) = .210\, B_\varepsilon(a_0^6/mole^2) .$$

The conversion of B_K to esu's is also straightforward. To begin, we recall Eq. (1.45),

$$B_K = \frac{8\pi^2 N^2}{405kT} \int_0^\infty dR\ R^2\ \beta^2(R)\ g(R)\ ,$$

and note that, in general, the units of B_K are length^9/mole^2-energy. One esu, then corresponds to taking the cm as the unit of length and one erg as the unit of energy. Taking $k = 1.380622 \times 10^{-16}$ erg/°K and noting that the atomic units of the integral are a_0^9, it immediately follows that B_K is obtained in esu's by multiplying the integral (in atomic units) by the factor:

$$C = (16.61399/T) \times 10^{-13}\ \text{cm}^9/a_0^9\text{-erg-mole}^2\ .$$

The particular values of C for T = 4°K and 322°K are respectively:

$$C(4°K) = 4.153497 \times 10^{-13}\ \frac{\text{cm}^9}{a_0^9\text{-erg-mole}^2}\ ,$$

and

$$C(322°K) = .0515962 \times 10^{-13}\ \frac{\text{cm}^9}{a_0^9\text{-erg-mole}^2}\ .$$

Throughout our work, the values of the various physical constants were taken from reference (83).

REFERENCES

1. (a) R. H. Orcutt and R. H. Cole, J. Chem. Phys. 46, 697 (1967); (b) E. C. Kerr and R. H. Sherman, J. Low Temp. Phys. 3, 451 (1970).
2. A. D. Buckingham and D. A. Dunmur, Trans. Faraday Soc. 64, 1776 (1968).
3. H. B. Levine, J. Chem. Phys. 56, 2455 (1972).
4. (a) E. Schrödinger, Ann. d. Physik 79, 489 (1926); see also (b) P. S. Epstein, Phys. Rev. 28, 695 (1926).
5. M. F. Barnsley, Ph.D. Thesis, University of Wisconsin, Madison, 1972; University of Wisconsin Theoretical Chemistry Institute Report WIS-TCI-408 (1972).
6. (a) F. P. Billingsley and M. Krauss, Phys. Rev. A6, 855 (1972); (b) W. J. Stevens and F. P. Billingsley, Phys. Rev. A8, 2236 (1973).
7. A. D. Buckingham and P. G. Hibbard, Symp. Faraday Soc. 2, 41 (1968).
8. W. Kolos and L. Wolniewicz, J. Chem. Phys. 46, 1426 (1967).
9. J. E. Lennard-Jones, Proc. Roy. Soc. (London), A106, 463 (1924).
10. (a) P. J. Bertoncini and A. C. Wahl, Phys. Rev. Lett. 25, 991 (1970); (b) P. J. Bertoncini and A. C. Wahl, J. Chem. Phys. 58,

1259 (1973); (c) D. R. McLaughlin and H. F. Schaefer III, Chem. Phys. Lett. 12, 244 (1971).

11. B. Liu and A. D. McLean, J. Chem. Phys. 59, 4557 (1973).

12. L. W. Bruch and I. J. McGee, J. Chem. Phys. 52, 5884 (1970).

13. (a) A. D. Klemm and R. G. Storer, Australian J. Phys. 26, 43 (1973); (b) A. D. Klemm, Ph.D. Thesis (unpublished) (The Flinders University of South Australia, 1971).

14. A. D. Buckingham, "Permanent and Induced Molecular Moments and Long-Range Intermolecular Forces" in Advances in Chemical Physics Vol. XII, edited by J. O. Hirschfelder (Interscience, New York, 1967).

15. H. A. Lorentz, Theory of Electrons (1908).

16. H. H. Uhlig, J. G. Kirkwood, and F. G. Keyes, J. Chem. Phys. 1, 155 (1933).

17. J. G. Kirkwood, J. Chem. Phys. 4, 592 (1936).

18. L. Jansen and P. Mazur, Physica 21, 193,208 (1955).

19. A. D. Buckingham and J. A. Pople, Trans. Faraday Soc. 51, 1029 (1955).

20. D. A. McQuarrie and H. B. Levine, Physica 31, 749 (1965); H. B. Levine and D. A. McQuarrie, J. Chem. Phys. 44, 3500 (1966).

21. A. D. Buckingham, Trans. Faraday Soc. 52, 1035 (1956).

22. H. B. Levine and D. A. McQuarrie, J. Chem. Phys. 49, 4181 (1968).

23. D. B. DuPré and J. P. McTague, J. Chem. Phys. 50, 2024 (1969).

24. T. K. Lim, B. Linder, and R. A. Kromhout, J. Chem. Phys. 52, 3831 (1970).

25. L. W. Bruch, D. Berman, and P. J. Fortune, to be published.

26. A. D. Buckingham and R. J. Watts, to be published.

27. E. F. O'Brien, V. P. Gutschick, V. McKoy, and J. P. McTague, Phys. Rev. A8, 690 (1973).

28. J. Kerr, Phil. Mag. 50, 337,446 (1875).

29. G. Otterbein, Phys. Z. 35, 249 (1934).

30. A. D. Buckingham and J. A. Pople, Proc. Phys. Soc. A68, 905 (1955).

31. A. D. Buckingham, Proc. Phys. Soc. A68, 910 (1955).

32. A. D. Buckingham and D. A. Dunmur, Trans. Faraday Soc. 64, 1776 (1968).

33. M. F. Crawford, H. L. Welsh, and J. L. Locke, Phys. Rev. 75, 1607 (1949).

34. J. P. McTague and G. Birnbaum, Phys. Rev. Lett. 21, 661 (1968); Phys. Rev. A3, 1376 (1971).

35. J. I. Gersten, R. E. Slusher, and C. M. Surko, Phys. Rev. Lett. 25, 1739 (1970).

36. F. R. Pike and J. M. Vaughan, J. Phys. C4, L362 (1971).

37. H. B. Levine and G. Birnbaum, J. Chem. Phys. 55, 2914 (1971).

38. W. M. Gelbart, Mol. Phys. 26, 873 (1973).

39. C. C. J. Roothaan, Rev. Mod. Phys. 23, 69 (1951); ibid. 32, 179 (1960).

40. B. J. Ransil, J. Chem. Phys. 34, 2109 (1961).

41. N. R. Kestner, J. Chem. Phys. 48, 252 (1968).

42. T. L. Hill, J. Chem. Phys. 28, 61 (1958).

43. A. Ishihara and R. V. Hanks 36, 433 (1962).

44. A. V. Tulub, M. D. Bal'makov, and S. A. Khallaf, Soviet Physics-Poklady 16, 18 (1971).

45. For a discussion of the theorem, see: A. Messiah, Quantum Mechanics Vol. II (1962), p. 573.

46. J. F. Hart and G. Herzberg, Phys. Rev. 106, 79 (1957).

47. P. Sitz and R. Yaris, J. Chem. Phys. 49, 3546 (1968).

48. D. M. Whisnant, Ph.D. Thesis, University of Wisconsin, Madison, 1970; University of Wisconsin Theoretical Chemistry Institute Report WIS-TCI-395 (1970).

49. A. Dalgarno and S. T. Epstein, J. Chem. Phys. 50, 2837 (1969).

50. C. L. Pekeris, Phys. Rev. 115, 1216 (1959).

51. J. L. Calais and P. O. Löwdin, J. Molec. Spect. 8, 203 (1962).

52. A. D. Buckingham, P. H. Martin, and R. S. Watts, Chem. Phys. Lett. 21, 186 (1973).

53. J. O. Hirschfelder and J. W. Linnett, J. Chem. Phys. 18, 130 (1950).

54. J. O. Hirschfelder, J. Chem. Phys. 3, 555 (1935).

55. J. G. Kirkwood, Physik. Z. 33, 57 (1932).

56. P. W. Langhoff, M. Karplus, and R. P. Hurst, J. Chem. Phys. 44, 505 (1966).

57. H. D. Cohen and C. C. J. Roothaan, J. Chem. Phys. 43, S35 (1965).

58. H. D. Cohen, J. Chem. Phys. 43, 3558 (1965).

59. G. Herzberg, Electronic Spectra of Polyatomic Molecules (D. Van Nostrand, New York, 1966).

60. R. E. Sitter and R. P. Hurst, Phys. Rev. A5, 5 (1972).

61. T. L. Gilbert and A. C. Wahl, J. Chem. Phys. 47, 3425 (1968).

62. J. O. Hirschfelder, C. F. Curtiss, and R. B. Bird, Molecular Theory of Gases and Liquids (John Wiley and Sons, Inc., New York, 1954), p. 946.

63. H. F. Schaefer III, The Electronic Structure of Atoms and Molecules (Addison-Wesley, Inc., 1972).

64. A. C. Wahl, P. J. Bertoncini, K. Kaiser, and R. H. Land, Argonne National Laboratory Report No. ANL-7271 (1968), unpublished.

65. R. R. Teachout and R. T. Pack, At. Data 3, 195 (1971).

66. E. Clementi, J. Chem. Phys. 40, 1944 (1964).

67. T. C. Caves and M. Karplus, J. Chem. Phys. 50, 3649 (1969).

68. V. P. Gutschick and V. McKoy, J. Chem. Phys. 58, 2397 (1973).

69. A. Dalgarno, Advan. Phys. 11, 281 (1962).

70. T. D. Lee and C. N. Yang, Phys. Rev. 113, 1165 (1959); 116, 25 (1959).

71. S. Y. Larsen, J. Chem. Phys. 48, 1701 (1968).

72. S. Y. Larsen, K. Witte, and J. E. Kilpatrick, J. Chem. Phys. 44, 213 (1966).

73. J. Poll and M. S. Miller, J. Chem. Phys. 54, 2673 (1971).

74. A. D. Klemm and R. G. Storer, Australian J. Phys. 26, 43 (1973).

75. A. D. Klemm, Ph.D. Thesis (unpublished) (The Flinders University of South Australia, 1971).

76. R. G. Storer, J. Math. Phys. 9, 964 (1968).

77. R. G. Storer, Phys. Rev. 176, 326 (1968).

78. M. Abramowitz and I. Stegun, Handbook of Mathematical Functions (1964), p. 444.

79. FORTRAN V Compiler Reference Manual for the 1108, Academic Computing Center, University of Wisconsin, Madison.

80. 1108 Computing Handbook, Academic Computing Center, University of Wisconsin, Madison (February, 1973), pp. V-35 - V-38.4.

81. A. Ben-Reuven and N. D. Gershon, J. Chem. Phys. 51, 893 (1969).

82. J. O. Hirschfelder and W. J. Meath, "The Nature of Intermolecular Forces" in Advances in Chemical Physics Vol. XII, edited by J. O. Hirschfelder (Interscience, New York, 1967).

83. B. N. Taylor, W. H. Parker, and D. N. Langenberg, Rev. Mod. Phys. 41, 375 (1969), see especially Table XXXII.